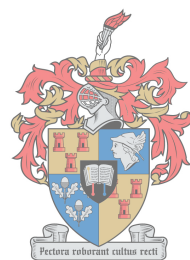


Characterization of a novel antibiotic isolated from *Xenorhabdus khoisanae* and encapsulation of vancomycin in nanoparticles

by
Elzaan Booysen



UNIVERSITEIT
iYUNIVESITHI
UNIVERSITY
*Thesis presented in fulfilment of the requirements for the degree of Master of Science in the
Faculty of Science at Stellenbosch University*



Supervisor: Prof. Leon M.T. Dicks

Co-supervisor: Dr. Hanél Sadie-Van Gijzen

March 2018

Declaration

By submitting this thesis electronically, I declare that the entirety of the work contained therein is my own, original work, that I am the sole author thereof (save to the extent explicitly otherwise stated), that reproduction and publication thereof by Stellenbosch University will not infringe in any third-party rights and that I have not previously in its entirety or in part submitted it for obtaining any qualification.

March 2018

Elzaan Booysen

Copyright © 2018 Stellenbosch University
All rights reserved

Summary

Periprosthetic joint infection (PJI) is the major cause of total joint arthroplasty failures and is often caused by methicillin-resistant *Staphylococcus aureus* (MRSA). The ability of these bacteria to rapidly acquire resistance against antibiotics has made it nearly impossible to treat these persistent infections. The number of novel antibiotics that have successfully completed clinical trials has declined rapidly in the last 50 years. The search for novel antibiotics and alternative delivery routes is thus of utmost importance.

Entomopathogenic bacteria, living in close association with nematodes, are a potential source of novel antibiotics. One such genus, *Xenorhabdus*, produces a variety of secondary metabolites, including antimicrobial compounds. The majority of these compounds are active against numerous so-called multidrug resistant pathogens. Antibiotics produced by *Xenorhabdus* spp. may thus be an alternative treatment for PJI.

Numerous drugs fail phase II and III clinical trials due to insolubility, toxicity and instability at pharmaceutically active levels. This can be overcome by encapsulating the therapeutic drugs in nanoparticles. The polymer poly(DL-lactide-co-glycolide) (PLGA) has significant attention as a colloidal drug delivery device and is well-known for its biocompatibility.

In this study, *Xenorhabdus khoisanae* was screened for the production of novel antibiotics. Three antibiotics were isolated from a *X. khoisanae* culture, two were similar to xenocoumacin-2 and one a novel antibiotic with a mass-to-charge ratio of 671, designated rhabdin. Rhabdin is active against two clinical strains of *S. aureus* (including MRSA). The osteogenic and cytotoxic effects of rhabdin were evaluated on two populations of rat femora-derived mesenchymal stem cells (MSC). Rhabdin was cytotoxic to the bone marrow-derived mesenchymal stem cells (bmMSC) at concentrations exceeding 3.5 µg/ml, but had no anti-osteogenic effects. In contrast, rhabdin was completely cytotoxic to proximal femur-derived mesenchymal stem cells (pfMSC). Vancomycin, traditionally used to treat MRSA, was also evaluated and no cytotoxicity was observed in bmMSC or pfMSC, but vancomycin had an anti-osteogenic effect on pfMSC.

Vancomycin was encapsulated in PLGA nanoparticles (VNP) by electrospraying. The mean hydrodynamic diameter of VNP was 247 nm. The antimicrobial activity of free vancomycin and encapsulated vancomycin was compared and VNP showed enhanced antimicrobial activity. Vancomycin release was monitored for 10 days and followed first-order release. After 10 days, only 50% of the encapsulated vancomycin was released from the nanoparticles.

To our knowledge, this is the first study to report on antibiotics produced by *X. khoisanae*, the anti-osteogenic effects of vancomycin and the encapsulation of vancomycin in PLGA nanoparticles by electrospraying.

Opsomming

Post-chirurgiese infeksie van 'n prostetiese gewrig is die mees algemene oorsaak vir onsuksesvolle totale gewrigs vervangings. Hierdie infeksies word meestal deur metisillien-weerstandige *Staphylococcus aureus* (MWSA) veroorsaak. Die vermoë van hierdie bakterieë om vinnige weerstandigheid teen antibiotika op te bou, maak dit bykans onmoonlik om weerstandige infeksies te behandel. In die laaste 50 jaar het die aantal antibiotika wat kliniese toetse suksesvol voltooi het, vinnig gedaal. Die soektog na unieke en nuwe antibiotika en alternatiewe middels is dus van uiterste belang.

Die entomopatogeniese genus, *Xenorhabdus*, wat in 'n eng gemeenskaplike verwantskap met nematodes leef, is 'n moontlike bron van unieke antibiotika. *Xenorhabdus* spp. produseer n verskeidenheid sekondêre metaboliete, insluitend antimikrobiese verbindings. Die meederheid van hierdie verbindings is teen 'n verskeidenheid veelvuldige antibiotika-weerstandige patogene aktief. Daar, is dus 'n moontlikheid dat antibiotika van *Xenorhabdus* spp. as behandeling teen prostetiese gewrigs-infeksies kan dien.

As gevolg van onoplaasbaarheid, toksisiteit en onstabiliteit teen farmakologies-aktiewe vlakke, misluk veelvuldige antibiotia tydens fase II and III kliniese toetse. Hierdie negatiewe punte kan oorkom word deur die terapeutiese middels in nanopartikels te omsluit. Die polimeer "poly(DL-lactide-co-glycolide) (PLGA)" geniet baie aandag as 'n kolloïdale toedieningsstelsel en is wêreldbekend as 'n biologies-versoenbare polimeer.

In hierdie studie is *Xenorhabdus khoisanae* vir die produksie van unieke antibiotika getoets. Drie antibiotika is van 'n *X. khoisanae* kultuur geïsoleer, twee is soortgelyk aan xenocoumacin-2 en een is 'n unieke verbinding met 'n massa-tot-lading verhouding van 671, aangewys as rhabdin. Rhabdin is aktief teen twee klinies-verwante *S. aureus* rasse (insluitend MWSA). Die osteogeniese en sitotoksiese effek van rhabdin is teen twee populasies van rot femur-afgeleide mesenkiem-stamselle (MSS) getoets. Rhabdin is sitotoksies vir beenmurg-afgeleide mesenkiem-stamselle (bmMSS) teen konsentrasies hoër as 3.5 µg/ml, maar het geen anti-osteogeniese effek gehad nie. In teenstelling hiermee, is rhabdin heeltemal toksies vir proksimaal femur-afgeleide

mesenkiem-stamselle (MSS). Vankomisien word tradisioneel gebruik om MWSA infeksies te behandel en is vir toksisiteit en osetogeniese effek geëvalueer. Geen toksiese effek is waargeneem in bmMSS en pfMSS kulture nie, maar vankomisien het wel 'n antiosteogeniese effek teen pfMSS getoon. Vankomisien is in PLGA nanoparticles (VNP) deur middel van elektrospoei omsluit. Die hidrodinamiese deursnit van VNP is 247 nm. Die antimikrobiese aktiwiteit van vrye vankomisien en PLGA-omsluite vankomisien is vergelyk. Vankomisien omsluite partikels het meer antimikrobiese aktiwiteit getoon.. Vankomisien vrystelling is vir 10 dae gemonitor en het eerste-orde vrystelling getoon. Na 10 dae was 50% van die omsluite vankomisien vrygestel.

So ver ons kennis strek is hierdie die eerste studie wat die werking van 'n antibiotikum, geproduseer deur *X. khoisanae*, raporteer. Hierdie is ook die eerste studie op die anti-osteogeniese effek van vankomisien en die omsluiting van vankomisien in 'n PLGA polimeer deur middel van die elektrospoei tegniek.

This thesis is dedicated to my two grandfathers, Jan Daniel Tolken and Barend Cornelius Booyesen.

Biographical Sketch

Elzaan Booysen was born in Cape Town, South Africa on the 21st of December, 1992. She matriculated at Paarl Girls' High, South Africa, in 2011. In 2012, she enrolled as B.Sc. student in Molecular Biology and Biotechnology at the University of Stellenbosch and obtained the degree in 2014. She obtained her HonsBSC in Microbiology in 2015, also at the University of Stellenbosch. In January 2016 she enrolled as M.Sc. student in Microbiology.

Preface

This thesis is presented as a compilation of manuscripts. Each chapter is introduced separately and is written according to the style of the respective journal.

Acknowledgements

I would like to sincerely thank the following people and organizations:

My family and friends for always believing in me and supporting me every step of the way.

Prof. L.M.T Dicks for granting me this opportunity and all his support and guidance.

Dr. Hanél Sadie-van Gijzen for her valuable insight, assistance with experiments and critical reading of the manuscripts.

Dr. Shelly Deane for her valuable insights and critical reading of the manuscripts.

Prof. Marina Rautenbach for her assistance with HPLC training and MS analysis.

All my co-workers in the Department of Microbiology for their insight and support.

The National Research Foundation (NRF) of South Africa and FraunHofer for their financial support and funding of the research.

Contents

	Page
Chapter 1: General Introduction	
General Introduction	5
References	7
Chapter 2: Literature Review	
Introduction	9
Novel sources	11
Nanotechnology	15
History	16
Types of nanoparticles	18
Nanoparticle synthesis	36
Current applications of nanoparticles	46
Mesenchymal stem cells	53
References	55
Chapter 3: Characterization of antibiotics from <i>Xenorhabdus khoisanae</i>	
Abstract	75
Introduction	76
Materials and methods	78

Results	83
Discussion	88
References	91
Supplementary information	94

Chapter 4: Evaluation of the osteogenic and cytotoxic effects of vancomycin on rat femora-derived mesenchymal stem cells

Abstract	97
Introduction	97
Materials and methods	99
Results and discussion	102
Conclusion	105
References	106

Chapter 5: Antibacterial activity of vancomycin encapsulated in poly(DL-lactide-co-glycolide) nanoparticles

Abstract	109
Introduction	109
Materials and methods	111
Results and discussions	115
Conclusion	119
References	120

Chapter 6: General Discussion and Conclusions

General Discussion	124
Final Conclusion	126
References	127

STELLENBOSCH UNIVERSITY

Chapter 1

General Introduction

General Introduction

Osteoarthritis (OA) is a debilitating bone disease that effects 22.7% of the world population (1). Treatment varies from following a pharmacologic approach to using complementary and alternative medicine and surgery (2). Surgery is only used when pharmacological and behavioural treatments failed to improve mobility and alleviate pain (2). Treating OA with total joint arthroplasty (TJA) is a well-known technique and delivers excellent results, with total hip arthroplasty (THA) being the most popular and successful (3, 4). With a success rate of 95%, many might believe that THA failures are a minor issue, but since the major cause of failure is infection, this is unfortunately the contrary (5). Periprosthetic joint infection (PJI) is defined by the Musculoskeletal Infection Society (MSIS) as a condition caused when a sinus tract (wound tunnel) comes in contact with the prosthesis, the isolation of pathogens, by culture, from two separate tissue or fluid samples near the prosthesis, elevated concentrations of C-reactive protein and serum erythrocyte sedimentation, elevated leukocyte count and the presence of purulence in the affected joint (6). In 2008, Pulido and co-authors reported that 53% of all PJI are caused by methicillin-resistant *Staphylococcus* spp. (MRS), of which 19% was *Staphylococcus aureus* and 11% *Staphylococcus epidermidis*. The same authors also reported that 11% of PJI was caused by Gram-negative bacteria, with *Klebsiella pneumoniae* and *Escherichia coli* being the most prevalent (7). Biofilm formation by these bacteria further complicates PJI treatment is. Traditionally, methicillin resistant infections were treated with vancomycin, but Kirby and co-authors reported in 2010 on the discovery of MRS with reduced sensitivity to vancomycin (8).

Although antibiotic resistance has always been an intrinsic part of antibiotic treatment, the misuse and over-prescription of antibiotics is contributing to the acceleration seen in antibiotic resistance (9). Further aggravating the situation is the decline in the discovery and approval of novel antibiotics. For decades, antibiotics have mainly been isolated from a handful of soil micro-organisms, including *Bacillus*, *Streptomyces* and *Pseudomonas* species; all belonging to the group Actinomycetes (10). This narrow-minded approach has led to the exclusion of numerous unique niches with antibiotic potential. One such niche, nematodes and their mutualistic bacteria, holds great potential as a possible source for novel antibiotics

(10–12). *Xenorhabdus* spp. co-exist in mutualistic relationship with *Steinernema* nematodes and produce various antimicrobial metabolites, including indole derivatives, iodinine, phenethylamides and more complex molecules derived from a hybrid non-ribosomal peptide synthetase/peptide polyketide synthase (NRPS/PKS) system (12).

Another reason for the decline in approval of novel antibiotics is that, after going through the different phases of clinical evaluations, a large percentage turn out to be toxic, whereas others are water-insoluble or unstable (13). Many researchers have shown that these negative characteristics can be overcome by incorporating therapeutically active drugs in nanoparticles. Recently, Turos and co-authors (14, 15) also reported that the antimicrobial activity can be enhanced by encapsulation in nanoparticles.

A novel antibiotic from an entomopathogenic bacterium that engages in a mutualistic relationship with a *Steinernema jeffreyense* nematode, was isolated and partially characterised in this study. This new antibiotic with a mass-to-charge ratio of 671 is and was evaluated for cytotoxicity *in vitro* on bone marrow mesenchymal stem cells (bmMSC) and proximal femur mesenchymal stem cells (pfMSC). Vancomycin was encapsulated in poly(lactide-co-glycolide) (PLGA) nanoparticles to enhance its antibiotic potential. The nanoparticles were characterised based on size, morphology and release profile. The antibiotic activity was evaluated *in vitro* against *Staphylococcus aureus* Xen 31 (methicillin resistant) and Xen 36 (methicillin sensitive).

References

1. Barbour KE, Helmick CG, Boring M, Brady TJ. 2017. Vital signs: Prevalence of doctor-diagnosed arthritis and arthritis-attributable activity limitation — United States, 2013–2015. *Morb Mortal Wkly Rep* 66:246–253.
2. Sinusas K. 2012. Osteoarthritis: diagnosis and treatment. *Am Fam Physician* 85:49–56.
3. Knight SR, Aujla R, Biswas SP. 2011. Total hip arthroplasty - over 100 years of operative history. *Orthop Rev (Pavia)* 3:72–74.
4. Learmonth ID, Young C, Rorabeck C. 2007. The operation of the century: total hip replacement. *Lancet* 370:1508–1519.
5. Song Z, Borgwardt L, Høiby N, Wu H, Sørensen TS, Borgwardt A. 2013. Prosthesis infections after orthopedic joint replacement: the possible role of bacterial biofilms. *Orthop Rev (Pavia)* 5:65–71.
6. Parvizi J, Zmistowski B, Berbari EF, Bauer TW, Springer BD, Della Valle CJ, Garvin KL, Mont MA, Wongworawat MD, Zalavras CG. 2011. New Definition for periprosthetic joint infection: from the workgroup of the Musculoskeletal Infection Society. *Clin Orthop Relat Res* 469:2992–2994.
7. Pulido L, Ghanem E, Joshi A, Purtill JJ, Parvizi J. 2008. Periprosthetic Joint Infection: the incidence, timing, and predisposing factors. *Clin Orthop Relat Res* 466:1710–1715.
8. Kirby A, Graham R, Williams NJ, Wootton M, Broughton CM, Alanazi M, Anson J, Neal TJ, Parry CM. 2010. *Staphylococcus aureus* with reduced glycopeptide susceptibility in Liverpool, UK. *J Antimicrob Chemother* 65:721–724.
9. Fair RJ, Tor Y. 2014. Antibiotics and bacterial resistance in the 21st century. *Perspect Medicin Chem* 6:25–64.
10. Pidot SJ, Coyne S, Kloss F, Hertweck C. 2014. Antibiotics from neglected bacterial sources. *Int J Med Microbiol* 304:14–22.
11. Challinor VL, Bode HB. 2015. Bioactive natural products from novel microbial sources. *Ann N Y Acad Sci* 1354:82–97.
12. Bode HB. 2009. Entomopathogenic bacteria as a source of secondary metabolites. *Curr Opin Chem Biol* 13:224–230.
13. Adair JH, Parette MP, Altinoglu EI, Kester M. 2010. Nanoparticulate alternatives for

drug delivery. ACS Nano 4:4967–4970.

14. Turos E, Shim JY, Wang Y, Greenhalgh K, Reddy GSK, Dickey S, Lim D V. 2007. Antibiotic-conjugated polyacrylate nanoparticles: New opportunities for development of anti-MRSA agents. Bioorganic Med Chem Lett 17:53–56.
15. Turos E, Reddy GSK, Greenhalgh K, Ramaraju P, Abeylath SC, Jang S, Dickey S, Lim D V. 2007. Penicillin-bound polyacrylate nanoparticles: Restoring the activity of β -lactam antibiotics against MRSA. Bioorganic Med Chem Lett 17:3468–3472.

STELLENBOSCH UNIVERSITY

Chapter 2

Literature Review

Introduction

Although micro-organisms are blamed for the majority of diseases that plague humans, they produce secondary metabolites that may be developed into antimicrobial compounds (1, 2). Antibiotics play a big role in the modern health care industry, saving numerous lives, and have become even more important with the rise of HIV/AIDS. Anti-retrovirals improved the life expectancy of an HIV/AIDS sufferer by approximately 30 to 40 years (3), but in most cases, death is caused by a microbial infection. Resistance to antibiotics is thus a major challenge to HIV/AIDS sufferers.

In 1909, Sahachiro Hata, identified arsphenamine, an arsenical compound, that was, considered the 'magic bullet' for treatment of syphilis (4, 5). Initially known as compound 606, arsphenamine was later relabelled as Salvarsan. The next big discovery was made by Alexander Fleming in 1928 when he noticed a blue mold, *Penicillium notatum*, inhibiting the growth of *Staphylococcus aureus* (6). Although Alexander Fleming was not able to demonstrate the therapeutic value of penicillin, his research paved the way for the antibiotic era. Many of the techniques used by Fleming are still widely used in antibiotic development (7). In August 1940, a paper was published by HW Florey and his colleagues demonstrating the therapeutic value of Penicillin (8) and by the end of 1943, penicillin was mass produced and used to treat soldiers in World War II (7). Sulfonamides, a azo dye derivative, was clinically introduced by Dogmagk in 1935 as protonsil, before the wide spread use of penicillin (9, 10). Following the success of penicillin Merck invested in the research of a soil scientist, Selman Waksman, who noticed that as many as 50% of actinomycetes inhibited the growth of other micro-organisms (11, 12) and isolated more than 10 different compounds with antimicrobial activity. Streptomycin, the first aminoglycoside isolated from *Streptomyces griseus* in 1943 and clinically introduced as a tuberculosis treatment in 1946, was one of those compounds (7, 13, 14). The discovery of streptomycin also led to the first randomized, double-blind, placebo- controlled clinical trials throughout Europe (15).

The next 30 years of antibiotic discovery was fruitfull and no less than 8 antibiotic classes were discovered, including amphenicols (16–18), polymyxins (19–22), macrolides (23),

tetracyclines (24), rifamycins (25, 26), glycopeptides (27), lincosamides (28) and quinolones (29). In the last 50, years only seven new classes of antibiotics have been discovered and approved by the FDA for human consumption, of which streptogramins and pleuromutilins were discovered before the 1970's (13). The timeline of clinical introduction of the antibiotic classes are depicted in Fig. 1.

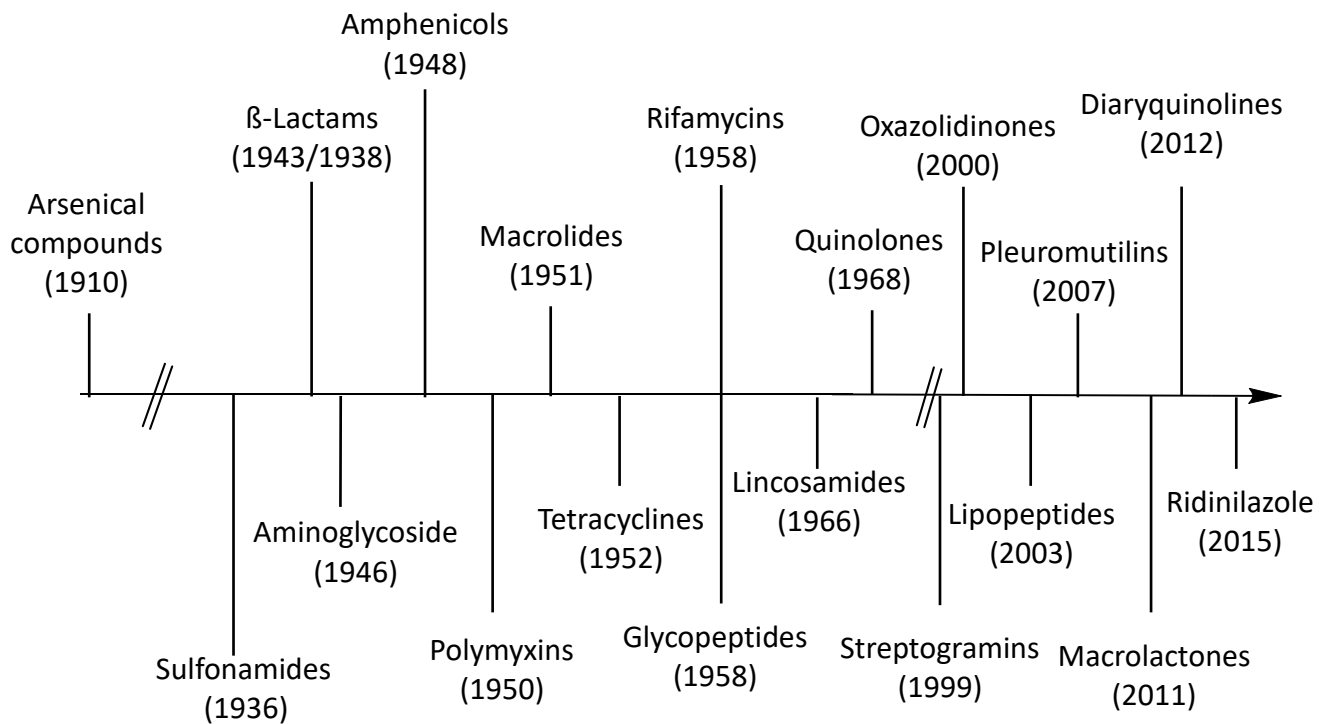


Fig. 1: Timeline of clinical introduction of antibiotic classes.

This golden era of antibiotics was short-lived, because bacteria developed resistance faster than new antibiotics were discovered (15). Three factors contributed to the rise in resistance and the decline in usable antibiotics: a decline in pharmaceutical investments, are over-use of antibiotics and the misuse of antibiotics by the food and agricultural sectors (13, 30).

Since 1970, only seven new classes of antibiotics entered the market, compared to the 11 novel classes licenced from the 1930s to 1960s (31). This lack in investment is due to various reasons, including reduced profit since novel antibiotics are used as last resort, shorter period of administration compared to other drugs, generic competitors and regulatory hurdles rendering it nearly impossible to obtain FDA approval (13). There are 18 classes of antibiotics on the market namely, β-lactams, streptogramins, amphenicols, polymyxins, macrolides,

tetracyclines, rifamycins, glycopeptides, lipopeptides, quinolone, oxazolidinone, pleuromutilins, macrolactones, diarylquinoline and ridinilazoles. The majority of these classes were isolated from *Streptomyces* spp. This lack in novel sources for antibiotics and thus limited structural diversity, have also contributed to the rise in antibiotic resistance (32).

Another factor contributing to the reduced output of novel antibiotics is the instability, low bio-distribution, short-half life and toxicity of natural compounds (33). This can be overcome by encapsulating antibiotics in nanoparticles. Numerous researchers have shown that by encapsulating pharmaceutically active drugs in nanoparticles, the bio-distribution can be improved, half-life prolonged, toxicity decreased, therapeutic effects enhanced and the drug protected against *in vivo* conditions (34–38).

For the past 100 years, soil microbes have been the main source of antibiotics (1). Numerous other potential antibiotic producers have been neglected, for example the Burkholderiales order, *Lysobacter* sp. from the Xanthomonadales order and bacteria associated with nematodes (1, 2).

Order Burkholderiales

The order Burkholderiales belongs to the class β -proteobacteria and contains two genera with the potential to be novel sources of antibiotics, namely *Burkholderia* and *Janthinobacterium* (2). Bacteria from the order Burkholderiales are well known for the production of various secondary metabolites, including antifungals and pesticides (39). These species can be isolated from various niches. Bacteria from the genus *Burkholderia* are infamous for nosocomial infections and is often isolated from patients with cystic fibrosis (1), but Santos *et al.* (40), Kang *et al.* (41) and El-Banna *et al.* (42) have shown that *Bulkolderia* species have potential as novel sources of antimicrobials. The first compounds with broad spectrum antibiotic activity isolated from a species of *Burkholderia*, was enacyloxins (43), originally isolated from *Frateuria* spp. W-315 (44).

The antimicrobial potential of *Janthinobacterium* spp. was first reported by O'Sullivan and co-authors in 1990 (45). Strains from the genus *Janthinobacterium* are motile Gram-negative

bacteria isolated from various niches including the Antarctic, plants and as symbionts of amphibians and insects (1). O'Sullivan reported that janthinocins, a peptide lactone antibiotic, produced by *Janthinobacterium lividum* was not only active against *Staphylococcus aureus*, but two to four times more potent than vancomycin. More recently, Graupner and co-authors reported the production of jagaricin, a novel cyclic lipopeptide with antifungal properties (46).

Genus *Lysobacter*

Species from the *Lysobacter* genus are Gram-negative and motile by gliding. They are strictly aerobic and produce lytic enzymes (47). The first antibiotic isolated from a *Lysobacter* sp. was cephabacin, classified as a β -lactam antibiotic. Cephabacin inhibits cell wall synthesis and is active against a wide variety of Gram-positives, including β -lactam resistant bacteria (48).

The cyclic peptides produced by *Lysobacter* spp. are known for their potent activity against methicillin-resistant *S. aureus* (MRSA) and methicillin-sensitive *S. aureus*. The first cyclic peptide, lysobactin, was described by O'Sullivan and co-authors in 1988 (49). This was followed by the discovery of WAP-8294A compounds in 1998 by Kato and co-authors (50). Kato and co-authors reported that compound WAP-8294A did not only have potent activity against MRSA, but was 14 times more potent compared to vancomycin and is undergoing phase I and II trials at aRigen, a pharmaceutical company situated in Tokyo (48, 50, 51). Lysocin E, an unique cell wall synthesis inhibitor, discovered by a Japanese group in 2015 (52), is known for its wide-spread activity against Gram-positive and Gram-negative bacteria by binding to menaquinone (52, 53). Tripropeptins, another cyclic peptide produced by *Lysobacter* spp., was first described by Hashizume and co-workers in 2011 (54). Tripropeptins inhibits bacterial cell wall biosynthesis and works synergistically with β -lactams, but is active against β -lactam resistant bacteria (55).

Nematodes

Steinernema nematodes are entomopathogenic and synergistically associated with bacterial species from the genus *Xenorhabdus* (56). The nematode-bacterium life cycle is unique and involves both symbiotic and pathogenic associations (Fig 2). The *Xenorhabdus* bacterium is

carried in the gut of the infective juvenile nematode. Infective juveniles (IJ) are a specialized free-living form of the nematode that search for insect larvae in the soil to prey on and enter through the larval haemocoel. Once the IJs infect the insect, *Xenorhabdus spp.* are released into the insect haemolymph to proliferate and produce various secondary metabolites. The secondary metabolites produced by the bacteria include hydrolytic exoenzymes, immune suppressors and antimicrobial compounds. Hydrolytic exoenzymes are responsible for the bioconversion of the insect larva to nutrients used by the nematodes. The IJ then moults into third (3J) and fourth (4J) stage juveniles. The juveniles mature into first generation (1G) males and females. The 1G nematodes mate and female nematodes lay eggs. The eggs hatch as first-stage juveniles (1J) that matures successively into 2J, 3J and 4J juveniles (long life cycle, Fig 2) or IJs depending on food supply (short cycle, Fig 2). The 4J stage nematodes mature into 2G adults that reproduce by mating and laying eggs. The eggs hatch and replication continue until cadaver (host) resources are depleted. Once the resources are depleted, individuals in late 2J stages stop feeding and incorporate a pellet of bacteria. This is followed by moulting into pre-infective (PJ) and infective juveniles. The nematodes leave the cadaver in search of new prey. The antimicrobial compounds prevent secondary infection of the insect larva and retains a “sterile” environment within the insect larva. Thus, the nematode provides protection and a mode of dispersal to the bacterium, while the bacterium provides the necessary enzymes and immune suppressors to the nematode (57).

In 1959, Dutky was the first to report that the bacterial symbiont of *Steinernema carpocape* produced antibiotics (58). Two decades later, the bacterial symbiont of *Steinernema* nematodes was identified as *Xenorhabdus*.

Only a handful of *Xenorhabdus spp.*, namely *X. nematophilia*, *X. bovienii*, *X. szentirmaii*, *X. doucetiae* and *X. budapestensis* have been studied for production of antimicrobial compounds. Antimicrobials isolated from *Xenorhabdus spp.* can be divided into four groups of metabolites, namely indole derived, mixed peptide-polyketide, pyrrothine and peptides. Indoles derivatives were the first antimicrobials isolated and characterized from *X. bovienii* (59). Indole-derived metabolites are active against a broad spectrum of organisms, including bacteria, fungi and insects (60). Xenocycloins and nematophin are well-known indole-derived

metabolites produced by *X. bovienii* (61) and *X. nematophilia* (62), respectively. In 1997, Jianxion Li and co-authors reported that the antimicrobial activity of nematophin against multidrug resistant *S. aureus* strains is comparable to the activity of vancomycin (63). Xenocoumacins, mixed peptide-polyketide derivatives, a group of antimicrobial compounds produced by *X. nematophilia* that are known to be active against both Gram-positive and -negative bacteria (64). Most active secondary metabolites produced by *Xenorhabdus* spp. are classified as peptide metabolites. *Xenorhabdus* peptide metabolites are either cyclic or linear peptides. Cyclic peptide metabolites are produced by *X. nematophilia*, *X. szentirmaii* and *X. doucetiae*, and are active against a range of parasites, including *Plasmodium falciparum* (causes malaria) and *Trypanosoma brucei* (causes sleeping sickness). Linear peptide metabolites are more known for their antifungal properties and are produced by *X. nematophilia* and *X. budapestensis* (2).

Most antimicrobial compounds produced by *Xenorhabdus* spp. have a broad activity spectrum. The rise in antibiotic resistant pathogens is a major threat to the health of immunocompromised patients. Hospitals are the main breeding ground for antibiotic resistant pathogens, thus putting immunocompromised patients at an ever-bigger risk for infection by multiple pathogens. The advantage of broad-spectrum antibiotics is that they can be used to treat multiple infections at once, thus eliminating the need for multiple treatments.

To ensure the longevity of *Xenorhabdus* antibiotics, they can also be encapsulated in colloidal drug delivery systems. These systems can be used to target a specific site of infection, thus decreasing the spread of antibiotic resistance and cytotoxicity. Nanofibers loaded with antibiotics can be used as bandages to treat severe burn wounds (65), while nanoparticles can be prophylactically used in prostheses (66).

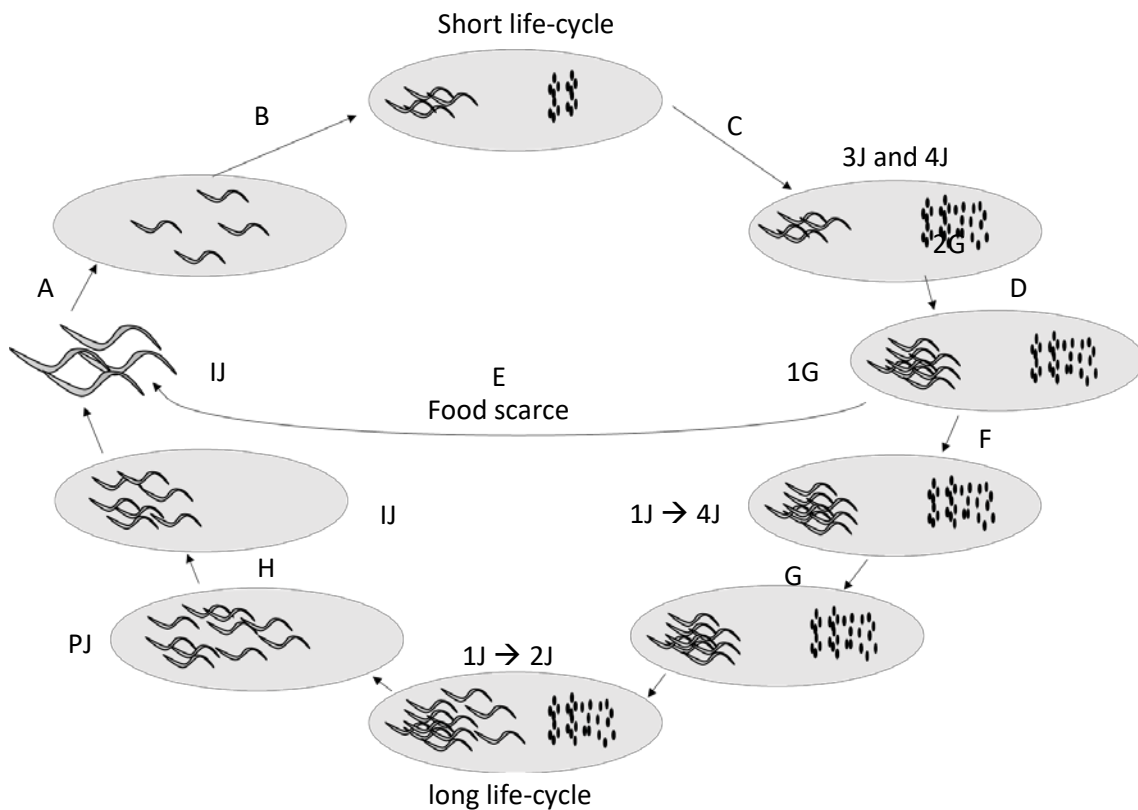


Fig. 2: Diagram of the life-cycle of *Steinernema* nematodes, illustrating the various life-stages of a nematode in a food limiting environment (top) and food rich environment (bottom). A) Infective juvenile (IJ) searches for prey and enters host through haemocoel. B) Bacteria are released and C) IJ molts into third-stage (3J) and fourth-stage (4J) juveniles. D) Juveniles mature into first generation (1G) males and females. The 1G adults mate and females lay eggs, that hatch as first-stage juveniles (1J). E) If food supply is insufficient 1J molt into IJ, leave the cadaver and hunt for new prey. F) Eggs hatch into first stage juveniles (1J) that successively mature into second-stage (2J), 3J and 4J juveniles. G) The juveniles mature into second generation (2G) adults, mate and lay eggs. Depending on food supply cycle is repeated or (H) 2J molt into pre-infective juveniles (PJ), that mature into IJ and exit the depleted cadaver.

Nanotechnology:

Since the start of modern medicine in the 1700s, a number of so called “incurable diseases” and plagues have been treated and in many cases completely eradicated, e.g. small pox (67, 68). For decades, the focus has been on the development of drugs to cure medically important and life-threatening infections, but with the rise in multidrug resistance, it has become clear

that alternative drugs and novel delivery systems are required to reach target sites (33). Oral and intravenous administration of drugs are still the norm, but with the advances in material sciences and nanotechnology, this may soon change (69). Some of the latest techniques include transdermal, transmucosal, ocular and pulmonary administration of drugs with nanoparticle delivery systems constructed from polymers, metals, carbon-based and silicon-based materials (69). Drugs delivered to target sites in an encapsulated form are then released from the nanoparticles by diffusion, change in osmotic pressure or disintegration of the particles (70). Erodible drug delivery devices are preferred since they eliminate the need for device retrieval.

History

Since the first experiments on nanoparticles in the 1960s, nanotechnology has revolutionized modern medicine (37, 71). In 1964, Alec Bangham and his colleagues published the first article on lipid vesicles, now known as liposomes (37, 72–74). This discovery opened the gateway for other research groups in the nanotechnology drug-delivery field. The major breakthroughs in nanoparticle-based drug delivery are listed in Fig. 3. Robert Langer and Judah Folkman developed the first polymer drug-delivery system in 1976 (75), when they produced macromolecules from ethylene-vinyl acetate, hydron and polyvinyl alcohol (75). Today, many research groups still use polyvinyl alcohol as a drug carrier (76).

Dendrimers, a unique class of polymers, were first described in 1978 by Fritz Vogtle. A dendrimer is a nano-sized, monodispersed, radially symmetric molecule consisting of tree-like branches (77). With the advances in materials science, more advanced drug delivery systems for targeted delivery have been developed. In 1980, two independent research groups led by Shinitzky and Weinstein, constructed the first liposome used in targeted delivery (37). The Shinitzky group used the pH difference between healthy and cancerous cells to elicit a targeted release of the encapsulated drugs (78), whereas the Weinstein group coupled site-directed monoclonal antibodies to the outer layer of the liposome (79). Despite the advances made in this field, the short half-life of liposomes made this method of drug delivery less optimal. This led to the production of PEGylated liposomes, later relabelled as “stealth liposomes”. PEGylated liposomes are produced by coupling polyethylene glycol (PEG) to the outer layer

of the liposome (80). PEGylation increased the half-life of liposomes and polymeric nanoparticles. Building onto this, a liposome conjugated with the anticancer drug doxorubicin was developed and named Doxil® (81). This was the first FDA-approved nanoparticle and paved the way for the approval of many other drug nanocarriers. Since then, more than 50 drug nanocarriers developed for various infections, cancer and degenerative eye diseases, have been approved by the FDA (82).

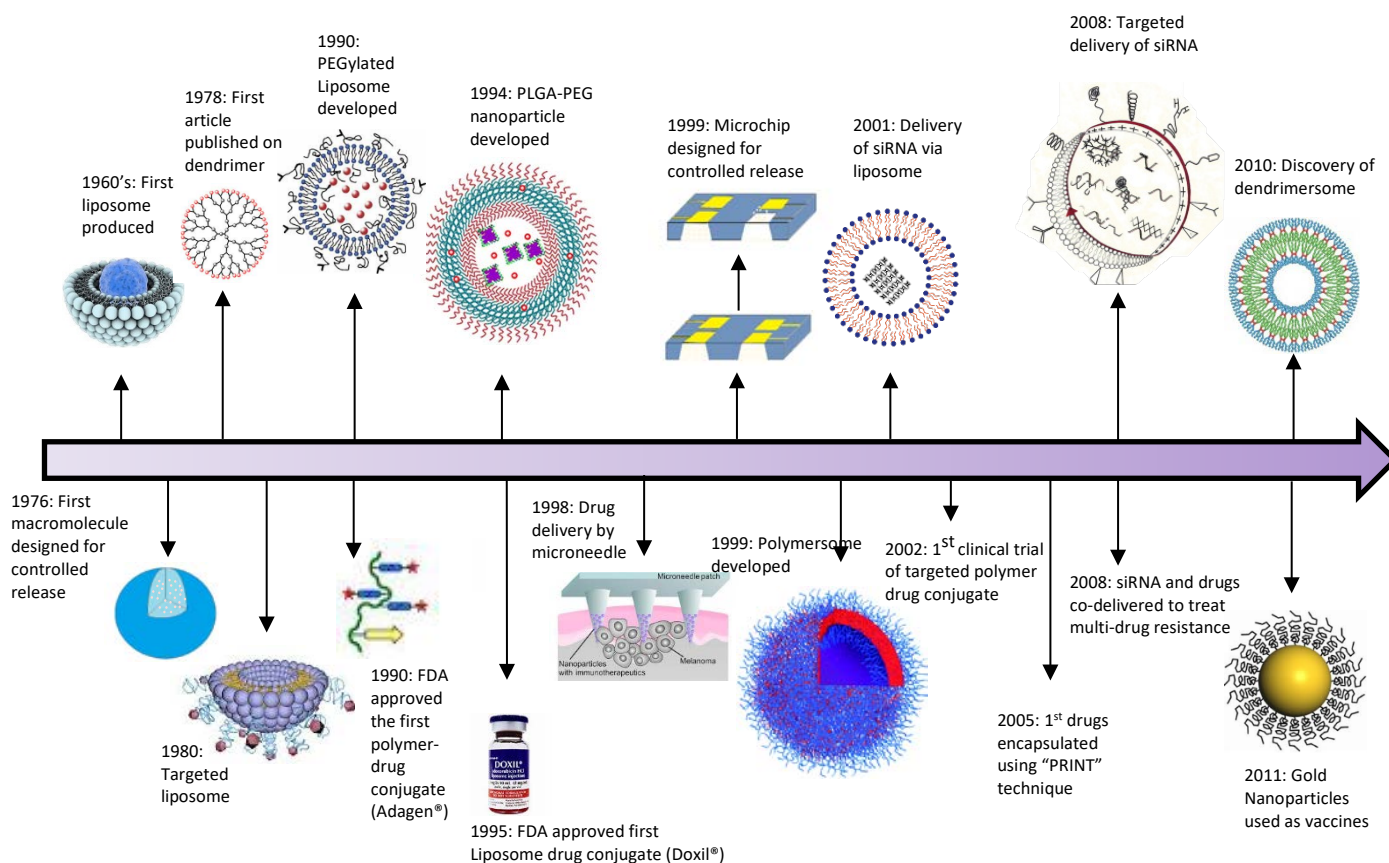


Fig. 3: Major breakthroughs in nanoparticle-based drug delivery.

With all the advances made in drug-delivery systems, the only shortcoming was the route of administration. In 1998, Henry and co-workers (83, 84) designed a microneedle consisting of a patch of needles with a radius curvature smaller than 1 μm and 150 μm in length. This device allowed pain-free administration of drugs through all three layers of the human skin (83, 84). In 1999, Discher and co-workers (85) reported a new group of polymer vesicle with enhanced controlled drug-delivery, which they referred to as a polymersome. Amphiphilic block copolymers were used to construct the vesicles (85, 86).

One of the major drawbacks of nanotechnology-based drug delivery is the inability to mass produce uniform particles. In 2005, a new method referred to as Particle Replication in Non-wetting Templates (PRINT) was introduced (87). PRINT is based on soft lithography and produces nanoparticles with a narrow size and shape distribution. Five years later, the dendrimersomes were developed. These nano-vesicles are prepared using amphiphilic Janus dendrimers (88). Today, nanomedicine has an impact on all forms of medicine and even plays a role in vaccine development. Research groups from across the world are exploring the idea of using gold nanoparticles in the delivery of vaccines. The particles are small enough to cross the blood-brain barrier, which allows, site-directed delivery of vaccines to brain tissue (89–91).

Types of nanoparticles

Nanoparticles are defined as small particles that act as a unit in terms of properties and transport, each with a diameter less than 1000 nm and prepared from a variety of materials (92, 93). Depending on the shape, size and chemical properties, nanoparticles are classified as fullerenes, solid lipid nanoparticles, liposomes, nanoshells, quantum dots, metallic and inorganic nanoparticles, dendrimers, dendrimersomes, micelles, nanocrystals or polymer nanoparticles (94, 95).

Fullerenes

Fullerenes are hollow spheres, ellipsoids or tubes constructed from carbon atoms (maximum 300) and are similar in structure to graphite (93). Fullerenes are produced by vaporising graphite and collecting the by-product (96). Carbon atoms are arranged to form pentagonal, hexagonal or heptagonal rings. Two separate studies have shown that C₆₀ fullerenes (which are the most abundant form) have pharmaceutically important properties (95). Friedman and co-workers (97) demonstrated the antiviral activity of C₆₀ fullerenes by showing its interaction with the active site of the human immunodeficiency virus 1 protease (HIVP). In another study, Yamakoshi and co-workers (32) reported on the antimicrobial activity of C₆₀ fullerenes and attributed this to the formation of reactive oxygen species.

Solid Lipid Nanoparticles

The first solid lipid nanoparticles (SLPs) were reported in the early 1990s. These particles are 50 to 1000nm in size and consist of a solid lipid core and a surfactant as emulsifier (93, 95, 98). The small size, large surface-to-area ratio, stability and vast range of lipids to choose from (fatty acids, triglycerides, steroids and waxes) made the construction of particles with unique properties possible (93). Soybean lecithin, phosphatidylcholine, poloxamer 188, sodium cholate and sodium glycocholate are just some of the surfactants that are used to produce SLPs (93, 98). A variety of different methods are used for the production of SLPs, namely spray-drying, ultra-sonication, microemulsion and high-pressure homogenization (93, 98, 99). SLPs have gained significant popularity as a colloidal drug-delivery system. This is due to the use of physiological lipids, high entrapment efficiency, no need for organic solvents during production and improved bioavailability compared to other nanoparticles. Furthermore, SLP particles are used to encapsulate hydrophobic and hydrophilic drugs and are easy to mass produce and sterilize (38, 93, 98). Despite these positive attributes, SLPs gelatinize under certain conditions, changing the polymorphic characteristics of the SLP (95, 99).

Liposomes

The first liposomal-like structure was reported by Alec Bangham in 1965 (37, 72, 73). Liposomes are defined as small spherical vesicles, ranging from 15 nm to several μm in size and with an aqueous core surrounded by phospholipids. The phospholipids form a lipid bilayer due to their hydrophobic and hydrophilic properties (38, 93, 95). Liposomes are classified as either unilamellar, consisting of a single phospholipid bilayer, or multilamellar (98). The inherent properties of liposomes render them ideal carriers of hydrophobic and hydrophilic drugs. Liposomes fuse with cell membranes and release drugs intracellularly. Furthermore, a range of 'stealth' molecules are easily added to the surface of liposomes (38, 93). The only major disadvantage of liposomes is their relatively short shelf life, making long-term storage impossible (95). Techniques used to produce liposomes include thin-film hydration, reverse phase evaporation, solvent injection and lastly detergent dialysis (98). Doxil[®] was the first liposome based drug approved by the FDA for medical use (81).

Nanoshells

Nanoshells are spherical dielectric cores surrounded by a thin layer of metal, usually between 1 and 20 nm in diameter (93, 100, 101). The dielectric core normally consists of silica or polystyrene, while the shell is often gold (93, 100, 101). Nanoshells are highly functional and show improved function compared to single composite particles of the same size (93). The properties of nanoshells can be modified as desired by changing the constituent material and core-to-shell ratio. Although nanoshells can be used for drug delivery their; optical, chemical and thermal properties render them ideal in bioimaging and biosensing applications (101). By altering the shell thickness, the optical properties are altered, as observed with a shift in wavelength from visible to invisible (UV) on the electromagnetic spectrum. Encapsulating the nanoshells in silica forms a multishell with three layers (silica-gold-silica), which improves the thermal stability of the nanoshells. The surface chemical properties of some nanoshells are altered by coating the gold outer shell with a material of desired properties (101).

In a study done by Mirkin *et al.* (102), DNA was immobilised on gold nanoshells and used to detect the presence of complementary DNA strands in a biological environment. Antibodies specific for a disease or tumour can also be immobilised on gold or metal nanoshells. Once the nanoshells are inserted into the body, they bind with the specific diseased cells and are detected with lasers (93, 101).

Nanoshell synthesis is a complicated two-step process. Various techniques have been developed to synthesise the core structure of nanoshells, e.g. precipitation, micro emulsion, sol-gel condensation, grafted polymerization and layer-by-layer absorption (101). To ensure a homogeneous coating (shell), the surface of the core is first coated with a primer (coupling agent). That enhances the coupling of the shell material with the core material (103). Although many advances have been made, nanoshell technology still has a long way to go in regard to synthesis.

Quantum dots

Quantum dots are defined as a group of heterogeneous nanoparticles consisting of a semiconductor nanocrystal, or core, containing an interface between different semiconductor materials (93). Their size ranges between 2 and 100 nm depending on the thickness of the coating (71). Originally quantum dots consisted of Cadmium-Selenide (CdSe), but an alternative material had to be used because of the cytotoxicity of Cd. This led to the development of quantum dots consisting of a Copper-Indium-Sulphide (CuInS₂) core (104). Due to the small size of quantum dots, they possess unique photostable properties rendering them perfect for bioimaging (82). However, before quantum dots can be used in a clinical setup, more research on cytotoxicity needs to be done (71).

Inorganic nanoparticles

Metallic nanoparticles consist of a metal that exhibits antibacterial activity. Silver has been known for its antibacterial properties since ancient times and have been used by the medical industry for centuries (38). Metal nanoparticles have various shapes and sizes ranging between 10 and 100 nm. These nanoparticles are produced by physical methods, which include electrochemical reduction, solution irradiation, spark discharging and cryochemical synthesis (95). Traditionally, metal oxide nanoparticles, such as Zinc Oxide (ZnO), were used as drug carriers, but it was recently discovered that these nanoparticles are also active against pathogenic *Escherichia coli* (105). Titanium Oxide (TiO₂) particles are other metal oxide nanoparticles well-known for their antibacterial activity (38). Superparamagnetic iron oxide particles (SPIONS) are defined as particles (5 – 100 nm in diameter) attracted to a magnetic field, but which do not retain residual magnetism once the magnetic field is removed. The unique paramagnetic property of SPIONS renders them ideal to be used in MRI imaging and controlled drug release. To date, eight different inorganic nanoparticles have been approved by the FDA for clinical use. Five of these are used as an iron supplement, two as an imaging agent and one to treat glioblastoma (Table 2) (82).

Dendrimers and dendrimersomes

Dendrimers are a unique group of highly branched, unimolecular and monodispersed polymer nanoparticles. Dendrimers are between 1 and 20 nm in diameter and are known for their well-defined branches (69, 71, 93). Dendrimers consist of three distinct structures, namely the core, containing the drug, layers of polymer branches and functional end groups on the outer layers of the branches (77, 93). Convergent and divergent step growth polymerization are used to synthesize the branches, while the drug molecules can be incorporated either via encapsulation or complexation (69, 77). Hydrophobic and hydrophilic drugs can be incorporated in dendrimers rendering them ideal drug delivery vehicles. Furthermore, the large surface area-to-size ratio ensures optimal release of the incorporated drugs (38). The first dendrimer consisted of polyamidoamine (PAMAM), but the toxicity of the polymer made it unsuitable for use in a clinical setting. However, by modifying the terminal ends of PAMAM, the cytotoxicity has been greatly reduced (38). A new group of dendrimers, dendrimersomes, are nanosized vesicles consisting out of Janus dendrimers (88). Janus dendrimers are synthetic amphiphilic dendrimers with two dendrimeric wedges terminated by different functional groups at their terminals (106). This allows the dendrimersome to interact with multiple cellular targets. The defined structure, monodispersed size, stability and functionalization of terminal ends makes dendrimers and dendrimersomes ideal for targeted drug delivery (69).

Micelles

Micelles are aggregates of surfactant molecules/amphiphilic block copolymers that self-assemble in aqueous solutions to form a hydrophobic core. Although they are similar in structure to liposomes, they are more stable and thus better suited for controlled drug release (82, 107). By balancing the hydrophobic and hydrophilic ends of the copolymers in the amphiphile, the size and morphology of micelles can easily be controlled (82) Micelles range from 1 to 50 nm in size, depending on the type of block copolymer used. Due to the hydrophobic core of micelles, they can be used to entrap poorly water-soluble drugs, while the amphiphilic exterior promotes dissolution of the drug (108). Micelles are produced using one of two methods depending on the hydrophobicity of the copolymer. The direct dissolution method is used for water soluble polymers, whilst oil-in-water emulsification is used for a

water insoluble polymer (107). The outer surface of a micelle is formed by constructing micelles from a variety of end-functionalized block copolymers (109). Currently, a number of micelles are being subjected to clinical trials (82).

Nanocrystals

Nanocrystals are defined as nanoparticles with a crystalline structure, solely composed of the active drug (82, 110). The increased surface area-to-size ratio compared to the free drug increases the dissolution velocity and saturation stability of pharmaceutical drugs (82). A big disadvantage of nanocrystals is that they need to be stabilized with additives (110). One of three methods can be used to synthesise nanocrystals, namely precipitation, milling and homogenization. The precipitation method was developed by Sucker for the preparation of hydrosols (111). In this method, the drug is dissolved in a solvent, the solution is then added to a nonsolvent, leading to precipitation of nanocrystals. Disadvantages of using this method are that a stabilizer needs to be added and residues of the organic solvent and surfactant are detected in the sample (110).

Milling is a more robust method and uses ball mills to reduce the size of nanocrystals. The ball mills are typically made from stainless steel, glass, ceramics or highly crosslinked polystyrene. Although the milling process is slow and only small batches of nanocrystals can be synthesized, the FDA has approved four nanocrystals for clinical use.

The homogenization methods for nanocrystal synthesis use high pressure and shear force to reduce the size of the particles. Various different technologies are used to synthesis nanocrystals via homogenization. Microfluidizer technology, developed by Bruno and McIlwrick in 1999, generates small particles via frontal collision of two fluid streams under high pressure. Piston gap homogenization in water (Dissocubes[®] technology), developed by Müller and co-workers, forces the drug through a homogenization gap with pressures up to 4000 bar (112). This increases the dynamic pressure of the solution, which is compensated for by reducing the static pressure below the vapor pressure of the solution, resulting in the formation of gas bubbles. Once the solution has passed through the gap, the bubble collapses due to the lowering in pressure. Shockwaves are generated by the formation and implosion of

the bubbles. The shear forces generated, turbulent flow and the power of the shockwaves reduce the size of the drug particles (113).

The last technology, Nanopure® technology, is also based on the piston gap homogenizer and was developed by Pharma Sol GmbH. Instead of using water as with Dissocubes® technology, Nanopure® technology uses a dispersion medium with a low vapor pressure to generate nanocrystals (112). Although homogenization is universally applicable and a rapid method, it is energy intensive and experience is needed to operate the machinery (110).

Polymer nanoparticles

Polymer nanoparticles are the most widely used and studied and are defined as particles with diameter less than 1000 nm consisting of either natural or synthetic polymers (92). A wide variety of polymers can be used for the synthesis of polymeric nanoparticles and the polymer type has an enormous influence on the structure, possible applications and physio-chemical properties of the particles. These polymers can be divided into two groups, natural and synthetic polymers. Although natural polymers are not as widely used as synthetic polymers, they are still important to keep in mind (92).

Polymer nanoparticles are constructed of various polymeric materials, including two natural polymers, chitosan and gelatin, or 5 groups of synthetic polymers, poly(esters), poly(ortho esters), poly(anhydrides), poly(amides) and polyphosphazenes (Refer to Table 1 for the structures of the synthetic polymers). Polymers used in controlled drug delivery vehicles have to be biodegradable and form small, water-labile, nontoxic products during degradation. The erosion rate must be easily adjustable by manipulating the backbone of the polymer, and directly linked to the release rate (114).

Natural polymers

Chitosan

Chitosan is a natural carbohydrate derived from chitin, the main component of the exoskeleton in crustaceans, and is isolated by decolourization of the shell with potassium permanganate followed by boiling in NaOH to N-deacetylate the chitin (115–117). Chitosan was first discovered by Rouget in 1859, but formally named by Hoppe-Seyler in 1894 (117, 118). Due to the low production costs, FDA approval, biodegradability and biocompatibility, the use of chitosan in the medical and food industries has increased immensely over the last two decades (119). Chitosan nanoparticles can be synthesised by ionotropic gelation, microemulsion, emulsification solvent diffusion, polyelectrolyte complex (PEC), emulsification-cross linking, complex coacervation, solvent evaporation or coprecipitation (116, 117).

Ionotropic gelation is based on the electrostatic interactions between the amine groups of chitosan and negatively charged polyanion groups. In short, chitosan is dissolved in acetic acid, followed by the addition of a polyanion or an anionic polymer (120, 121). Microemulsion is a more complex method. Firstly, a surfactant is dissolved in hexane, followed by the addition of chitosan dissolved in acetic acid and glutaraldehyde. The solution is stirred overnight at room temperature (25°C). After 24 h hexane is allowed to evaporate, and excess surfactant is removed by precipitation. Nanoparticles are collected via centrifugation, dialysis and lyophilization (122, 123).

The emulsification solvent diffusion method is only suitable for hydrophobic drugs. For this method, an organic phase is injected into chitosan dissolved in acetic acid containing a stabilizer. The polymer formation is obtained by diluting the organic phase with water under mechanical stirring and high-pressure homogenization, leading to particle precipitation (122, 124). Synthesis via the PEC method is also based on electrostatic interactions between anions and the cationic polymer (chitosan). This method is preferred because it is simple, lacks any harsh conditions and the formation of the nanoparticles is spontaneous (118, 125). The emulsification-cross linking method is used to encapsulate water-soluble drugs. Nanoparticles

are produced by adding dioctyl sodium sulfosuccinate (AOT) to a sodium Alg (a biodegradable co-polymer of mannuronic acid and guluronic acid) solution, followed by vortexing the solution and emulsification over an ice bath. Polyvinyl alcohol (PVA) is then added and emulsified by sonication, followed by the addition of an aqueous calcium chloride solution. Methylene chloride is allowed to evaporate and nanoparticles are collected with ultracentrifugation, washing and lyophilization (126, 127).

The complex coacervation method is used for the production of chitosan-DNA nanoparticles. Chitosan-DNA nanoparticles are produced by vortexing a heated solution of chitosan (dissolved in acetic acid) and plasmid DNA (pDNA, dissolved in sodium sulphate/dextran sulphate) (128, 129). The solvent-evaporation method is also used to produce chitosan-DNA nanoparticles. Briefly, chitosan is dissolved in ethanol and added to a poly-L-lisin solution (dissolved in ethanol) and mixed, followed by the addition of pDNA-Tris buffer. Ethanol is allowed to evaporate under reduced pressure and nanoparticles are collected (128). Chitosan-Alg nanoparticles have also been produced by the solvent evaporation method to encapsulate antibiotics. Coprecipitation is used to produce lactic acid-grafted chitosan nanoparticles. This method produces nanoparticles with a high degree of uniformity and has a high encapsulation efficiency. To produce lactic acid-grafted chitosan nanoparticles, chitosan dissolved in lactic acid is dehydrated using ammonium hydroxide (130).

Chitosan nanoparticles has numerous applications in the medical industry, including intravenous delivery of anticancer drugs, oral delivery of numerous drugs, delivery of DNA (119), vaccines (131), ocular drugs and drugs destined for the brain and lastly to carry and protect insulin (117).

Gelatin

Gelatin, well known for its use in the food industry, is obtained by partial alkaline or acid hydrolysis of animal collagen and is defined as a polyampholyte with cationic, anionic and hydrophilic groups (132, 133). Gelatin is a promising drug carrier due to its biocompatibility (non-toxicity), biodegradability, abundance and low production cost. Commercial gelatin is available in two forms (type A and type B) depending on the hydrolysis method used. Type

A is produced when collagen is treated with acid, while type B gelatin is produced when collagen is treated with alkali (134). In the past, gelatin has been used in the medical industry as a plasma extender and stabilizer (133). As in the case for chitosan nanoparticles, numerous methods exist for the synthesis of gelatin nanoparticles, namely two-step desolvation, simple coacervation, solvent evaporation, microemulsion, nanoprecipitation and self-assembly through chemical modifications (132, 135). Many of the synthesis techniques used for gelatin nanoparticles are similar to those used to synthesis chitosan nanoparticles. Thus, only the methods unique to gelatin nanoparticle production, namely two-step desolvation, nanoprecipitation and self-assembly through chemical modifications, will be further discussed.

Two-step desolvation, also referred to simply as desolvation, is a thermodynamic driven process (136). The nanoparticles are formed when a desolvation agent is added to a gelatin solution. The desolvation agent dehydrates the gelatine, inducing a conformational change. This step is repeated to ensure the formation of uniform nanoparticles. This is followed by a cross-linking step to harden the particles (135). In 2010, Ofokansi and co-workers developed a simpler one step desolvation method, in which it is no longer necessary to repeat the initial desolvation step (137). Although desolvation is a commonly used method, two disadvantages are associated with the method namely, the use of organic solvents and toxic crosslinkers (135). Nanoprecipitation, also known as solvent displacement, is a well-known technique in the polymeric nanoparticles field and is used to produce both natural and synthetic polymer nanoparticles (132, 138). Nanoprecipitation is a favourable method for the production of gelatin nanoparticles since it produces nanoparticles of a uniform size, is simple and easy to use and not energy intensive. The nanoparticles are produced by adding gelatin (dissolved in water) and the drug to ethanol containing poloxamer as a stabiliser, followed by the addition of glutaraldehyde as a crosslinking agent (132, 135). The final method, self-assembly through chemical modification, was first proposed by Kim and Byun in 1999. The authors proposed PEGylating gelatin, by coupling the carboxyl groups of deoxycholic acid (DOCA) and carboxylated monomethoxy polyethylene glycol (MPEG) to the amine groups of gelatin to form gelatin micelle like nanospheres. The self-assembled nanoparticles form when the gelatin/DOCA/MPEG solution is sonicated (132, 135, 139).

Synthetic polymer

Poly(ester)

Poly(ester) polymers are a group of biodegradable polymers produced when the ring structures of lactones and lactides are broken by either cationic or metalorganic catalysed polymerization, also known as ring-opening polymerization (ROP) (140, 141). The most extensively studied poly(ester) polymers are polylactide, polyglycolide, poly(lactide acid-co-glycolide acid), poly(ϵ -caprolactone) and lastly poly(ethylene glycol) (141). See table 2 for structures. Most poly(esters), especially polyglycolide and polylactide, were originally developed to be used as dissolvable sutures, but researchers later discovered that these polymers can be used to develop drug-delivery vehicle (142).

The first biodegradable poly(ester) synthesised was polyglycolide (142, 143). Polyglycolide, also referred to as poly(glycolic acid) (PGA), is not suitable for a slow-release system due to fast degradation and thus is often copolymerized with polylactide and caprolactone (144). Under biological conditions, polyglycolide undergoes bulk degradation and produces acetic acid as a by-product. The acetic acid is incorporated into biological pathways, thus making it safe to be used in biomedical products (145).

Polylactide, also referred to as poly(lactic acid) (PLA), occurs naturally as enantiomeric poly(L-lactic acid) and was first described by Carothers in 1932. Carothers produced low molecular weight PLA by heating lactic acid under vacuum and removing the condensed water. Later, high molecular weight PLA was produced by breaking the lactone ring (143). Polylactide has numerous uses in the medical industry, namely as dissolvable sutures, internal fixation devices used to support bone fractures and as drug-delivery vehicles (142, 145).

Poly(lactic acid-co-glycolic acid) (PLGA) is a copolymer of polylactide and polyglycolide. A wide variety of PLGA forms is commercially available, and they are classified according to the ratios of PLA and PGA used (146). This ratio can be used to change the physio-chemical properties of PLGA nanoparticles and a rule of thumb, the higher the concentration of PGA the faster the copolymer degrades and more hydrophilic the co-polymer (147). The success of PLGA as a drug-delivery vehicle is due to the biodegradability of this copolymer. In water, PLGA

undergoes hydrolysis of the ester bond and forms two by-products, namely glycolic acid and lactic acid. Both these monomers are incorporated into the Krebs cycle, a metabolic pathway present in all higher organisms, thus lowering the systemic toxicity of PLGA (148, 149). Both the FDA and European Medicine Agency have approved PLGA for use in drug-delivery systems in humans and has given PLGA generally regarded as safe (GRAS) status.

Poly(ϵ -caprolactone) (PCL) is a biodegradable nontoxic polymer produced by ROP of caprolactone and was first described by Van Natta and co-authors in 1934 (92, 150, 151). Once again, the hydrolysis of PCL forms a by-product, 6-hydroxycaproic acid, that is utilized in the Krebs cycle. Due to the slow degradation (even slower than PLA) and high protein permeability of PCL, it is mainly used as a delivery vehicle for vaccines. Furthermore, PCL does not create an acidic environment during degradation and can thus be used to encapsulate pH-sensitive drugs (150).

Poly(ethylene glycol) (PEG) is rarely used alone and is well-known for its use in conjunction with other polymers. The hydrophilic nature of PEG reduces aggregation and association with nontargeted organelles in the body, thus extending the circulation lifetime of PEGylated proteins and nanoparticles in biological environments. Another advantage of PEG is the ease of which functional groups can be added to the chain-end of PEG, thus making modification quick and simple (141).

Poly(ortho esters)

Poly(ortho esters) (POE) are biodegradable polymers that only release the encapsulated drug once hydrolysis of the polymer chains has started. This prevents diffusion of the drug out of the nanoparticle device. POE was first described by Choi and Heller in the late 1970s (70, 152–155). Four different POE families have been developed, POE I at the Alza corporation and the other three, POE II, POE III and POE IV, at the Stanford Research Institute, also referred to as SRI International (153).

POE I development has stopped due to its autocatalytic nature and low glass transition temperature, although it was used in the past to treat burn wounds (156), deliver naltrexone (157), a narcotic antagonist and contraceptive steroids (158). Another disadvantage of POE I

is its complex and time-consuming synthesis procedure. POE I is synthesised by the transesterification of diethoxytetrahydrofuron with diols at high temperatures and under vacuum (159). Due to the limitations and complex synthesis of POE I, and desire to develop their own POE, SRI International invested in the development of improved families of POE (155).

The first POE developed by SRI International was POE II, a unique polymer that forms dense crosslinked matrices that biodegrade to small water-soluble molecules (153). This POE is synthesised by simply dissolving the two constituents, diol and diketene acetal 3,9-diethylidene 2,4,8,10-tetraoxaspiro[5.5]undecane, in a polymer solvent and adding an acidic catalyst (155). Thus, it is clear that POE II synthesis is a lot less complicated compared to POE I synthesis, and the thermal properties of POE II can also easily be adjusted by using diols with different chain flexibilities. Furthermore, unlike POE I, POE II does not have an autocatalytic nature since neutral products are initially formed during hydrolysis (70, 154). The hydrophobic nature of POE II contributes to its stability in physiological environments, since water can't easily reach the water-labile ester links in the polymer backbone. Furthermore, release can be controlled by altering the pH of the polymer-water-interface since the majority of the polymer backbone links are acid-labile (153).

The next POE developed by SRI international was the semi-solid polymer PEO III. This polymer has a flexible backbone and is in a semi-solid state at room temperature. Due to this property, drugs are easily encapsulated into POE III nanoparticles. The major downfall of this polymer is its complex and time-consuming synthesis procedure. Furthermore, it is near to impossible to produce constant polymers with similar molecular weights. Thus, although POE III showed promise to be used as a controlled drug-delivery system, development was stopped soon after its initial discovery (153).

POE IV was developed by SRI International and first described by Ng and co-authors in 1997 (153). POE IV, a modified form of POE II, consists of three parts, a lactic or glycolic acid, a diol and a diketene acetal (160). By adding an acid moiety (lactic acid or glycolic acid) in the backbone of the polymer, Ng and co-workers could ensure hydrolysis of the polymer without lowering the pH of the polymer-water interface (153, 154). This is due to the initial hydrolysis

of the water-labile ester bond in the acid moiety that produces a polymer with a carboxylic acid end. This acidic polymer is then responsible for the acid hydrolysis of the rest of the polymer backbone (161). A major advantage of this polymer is the ability to control the release rate by adding or removing the latent acid groups present in the polymer backbone. In other words, the less latent acid groups present, the more slowly the nanoparticle will be eroded and the encapsulated drug released (154, 160).

Today, POE nanoparticles are studied extensively to be used as controlled drug-delivery devices and numerous articles have been published on the use of POE nanoparticles to control post-surgery pain (154), to treat periodontal diseases (162), to use in ocular applications (154) and to use as a delivery mechanism for DNA-based vaccines (163).

Poly(anhydrides)

Poly(anhydrides) have a long and extensive history and were first synthesised by Bucher and Slade in 1909 when they heated isophthalic acid and terephthalic acid with acetic anhydride (164). Poly(anhydrides) consist of a hydrophobic polymer backbone with anhydride linkages (table 1) and were originally developed to be used in the textile industry but were deemed unsuitable for textile applications due to hydrolytic instability (164).

The medical potential of polyanhydrides was only discovered in 1980 by Rosen and co-workers (165), who used poly[bis(p-carboxyphenoxy) methane] as a poly(anhydride) polymer due to its hydrophobicity and toxicology (165, 166). Various techniques are used for the synthesis of poly(anhydrides), including melt condensation, ROP, interfacial condensation, dehydrochlorination and dehydrative coupling, and depending on the polymer, a specific method will be used (167). For example, melt condensation is used for monomers stable at high temperatures, while ROP is used to synthesise poly(adipic anhydride) polymers. The dehydrative coupling method is used to convert dicarboxylic acid to a poly(anhydride) and the major disadvantage of this technique is the presence of the polymerization by-products in the final product (168).

Since the initial discovery of the potential to use polyanhydrides as controlled drug-delivery

systems, hundreds of poly(anhydride) structures have been described by various researchers. These polymers are grouped into one of ten different classes depending on their structure. Therapeutic agents are encapsulated either by compression-molding or microencapsulation (141). The FDA have approved two poly(anhydride) drug delivery devices, namely Gliadel® (166), used to treat brain tumours, and Septacin™ (169), used to treat osteomyelitis (Table 2).

Poly(amides)

Poly(amides) (PA) are semi-crystalline polymers, consisting of monomers linked with an amide (-CONH-) bond (170). Poly(amino acids) are poly(amides) that show the most potential to be used for colloidal drug-delivery devices (141). Poly(amino acids) (PAA) are polymers consisting of repeating units of a single natural occurring amino acid (the monomer) linked with an amide bond (171). The physical and biochemical properties of PAA are easily adjusted by adding various moieties to the side chains of the amino acids. Since PAA are enzymatically degraded by proteinases, their release rate can be adjusted by modifying the amino acid side chains. Biodegradation of PAA produces nontoxic naturally-occurring metabolites that are incorporated into its metabolic pathways. The complex synthesis procedure of building PAA is their biggest downfall (171).

Polyphosphazenes

Polymers containing phosphorus atoms are referred to as polyphosphazenes (PPH). These polymers are inorganic-organic hybrids consisting of nitrogen molecules, phosphorus molecules and an organic or organometallic side chain (R). The nitrogen and phosphorus atoms are linked with single or double bonds while the R group is bound to the phosphorus atom (Table 2; 172, 173). The first PPH was synthesised by Stokes in 1897 (174) by ROP of hexachlorocyclotriphosphazene. The resulting polymer was unstable, insoluble and susceptible to hydrolytic cleavage, degrading to phosphates, hydrochloric acid and ammonia. These characteristics rendered this polymer unsuitable for use as a controlled drug delivery compound (172, 175, 176).

The first useable PPH, poly(dichlorophosphazene) was synthesised by Allcock and Kugel in

1965 (177) and in 1966 Allcock reported on the first hydrolytically stable phosphate containing polymer with a high-molecular weight (178). This PPH, poly(organophosphazene), was synthesised by replacing the chlorine atoms of poly(dichlorophosphazene) with organic or organometallic nucleophiles. Modern PPH polymers are synthesised by living cationic polymerization, a form of chain polymerization from which chain termination and chain transfer is absent, of phosphoranimines, a method designed by Allcock and co-workers in 1999 (178). This technique allows the synthesis of polymers with a controlled molecular weight and narrow polydispersity at room temperature. A unique property of PPH is that these polymers undergo bulk and surface erosion and the erosion rate of PPH can be adjusted by using different organic or organometallic side chains (175).

During PPH degradation the following nontoxic by-products are formed, ammonia, phosphoric acid and an organic or organometallic moiety, depending on the side chain. The unique characteristic, backbone flexibility, contributes to the biomedical potential of PPH (175). PPH has been used for a variety of biomedical applications including as supporting structures for bone and soft tissue regeneration (172) and in 2000 Calceti and co-authors. reported the use of PPH microspheres for the controlled delivery of insulin (179).

Table 1: The structures of synthetic polymers commonly used for controlled drug delivery


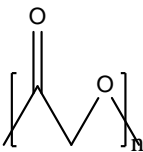
Group	Structure	Ref.
Poly(esters)	<p>PEG</p> 	(142, 152, 180, 181)
	<p>PGA</p> 	(143– 146)

Table 1 continued

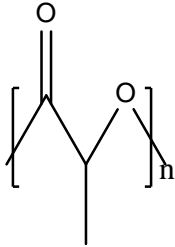
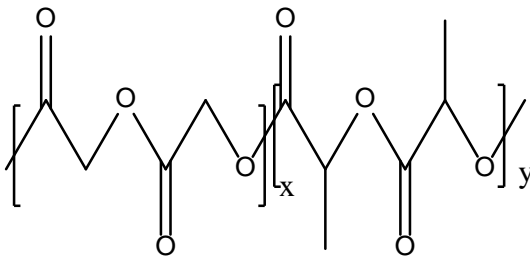

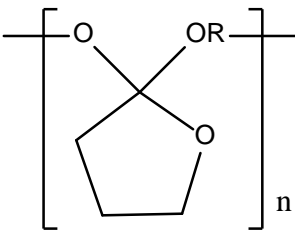
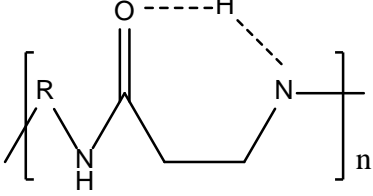
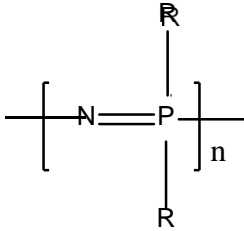
	Group	Structure	Ref.
Poly(ester)	PLA		(143, 144, 146)
	PLGA		(147– 150)
	PCL		(92, 151, 182)
Poly(ortho esters)	POE I		(153, 156– 159)

Table 1 continued

Group	Structure	Ref.
Poly(ortho esters)	POE II	(70, 153– 155)
	POE III	(153)
POE IV		153, 154, 160, 161)
Poly(anhydrides)		(141, 164– 169)

Table 1 continued

Group	Structure	Ref.
Poly(amides)		(141, 170, 171)
Polyphosphazenes		(172, 173, 175– 179)

Nanoparticle synthesis

From the section above, it is clear that nanoparticles are synthesized from various different polymers and each polymer has some advantages and disadvantages. Nanoparticles fabrication methods are divided into two groups: bottom-up methods and top-down methods (183). In bottom-up methods, nanoparticle and polymer formation is done simultaneously, while top-down methods use preformed polymers to encapsulate drugs (184, 185). Various top-down methods used to encapsulate drugs in a nanoparticle core or shell-like polymer matrix will be discussed below. Similar to the various polymers, each technique comes with a list of advantages and disadvantages. Figure 4 provides a short overview of all the techniques used to synthesise nanoparticles.

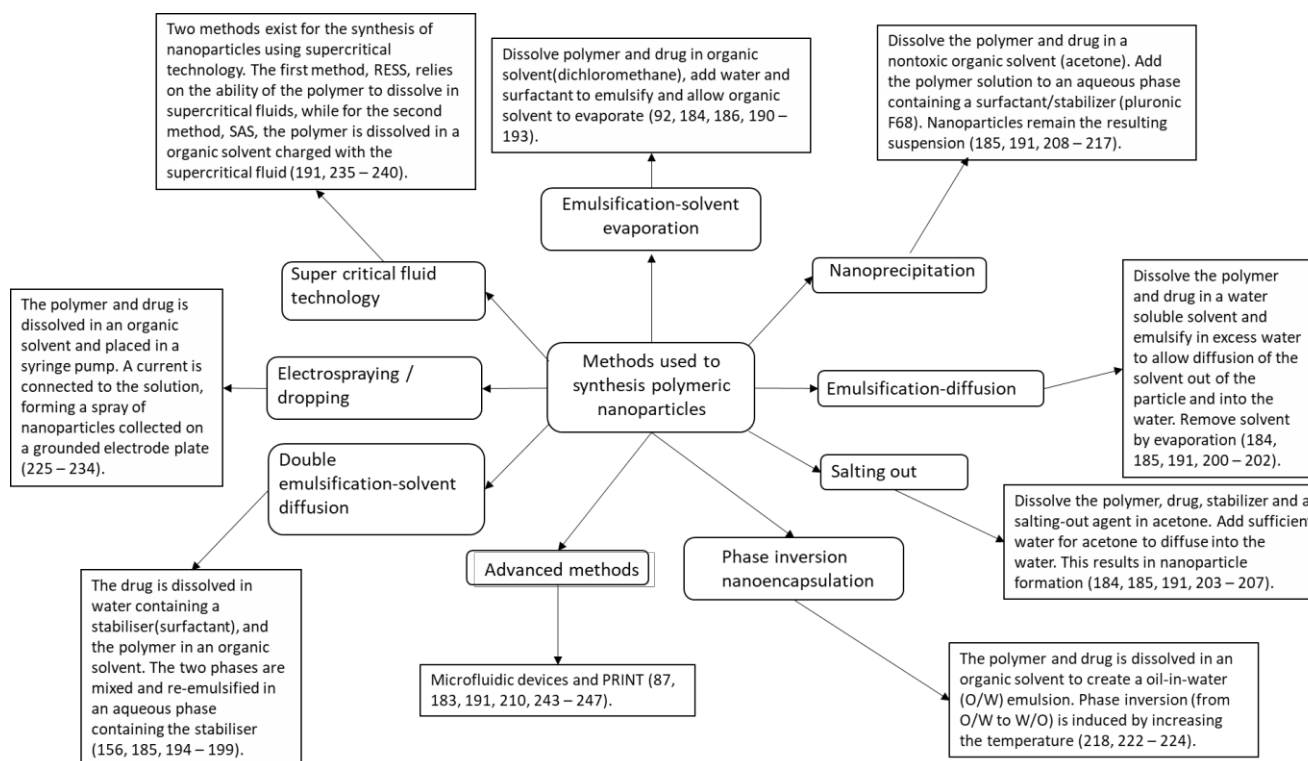


Fig. 4: General methods used for the synthesis of polymer nanoparticles, including a brief description of each method.

Emulsification-solvent evaporation technique

The most common and oldest technique used for the production of polymer nanoparticles are the emulsification-solvent evaporation technique, a two-step process (186–190). The polymer and therapeutic drug are emulsified in an aqueous solution followed by evaporation of an organic solvent (184). The evaporation of the organic solvent induces the precipitation of the polymer and drug as nanoparticles. Surfactants or stabilisers are added to prevent aggregation of the nanoparticles during formation (191) and sonication or homogenization are often used to ensure formation of nanosized particles (92).

The polymer and therapeutically active drug are dissolved in an organic solvent, dichloromethane is often used for PLGA nanoparticles. The polymer solution is, subsequently, emulsified in an aqueous solution, often water, containing a surfactant (PVA, methylcellulose and gelatin) as a stabiliser (192) and nanosized emulsions are induced by sonication. The

organic solvent is allowed to evaporate, inducing the formation of nanoparticles. Nanoparticles are collected by centrifugation and freeze-frying (186, 193). Unfortunately, this method can only be used to encapsulate hydrophobic drugs, thus a new method had to be developed, the double emulsification-solvent evaporation method.

Double emulsification-solvent evaporation

The double emulsification-solvent evaporation method, developed by Vracken and co-workers in 1970 (194), is a modified version of the emulsification-solvent evaporation method used to encapsulate hydrophilic drugs (156). The method is divided into three steps, formation of a water-in-oil (w/o) emulsion, formation of a water-in-oil-in-water (w/o/w) emulsion and lastly evaporation of the organic solvent. For the formation of the w/o emulsion, the hydrophilic drug is dissolved in an aqueous solution, often water, and the polymer dissolved separately in an organic solvent containing a surfactant. The organic solvent, containing the surfactant, and polymer are sonicated to induce formation of nanosized oil droplets. The w/o/w emulsion is produced by mixing and sonicating the aqueous and organic solutions. The mixing step is extremely important and should be controlled to prevent excessive diffusion of the drug into the external aqueous phase. Once the w/o/w emulsions have formed the organic solvent is allowed to evaporate and the nanoparticles are collected by centrifugation and freeze drying (195–198).

The disadvantages associated with this method are the size and the low encapsulation efficiency of nanoparticles. Song and co-workers (199) proposed using a second strong shear force during formation of the w/o/w emulsion to decrease the size of the nanoparticles, but it was also noticed that as the shear force increases the drug encapsulation efficiency decreases (185). Increasing the polymer concentration and using polymers with high molecular weight can improved the drug encapsulation efficiency.

Emulsification-diffusion

The emulsification-solvent-diffusion (ESD) method relies on the diffusion of an organic solvent

into an external aqueous solution for particle formation (191). The ESD method was first proposed by Niwa and co-workers in 1993 for the encapsulation of water soluble and insoluble drugs in PLGA (200, 201). The original method proposed by Niwa and co-workers used a mixture of acetone and dichloromethane or chloroform as the water-miscible solvent, but due to severe aggregation when the method was upscaled for industrial production, the method had to be modified. Murakami and co-workers proposed a modified version of the ESD method in 1999 (202).

The modified method, described below, uses two nontoxic organic solvents to dissolve the polymer and drug and form the organic phase. This eliminates the need to evaporate the organic solvent. The polymer and drug are dissolved in a combination of two water miscible organic solvents, such as methanol/acetone or ethanol/acetone, forming the organic phase. The organic phase is emulsified in the aqueous phase consisting of water and a suitable surfactant, such as nonionic PVA or anionic sodium dodecyl sulphate (SDS). Nanoparticle formation is induced by diffusion of the organic solvent into the external aqueous phase (185, 202).

Advantages associated with the modified ESD method are, absence of toxic organic solvents, low energy consumption (no need for sonication or homogenization), high encapsulation efficiency, low batch-to-batch variability and evaporation is avoided. Disadvantages associated with the modified ESD method are requires large amounts of water, timely process (takes a while for the emulsification to form) and can only be used to encapsulate hydrophobic drugs (184, 185, 202).

Salting out process

The salting-out process is a modified version of the ESD method (184). The salting-out process was first patented by Bindschaedler co-authors in 1988 (203), and later modified by Allémann co-workers to eliminate the use of surfactants (204).

The salting-out process consists of three steps, i.e. preparing the organic and aqueous phases, emulsification and precipitation. The polymer and drug are dissolved in an organic solvent, such as acetone, to create the organic phase. The aqueous phase consisting of water, a water soluble polymer and a high concentration of a salting out agent, often magnesium chloride hexahydrate or magnesium acetate tetrahydrate (185, 204, 205). Under magnetic stirring, the organic phase is emulsified in the aqueous phase, creating the o/w emulsion. The high salt concentration prevents the diffusion of the organic solvent into the aqueous phase by altering the miscibility of water. Nanoparticles are precipitated by adding an excess amount of water, subsequently diluting the salting out agent and allowing the organic solvent to diffuse into the aqueous phase, resulting in nanosized emulsions. The salting out agent and any remaining solvents are removed by cross flow filtration and centrifugation (184, 185, 204–207).

Unfortunately, although this method is free of nontoxic solvents and can be used to encapsulate sensitive hydrophobic peptides, upscaling for industrial use is not an option due to a low nanoparticle yield (191).

Nanoprecipitation

Nanoprecipitation, also known as interfacial deposition of solvent displacement, was developed by Fessi and co-workers in 1989 (208). The method is based on the interfacial deposition of a polymer due to the displacement of a semi-polar solvent (miscible in water) from a hydrophobic solution (the oil phase) (191, 209, 210). Nanoprecipitation is widely used for the development of poly(ester) controlled drug release systems, even though it is only used for the encapsulation of hydrophobic drugs (209, 211, 212).

Nanoparticles are produced by dissolving the polymer in an organic solvent, miscible with water, and adding the organic phase drop wise to the aqueous solution. The aqueous solution consists of a water miscible solvent, in which the polymer cannot dissolve, and a surfactant. As the organic solvent drops into the aqueous solvent, nanoparticles are formed by rapid solvent diffusion. The organic solvent is removed under reduced pressure (184, 185, 205, 209,

211, 212). Nanoparticles form due to the difference in surface tension of the organic/oil solvent and the aqueous solvent. Compared to the organic solvent the surface tension of the aqueous solvent is higher, causing interfacial turbulence and thermal inequalities. This leads to the formation of vortices on the surface of the solvents and the diffusion of the organic solvent out of regions with low tension. The diffusion causes the precipitation of the polymer and subsequently the formation of nanoparticles (213, 214).

Nanoprecipitation is known for producing small nanoparticles with a narrow size distribution, in the absence of toxic solvents and a high energy input. High reproducibility and low batch variation renders this method ideal for industrial production of nanoparticles encapsulating hydrophobic drugs. A modified nanoprecipitation method for encapsulating hydrophilic drugs was recently developed by Bilati and co-workers (185, 215–217). Unfortunately, evaporation of the organic solvent is a time-consuming process rendering this process less attractive for industrial production.

Phase inversion temperature

The phase inversion temperature (PIT) method is a low-energy emulsification method that is solvent-free (218, 219). The method was developed by Shinoda and Saito in 1968 (220) and is based on the phase transition of an emulsion due to a change in the curvature of a nonionic surfactant, brought on by a change in temperature (221). Phase transition is possible due to the unique curvature properties of nonionic surfactants. Nonionic surfactants have oxygen-containing hydrophilic groups covalently bound to the hydrophobic parent structure and the oxygen bonds are water soluble due to the hydrogen bonds (222). At low temperatures, nonionic surfactants have a positive curvature and are hydrophilic, while the nonionic surfactants are hydrophobic at high temperatures due to a negative curvature. At the PIT of the nonionic surfactant (curvature of zero), nanoemulsions appear and extremely small nanoparticles (50 – 120 nm) are produced due to the low interfacial tension (221). To encapsulate drugs with the PIT method an o/w emulsion is formed by dissolving the drug and nonionic surfactant in an aqueous solvent and subsequently mixing the aqueous and organic solvents. The o/w emulsions are then heated (to the PIT), resulting in inversion (w/o) of the emulsions. This is followed by rapid cooling of the solution and the formation of stable

nanoparticles (218,221, 223, 224).

Electrospraying/dropping method

Electrospraying is a one-step synthesis technique based on electrospinning, a technique used to produce nanofibers (225). Electrospraying and electrospinning are based on the ability of an electrical current to deform the surface of a liquid. The principle was first established by Lord Rayleigh in 1882 (226) and later improved on by Zeleny in 1917 (227) and Sir Taylor in 1964 (228). When comparing electrospraying to more traditional emulsification methods, a few advantages can be identified. The advantages include the synthesis of nanosized particles with a narrow size distribution, the absence of toxic organic solvents and solvent evaporation and a high encapsulation efficiency of hydrophobic and hydrophilic drugs at ambient conditions. The single syringe system can be adapted to a multiple syringe system for industrial production purposes (229–233).

An electrospraying setup consists of three components a power supply, syringe pump and a grounded collector (230). The polymer and drug are dissolved in a water miscible organic solvent and placed in the pump syringe. The high voltage power supply is connected to the tip of the syringe and the particles are collected at the grounded collector. Nanoparticles can be collected in one of two methods, on a grounded plate or in a grounded solution (231). The nanoparticles form when the polymer solution enters the electrical field, elongating the meniscus to form a Taylor cone-jet (a conical shaped meniscus). Once the cohesion forces in the drop overcome the coulomb force, created by the electrical current, the surface tension is released and nanodroplets are formed. As the droplets migrate to the grounded collector, the solvent evaporates, producing nanosized particles (225, 229–234).

The size and shape of the particles depend on various factors, including the polymer concentration, distance from the grounded collector and voltage applied (229, 231, 234). By adding a surfactant or protective colloid to the electrospraying solution, aggregation of the particles can be prevented. This is especially useful when the system is upscaled and a multi-syringe system is being used (191).

Supercritical fluid technology

The existence of supercritical fluids (SCF) was first observed by Cagniard de la Tour in 1822 (235) and the enhanced solubility of solids in SCFs was reported by Hannay and Hogarth in 1879 (236). A SCF is defined as a monophasic fluid above its critical temperature and pressure, with properties of both liquids and gaseous substances (191, 237). Supercritical fluid technology (SFT) is a term used to refer to all techniques that use SCFs (238). Due to the non-toxic, “green” (non-polluting) and economical properties of SCFs, the technology has attracted the interest of the pharmaceutical industry for the production of nanosized drug-delivery devices (239). SCFs can be used as solvents, anti-solvents and plasticisers for the synthesis, purification and modification of synthetic polymers. In contrast to conventional techniques SFT is used to “grow” the particle to the appropriate size, instead of reducing the size of a larger particle formed by emulsification (238). The most commonly used SCF is supercritical CO₂ (SC-CO₂), due to FDA approval for use in pharmaceutical processes, low toxicity, low cost, low density and mild supercritical conditions (237, 239, 240).

Various techniques have been developed for the production of nanoparticles using SFT, and these techniques can be categorized based on whether the SCF is used as a solute, solvent or anti-solvent (239). Particle formation from gas-saturated solutions (PGSS), rapid expansion of supercritical solutions (RESS), supercritical anti-solvent (SAS), gaseous anti-solvent (GAS), aerosol solvent extraction system (ASES) and depressurization of an expanded liquid organic solution (DELOS) are techniques discussed in this review.

For the PGSS compressed SC-CO₂, the SCF, acts as the solute and is dissolved in a molten polymer. The solution is allowed to expand across a nozzle, allowing the SCF to evaporate and a fine dry powder of nanoparticles to form (238, 239). In the RESS technique, the SCF acts as a solvent. The main drawback of this method is the poor solubility of the polymers and pharmaceutical compounds in SCFs. Nanoparticles are formed when the saturated SCF is depressurized in a heated nozzle connected to a low-pressure chamber. The depressurization leads to rapid nucleation of the polymer/drug substrate, forming nanoparticles (238, 239). In principle the SAS and GAS techniques are similar. These two methods are used for polymers and

drugs with a poor solubility in SCFs, thus the SCF acts as an anti-solvent. In the SAS method, the polymer and drug are dissolved in an organic solvent. The organic solvent is charged with the SCF in a precipitation vessel. The pressure of the vessel is increased, allowing the SCF to enter a liquid phase and to saturate the organic solvent, leading to precipitation (116). In the GAS process, the organic solvent is saturated with a gas. Reducing the solubility of the solvent, leading to particle precipitation (238).

The ASES technique is closely related to the SAS and GAS techniques. The polymer and drug are dissolved in an organic solvent, but in contrast to the SAS technique, the organic phase is sprayed through an atomization nozzle into compressed SC-CO₂. This is followed by the dissolution of the SCF into the liquid drops, formed by the atomization nozzle, reducing the solubility of the liquid solvent, causing supersaturation of the liquid and the formation of nanoparticles (238, 241). The main downfall of the ASES procedure is its low drug-loading efficiency compared to the other techniques (239). The DELOS method uses SFCs as co-solvents. The method is preferred over SAS since it can be used for heat sensitive drugs, uses small amounts of SC-CO₂ and is upscaled with ease (239).

The DELOS process uses compressed SCFs, miscible with the organic solvents at a given temperature and pressure, as a co-solvent. The compressed SCF causes homogenous supercooling of the solution, leading to particle precipitation (242).

Advanced methods

A central problem of the above mentioned techniques is the inability to control the homogenous mixing of solvents and the subsequent controlling of the size distribution and physiochemical properties of nanoparticles (210). This led to the development of two advanced techniques for the production of nanoparticles, namely incorporation of microfluidic devices and PRINT (183, 191).

The use of microfluidic devices for the synthesis of nanoparticles was first reported by Kawakatsu and co-authors in 2000 (243, 244). Nanoparticles formed in microfluidic devices are fabricated by a competition between the interfacial force and shear stress, imposed by

the continuous flow of the organic and aqueous solvents (191). Kawakatsu and co-authors also reported that the geometry of the microfluidic device can greatly impact the size distribution of the particles (243, 244). Nano-emulsions are solidified by ionic crosslinking, solvent evaporation, solvent diffusion, radical polymerization or by condensation (191).

The advantages of this method are the ease of controlling nanoparticles size by manipulating the solution flow, the high encapsulation efficiency (more than 90%), the portability of the device for *in situ* production and low operating costs. This process is used for industrial scale production by modifying the microfluidic device to consist out of multiple channels(191).

Particle Replication In Non-wetting Template (PRINT), was developed by Rolland and co-workers in 2005 (245). It is a roll-to-roll, high resolution, continuous technique inspired by microelectronics and lithography (87, 191). PRINT is used to produce nanoparticles with a narrow size and shape distribution by using a perfluoropolyether mold with a defined pattern (87). Perfluoropolyether is a non-wetting, gas-permeable, nontoxic, inert polymer that is resistant to swelling in the presence of most organic acids and has a low surface energy (87, 183, 246). These characteristics ensure the production of monodispersed nanosized particles that are easily removed from the mold (247). The loading and encapsulation efficiency of the PRINT technique is extremely high when compared to the other top-down techniques (>90%) (191) and is used to encapsulate hydrophobic and hydrophilic drugs on an industrial scale at low cost (247). Due to the gas permeability of perfluoropolyether, the polymer can be dissolved in volatile organic acids, removed by evaporation during the hardening step (191). PRINT has been used to create polymeric nanoparticles from various materials including PLGA, PLA, PEG and poly(silyl ether) (183).

Nanoparticles are produced by dissolving the polymer and drug in an organic solvent and pouring the solution onto the mold. A roller is used to evenly disperse the solution and due to the low surface energy, the mold prevents overflow of the polymer solution to non-cavity areas. Individual nanoparticles are subsequently formed. Once the particles have cured in the mold and the organic solvent has evaporated, the particles are removed from the mold and collected with film-based techniques (87, 246, 247)

Current applications of nanoparticles

The majority of controlled drug delivery devices (nanoparticles) approved by the FDA for medical use are cancer-related (Table 2), which is due to the high toxicity of chemotherapy agents. Thus it is only natural that the first nanoparticle approved by the FDA was a chemotherapeutic agent, liposome encapsulated doxorubicin, Doxil[®] (approved 1995), (81). Although Adagen[®] (approved 1990) is classified as a nanoparticle, in truth it is only a PEGylated form of the adenosine deaminase enzyme to improve the circulation of the enzyme (248). The approval of Doxil[®] opened the door for numerous other nanoparticle formulations to be developed for the medical industry.

Doxil[®] approval was followed by the approval of Abelcet[®] in 1995, the first encapsulated antimicrobial agent (249). Abelcet[®] proved that nanoparticles can be used to reduce the toxicity of antimicrobials, and can be used to circumvent antimicrobial resistance. This led to a boom in the nanomedicine industry, and at least 45 nanoparticle formulations have been approved for various illnesses in the last 20 decades. In 1996, the first magnetic nanoparticle used as a liver-specific imaging agent, Feridex[®] (Endorem[®]), was approved by the FDA (250–252). In 2001 the first nanoparticle formulation, PegIntron[®], for the treatment of a viral disease, hepatitis C, was approved by the FDA (253), followed by the approval of Pegasys[®]. Pegasys[®] is a PEGylated form of interferon alpha 2a, for treating hepatitis B and hepatitis C infections (254). The first nanocrystal approved by the FDA was Rapamune[®], an immunosuppressant to prevent organ rejection (255). Megace EC was the first nanoparticle approved, for the treatment of mental disorders (255) and was followed by the approval of Ritalin LA[®] (256) and Focalin[®] (257). A number of nanoparticle formulations used as bone substitutes have been approved by the FDA, including Vitoss[®] (258), Ostim[®] (259), OsSatura[®] (260, 261), NanOss (262) and EquivanBone (263, 264).

It is thus clear that nanotechnology have made a great impact on the pharmaceutical industry in the last 20 decades and has become a big industry with a net worth of \$26 billion in 2014 (265). It is believed that as material science grows, the nanotechnology industry will grow even more and it is expected to have a net worth of \$64.2 billion by 2019.

Table 2: A list of all the nanoparticle formulations that have been approved by the FDA up to 2016

Type of Particle	Name	Production material	Treatments	Year approved	Ref.	
Synthetic Polymer Nanoparticle	Adagen®/ pegademase bovine (Sigma-Tau Pharmaceuticals)	PEGylated adenosine deaminase enzyme	Severe combines immunodeficiency disease (SCID)	1990	(266)	
	Septacin™	Gentamicin encapsulated in polyanhydride	Osetomyelitis	2002	(169)	
	Cimzia® / Certolizumab pegol (UCB)	PEGylated antibody fragments		Crohn's disease	2008	(231, 232)
				Rheumatoid arthritis	2009	
				Psoriatic arthritis	2013	
				Ankylosing Spondylitis	2013	
	Copaxone®/ Glatopa (Teva)	Copolymer of L-Glutamate, L- alanine, L-lysine and L-tyrosine	Multiple Sclerosis	1996	(268)	
	Eligard® (Tolmar)	Leuprolide acetate coupled to poly(DL- Lactide-co- glycolide)	Prostate cancer	2002	(269, 270)	
	Macugen®/ Pegaptanib (Bausch & Lomb)	PEGylated anti- vascular	Macular degeneration, neovascular age- related	2004	(271)	

Table 2 continued

Type of Particle	Name	Production material	Treatments	Year approved	Ref.
Synthetic Polymer Nanoparticle	Mircera [®] /Methoxy polyethylene glycol-epoetin beta (Hoffman-La Roche)	Chemically synthesized ESA	Anaemia associated with chronic kidney disease	2007	(272)
	Neulasta [®] / pegfilgrastim(Amgen)	PEGylated GCSF protein	Neutropenia, Chemotherapy induced	2002	(273, 274)
	Pegasys [®] (genentech)	PEGylated IFN alpha-2a protein	Hepatitis B, Hepatitis C	2002	(254)
	PegIntron [®] (Merck)	PEGylated IFN alpha-2b protein	Hepatitis C	2001	(253)
	Renagel [®] [sevelamer hydrochloride]/ Renagel [®] [sevelamer carbonate] (Sanofi)	Poly (allylamine hydrochloride)	Chronic kidney disease	2000	(275)
	Somavert [®] / Pegvisomant (Pfizer)	PEGylated HGH receptor antagonist	Acromegaly	2003	(276)
	Oncaspar [®] / pegaspargase (Enzon Pharmaceuticals)	Polymer-protein conjugate (PEGylated L-asparaginase)	Acute lymphoblastic leukaemia	1994	(277)
	Krystexxa [®] / pegloticase (Horizon)	Polymer-protein conjugate (PEGylated porcine-like uricase)	Chronic gout	2010	(278)

Table 2 continued

Type of Particle	Name	Production material	Treatments	Year Approved	Ref.
Synthetic Polymer Nanoparticle	Plegridy® (Biogen)	Polymer-protein conjugate (PEGylated IFN beta-1a)	Multiple Sclerosis	2014	(279)
	Adynovate (Baxalta)	Polymer-protein conjugate (PEGylated factor VIII)	Haemophilia	2015	(280)
	Gliadel® (MGI Pharma)	Carmustine encapsulated in polyanhydride	Recurrent glioma	1996	(281)
Liposome Nanoparticle	DaunoXome® (Galen)	Liposome Daunorubicin	Karposi's Sarcoma	1996	(282–284)
	DepoCyt® (Sigma-TAU)	Liposomal Cytarabine	Lymphomatous meningitis	1996	(284, 285)
	Marqibo® (Onco TCS)	Liposomal Vincristine	Acute Lymphoblastic Leukemia	2012	(286, 287)
	Onivyde® (Merrimack)	Liposomal Irinotecan	Pancreatic cancer	2015	(288)
	AmBisome® (Gilead Sciences)	Liposomal Amphotericin B	Fungal/Protozoal infection	1997	(284, 289)
	Visudyne® (Bausch and Lomb)	Liposomal Verteporfin	Macular degeneration, myopia, ocular histoplasmosis	2000	(284, 290)

Table 2 continued

Type of Particle	Name	Production material	Treatments	Year Approved	Ref.
Liposome Nanoparticle	DepoDur® (Pacira pharmaceuticals)	Liposomal Morphine Sulphate	Analgesia (Post-operative)	2004	(291)
	Doxil®/Caelyx™ (Janssen)	Liposomal doxorubicin	Karposi's sarcoma	1995	(81,
			Ovarian cancer	2005	284,
			multiple myeloma	2008	292)
	Abelcet® (Sigma-Tau)	Liposomal Amphotericine B lipid complex	Fungal infections	1995	(249)
Curosurf®/Poractant alpha (Chiesei farmaceutici)	Liposome-proteins SP-B and SP-C	Pulmonary surfactant for respiratory Distress syndrome	1999	(293)	
Micellar Nanoparticl	Estrasorb™ (Novavax)	Micellar Estradiol	Menopausal therapy	2003	(294, 295)
Protein nanoparticles	Abraxane®/ABI-007 (Celgene)	Albumin-bound paclitaxel nanoparticles	Breast cancer	2005	(232,
			NSCLC	2012	296,
			Pancreatic cancer	2013	297)
Ontak® (Eisai Inc)	Engineered protein combining IL-2 and diphtheria toxin	Cutaneous T-Cell Lymphoma	1999	(296)	

Table 2 continued

Type of Particle	Name	Production material	Treatments	Year Approved	Ref.
Nanocrystals	Emend® (Merck)	Aprepitant	Antiemetic	2003	(296)
	Tricor® (Lupin Atlantis)	Fenofibrate	Hyperlipidermia	2004	(298, 299)
	Rapamune® (Wyeth pharmaceuticals)	Sirolimus	Immuno- suppressant	2000	(255)
	Megace ES® (Par pharmaceuticals)	Megestrol acetate	Anti-anorexic/ weight gain	2001	(255)
	Avinza® (Ligand Pharmaceuticals)	Morphine sulphate	Severe pain	2002 (2015)	(300)
	Focalin XR® (Novartis)	Dexamethyl- phenidate HCL	Psychostimulant (ADHD treatment)	2005	(257)
	Ritalin LA® (Novartis)	Methyphenidate HCL	Psychostimulant (ADHD treatment)	2002	(256)
	Zanaflex® (Acorda)	Tizanidine	Muscle relaxant	2002	(301)
	Vitoss® (Stryker)	Calcium phosphate	Bone substitute	2000	(258)
	Ostim® (Heraeus Kulzer)	Hydroxyapatite	Bone substitute	2004	(259)
	OsSatura® (IsoTis Orthobiologics)	Hydroxyapatite and Calcium phosphate	Bone substitute	2003	(260, 261)
	NanOss® (Rti Surgical)	Hydroxyapatite	Bone substitute	2005	(262)

Table 2 continued

Type of Particle	Name	Production material	Treatments	Year Approved	Ref.
Nanocrystals	EquivaBone® (Zimmer Biomet)	Hydroxyapatite	Bone substitute	2009	(263, 264)
	Invega® Sustenna® (Janssen Pharmaceuticals)	Paliperidone Palmitate	Schizophrenia	2009	(302, 303)
			Schizoaffective Disorder	2014	
Ryanodex® (Eagle Pharmaceuticals)	Dantrolene sodium	Malignant hypothermia	2014	(304)	
Inorganic / metallic nanoparticles	Nanotherm® (MagForce)	Iron oxide	Glioblastoma	2010	(250 – 252)
	Feraheme™ / Ferumoxytol (AMAG pharmaceuticals)	Ferumoxytol SPION with polyglucose sorbitol carboxymethylether	Anemia iron deficiency in chronic kidney disease	2009	(305)
	Venofer® (Luitpold pharmaceuticals)	Iron sucrose	Iron deficiency in chronic kidney disease	2000	(306 – 309)
	Ferrelecti® (Sanofi Avertis)	Sodium ferric gluconate	Iron deficiency in chronic kidney disease	1999	(306, 308, 309)
	INFeD® (Sanofi Avertis)	Iron dextran (low MW)	Iron deficiency in chronic kidney disease	1992	(306 – 310)
	DexIron® / Dexferrum® (Sanofi Avertis)	Iron Dextran (high MW)	Iron deficiency in chronic kidney disease	1996	(307, 308, 311)

Table 2 continued

Type of Particle	Name	Production material	Treatments	Year Approved	Ref.
Inorganic / metallic nanoparticles	Feridex®/Endorem® (AMAG pharmaceuticals)	SPION coated with dextran	Liver-specific imaging agent	1996	(250– 252)
	GastroMARK™/ Lumiren™ (AMAG pharmaceuticals)	SPION coated with dextran	Gastro-intestinal tract imaging agent	2001	(312, 313)

Mesenchymal stem cells

Osteoarthritis (OA) is a bone disorder that occurs in about 22.7 % of the world population (314). The only treatment available for severe OA is total joint arthroplasty (TJA) surgery and 99% of all total hip arthroplasties (THA) are due to arthritis-related pain and functional limitations (315). According to a report released by the CDC in February 2015, the amount of THA performed more than doubled from the year 2000 to 2010 (316). This is due to the high success rate of THA and the ever-aging population of the 21st century. Even though THA is seen as one of the most successful operations of the century (317), complications do occur (318–322). One of the primary reasons for early THA failure is periprosthetic joint infection (PJI) (319, 323).

Periprosthetic joint infection (PJI) is defined as an infection of the joint prosthesis and adjacent tissue (320). According to the Musculoskeletal Infection Society (MSIS), PJI can be identified when one of the following symptoms is present, a sinus tract (wound tunnel) that makes contact with the prosthesis or when pathogens can be isolated from two separate tissue samples (318). *Staphylococcus aureus* biofilm formation is associated with 38% of PJI and is extremely difficult to eradicate, since 53% of these strains are methicillin-resistant (319, 322). In severe cases PJI, is treated by administrating different combinations of antibiotics intravenously for two to six weeks (324). If the infection persists the prosthesis is removed

and the joint flushed with antibiotics, followed by a 12-week course of antibiotic treatment (319). Once the infection has cleared, a new prosthesis is inserted.

The effect of this direct application of antibiotics on osteoblast cells is largely unknown. Osteoblast proliferation and function is traditionally evaluated *in vitro* using bone-derived mesenchymal stem cells (bmMSC). In 2006, the International Society for Cellular Therapy Position proposed a three-part criteria for identifying mesenchymal stem cells, (a) the ability to adhere to plastic *in vitro*; (b) the expression (e.g. CD105, CD90 and CD73) and absence (e.g. CD45, CD34, CD 19, CD79a, CD14, CD11b and HLA-DR) of a range of cell markers as assessed by flow cytometry; and (c) ability to differentiate into osteoblasts, chondroblasts and adipocytes (325). This criteria was proposed for human MSC, but may not apply uniformly to all species, since it has been shown that murine MSCs express different cell markers *in vitro* (326). The presence of MSCs in bone marrow was first reported by Cohnheim (327, 328) in 1867. In the 1970s, Friedenstein and co-authors reported the ability of these bone-marrow cells to form colonies on plastic *in vitro* (329), designating the cells as colony forming units. A few years later Castro-Malaspina (330) succeeded in isolating these cells from humans and in 1999, Pittenger and co-authors (331) reported that bone-marrow derived cells were multipotent and could give rise to various mesenchymal cell lineages *in vitro*. Recently, Jacobs and co-authors described a second phenotypically, but functionally distinct population of mesenchymal stem cells, isolated from the proximal end of murine femora (pfMSC) (332). These cells were shown to have a decreased osteogenic potential and increased sensitivity to the cytotoxic effects of glucocorticoids.

References

1. Pidot SJ, Coyne S, Kloss F, Hertweck C. 2014. Antibiotics from neglected bacterial sources. *Int J Med Microbiol* 304:14–22.
2. Challinor VL, Bode HB. 2015. Bioactive natural products from novel microbial sources. *Ann N Y Acad Sci* 1354:82–97.
3. Hughes J, Jelsma J, Maclean E, Darder M, Tinise X. 2004. The health-related quality of life of people living with HIV / AIDS. *Disabil Rehabil* 26:371–376.
4. Riethmiller S. 2005. From atoxyl to salvarsan: searching for the magic bullet. *Chemotherapy* 51:234–242.
5. Mcdonagh JER. 1910. A report on twenty cases treated with Ehrlich's specific for syphilis. *Lancet* 176:711–713.
6. Hare R. 1982. New light on the history of Penicillin. *Med Hist* 26:1–24.
7. Zaffiri L, Gardner J, Toledo-Pereyra LH. 2012. History of antibiotics. From salvarsan to cephalosporins. *J Investig Surg* 25:67–77.
8. Chain E, Florey H, Gardber A, Heatly N, Jennings M, Orr-Ewing J, Sanders A. 1940. Penicillin as a chemotherapeutic agent. *Lancet* 236:226–228.
9. Wainwright M, Kristiansen JE. 2011. On the 75th anniversary of Prontosil. *Dye Pigment* 88:231–234.
10. Cohen LS, Cluff LE. 1961. The sulfonamides. *Am J Nurs* 61:54–58.
11. Comroe J. 1978. R Pay Dirt : The Story of Streptomycin. Part 1. From Waksman to Waksman. *Am Rev Respir Dis* 117:773–781.
12. Kresge N, Simoni RD, Hill RL. 2004. Selman Waksman: the father of antibiotics. *J Biol Chem* 279:101–102.
13. Fair RJ, Tor Y. 2014. Antibiotics and bacterial resistance in the 21st century. *Perspect Medicin Chem* 6:25–64.
14. Waksman SA. 1953. Streptomycin: background, isolation, properties and utilization. *Science, New Ser* 118:259–266.
15. Fox W, Sutherland I, Daniels M. 1954. A five year assessment of patients in a controlled trial of streptomycin in pulmonary tuberculosis.
16. Carter HE, Gottlieb D, Anderson HW. 1948. Chloromycetin and Streptothricin. *Sci New Ser* 107:113.

17. Ehrlich J, Bartz QR, Smith RM, Joslyn DA, Burkholder PR. 1947. Chloromycetin, a new antibiotic from a soil actinomycete. *Sci New Ser* 106:417.
18. Smith RM, Joslyn DA, Gruhzt OM, Mclean WI, Penner MA, Ehrlich J. 1948. Chloromycetin: Biological studies. *J Bacteriol* 55:425–448.
19. Koyama Y, Kurosasa A, Tsuchiya A, Takakuta K. 1950. A new antibiotic “colistin” produced by spore-forming soil bacteria. *J antibiot* 3:457–458.
20. Falagas ME, Kasiakou SK. 2005. Colistin: The revival of polymyxins for the management of multidrug-resistant Gram-negative bacterial infections. *Clin Infect Dis* 40:1333–1341.
21. Vaara M. 2010. Polymyxins and their novel derivatives. *Curr Opin Microbiol* 13:574–581.
22. Elverdam I, Larsen P, Lund E. 1981. Isolation and characterization of three new polymyxins in polymyxins B and E by high-performance liquid chromatography. *J Chromatogr* 218:653–661.
23. GARROD LP. 1957. The erythromycin group of antibiotics. *Br Med J* 2:57–63.
24. Conover LH, Moreland WT, English AR, Stephens CR, Pilgrim FJ. 1953. Terramycin. XI. Tetracycline. *J Am Chem Soc* 75:4622–4623.
25. Maggi X, Arioli V, Sensi P. 1965. Rifamycins. XLI. A New Class of Active Semisynthetic Rifamycins. N-Substituted Aminomethyl Derivatives of Rifamycin SV. *J Med Chem* 8:790–793.
26. Wehrli W, Staehelin M. 1969. The rifamycins-relation of chemical structure and action on RNA polymerase. *Biochem Biophys Acta* 182:24–29.
27. Fairbrother RW, Williams BL. 1956. Two new antibiotics, antibacterial activity of novobiocin and vancomycin. *Lancet* 268:1177–1179.
28. hoeksema H, Bannister B, Blrkenmeyer RD, Kagan F, Magerlein BJ, MacKellar F a., Schroeder W, Slomp G, Herr RR. 1964. Chemical studies on lincomycin. I. The structure of lincomycin. *J Am Chem Soc* 86:4223–4224.
29. Shah PM. 1991. Ciprofloxacin. *Int J Antimicrob Agents* 1:75–96.
30. Centre for Disease Control and Prevention. 2013. Antibiotic resistance threats in the united states.
31. Coates ARM, Halls G, Hu Y. 2011. Novel classes of antibiotics or more of the same? *Br J Pharmacol* 163:184–194.
32. Butler MS, Buss AD. 2006. Natural products — The future scaffolds for novel antibiotics?

- Biochem Pharmacol 71:919–929.
33. Shi J, Votruba AR, Farokhzad OC, Langer R. 2010. Nanotechnology in drug delivery and tissue engineering: from discovery to applications. *Nano Lett* 10:3223–3230.
 34. Yao S, Liu H, Yu S, Li Y, Wang X, Wang L. 2016. Drug-nanoencapsulated PLGA microspheres prepared by emulsion electrospray with controlled release behavior. *Regen Biomater* 3:309–317.
 35. Zakeri-milani P, Loveymi BD, Jelvehgari M, Valizadeh H. 2013. The characteristics and improved intestinal permeability of vancomycin PLGA-nanoparticles as colloidal drug delivery system. *Colloids Surfaces B Biointerfaces* 103:174–181.
 36. Adair JH, Parette MP, Altinoglu EI, Kester M. 2010. Nanoparticulate alternatives for drug delivery. *ACS Nano* 4:4967–4970.
 37. Farokhzad OC, Langer R. 2009. Impact of nanotechnology on drug delivery. *ACS Nano* 3:16–20.
 38. Jung A, Jik Y. 2011. “ Nanoantibiotics ”: A new paradigm for treating infectious diseases using nanomaterials in the antibiotics resistant era. *J Control Release* 156:128–145.
 39. Depoorter E, Bull MJ, Peeters C, Coenye T, Vandamme P, Mahenthiralingam E. 2016. *Burkholderia*: an update on taxonomy and biotechnological potential as antibiotic producers. *Appl Microbiol Biotechnol* 100:5215–5229.
 40. Santos AV, Dillon RJ, Dillon VM, Reynolds SE, Samuels RI. 2004. Occurrence of the antibiotic producing bacterium *Burkholderia* sp. in colonies of the leaf-cutting ant *Atta sexdens rubropilosa*. *FEMS Microbiol Lett* 239:319–323.
 41. Kang Y, Carlson R, Tharpe W, Schell MA. 1998. Characterization of genes involved in biosynthesis of a novel antibiotic from *Burkholderia cepacia* BC11 and their role in biological control of *Rhizoctonia solani*. *Appl Environ Microbiol* 64:3939–3947.
 42. El-Banna NM, Quddoumi SS, Daradka H. 2007. Antimicrobial substances produced by bacteria isolated from different Jordanian sources that are active against methicillin-resistant *Staphylococcus aureus*. *African J Biotechnol* 6:1837–1839.
 43. Mahenthiralingam E, Song L, Sass A, White J, Wilmot C, Marchbank A, Boaisa O, Paine J, Knight D, Challis GL. 2011. Enacyloxins are products of an unusual hybrid modular polyketide synthase encoded by a cryptic *Burkholderia ambifaria* genomic island. *Chem Biol* 18:665–677.
 44. Watanabe T, Izaki K, Takahashi H. 1982. New polygenic antibiotics active against Gram-

- positive and -negative bacteria. Isolation and purification of antibiotics produced by *Gluconobacter* sp. W-315. *J Antibiot (Tokyo)* 35:1141–1147.
45. O’Sullivan J, McCullough J, Johnson JH, Bonner DP, Clark JC, Dean L, Trejo WH. 1990. Janthinocins A, B and C, novel peptide lactone antibiotics produced by *Janthinobacterium lividum*. I. Taxonomy, fermentation, isolation, physico-chemical and biological characterization. *J Antibiot (Tokyo)* 43:913–919.
 46. Graupner K, Scherlach K, Bretschneider T, Lackner G, Roth M, Gross H, Hertweck C. 2012. Imaging mass spectrometry and genome mining reveal highly antifungal virulence factor of mushroom soft rot pathogen. *Angew Chemie - Int Ed* 51:13173–13177.
 47. Christensen P, Cook FD. 1978. *Lysobacter*, a new genus of nonhiting, gliding bacteria with a high base ratio. *Int J Syst Bacteriol* 28:367–393.
 48. Panthee S, Hamamoto H, Paudel A, Sekimizu K. 2016. *Lysobacter* species: a potential source of novel antibiotics. *Arch Microbiol* 198:839–845.
 49. O’Sullivan J, McCullough JE, Tymiak AA, Kirsch DR, Trejo WH, Principe PA. 1988. Lysobactin, a novel antibacterial agent produced by *Lysobacter* sp. I. Taxonomy, isolation and partial characterization. *J Antibiot (Tokyo)* 41:1740–1744.
 50. Kato A, Nakaya S, Ohashi Y, Hirata H, Fujii K, Harada K. 1997. WAP-8294A2, a novel anti-MRSA antibiotic produced by *Lysobacter* sp. *J Am Chem Soc* 119:6680–6681.
 51. Xie Y, Wright S, Shen Y, Du L. 2012. Bioactive natural products from *Lysobacter*. *Nat Prod Rep* 29:1277–87.
 52. Hamamoto H, Urai M, Ishii K, Yasukawa J, Paudel A, Murai M, Kaji T, Kuranaga T, Hamase K, Katsu T, Su J, Adachi T, Uchida R, Tomoda H, Yamada M, Souma M, Kurihara H, Inoue M, Sekimizu K. 2015. Lysocin E is a new antibiotic that targets menaquinone in the bacterial membrane. *Nat Chem Biol* 11:127–133.
 53. Murai M, Kaji T, Kuranaga T, Hamamoto H, Sekimizu K, Inoue M. 2015. Total synthesis and biological evaluation of the antibiotic lysocin E and its enantiomeric, epimeric, and N-demethylated analogues. *Angew Chemie - Int Ed* 54:1556–1560.
 54. Hashizume H, Igarashi M, Hattori S, Hori M, Hamada M, Takeuchi T. 2001. Tripropeptins, novel antimicrobial agents produced by *Lysobacter* sp. I. Taxonomy, isolation and biological activities. *J Antibiot (Tokyo)* 54:1054–1059.
 55. Hashizume H, Takahashi Y, Harada S, Nomoto A. 2015. Natural lipopeptide antibiotic tripropeptin C revitalizes and synergistically potentiates the activity of beta-lactams

- against methicillin-resistant *Staphylococcus aureus*. *J Antibiot (Tokyo)* 68.
56. Malan AP, Nguyen KB, Addison MF. 2006. Entomopathogenic nematodes (*Steinernematidae* and *Heterorhabditidae*) from the southwestern parts of South Africa. *African Plant Prot* 12:65–69.
 57. Adams BJ, Nguyen KB. 2002. *Entomopathogenic Nematology*. CABI, Wallingford, Oxon.
 58. Dutkey S. 1959. *Insect Microbiology*. *Adv Appl Microbiol* 1:175–200.
 59. McInerney B V, Gregson RP, Lacey MJ, Akhurst RJ, Lyons GR, Rhodes SH, Smith DRJ, Engelhardt LM, White H. 1991. Biologically active metabolites from *Xenorhabdus* spp., Part 1. Dithiolopyrrolone derivatives with antibiotic activity. *J Nat Prod* 54:774–784.
 60. Paul V, Frautschv S, Fenical W, Neelson K. 1981. Antibiotics in microbial ecology: isolation and structure assignment of several new antibacterial compounds from the insect-symbiotic bacteria *Xenorhabdus* spp. *J Chem Ecol* 7:589.
 61. Li J, Chen G, Webster JM. 1995. Antimicrobial metabolites from a bacterial symbiont. *J Nat Prod* 58:1081–1086.
 62. Sundar L, Chang FN. 1993. Antimicrobial activity and biosynthesis of indole antibiotics produced by *Xenorhabdus nematophilus*. *J Gen Microbiol* 139:3139–3148.
 63. Li J, Chen G, Webster JM. 1997. Nematophin, a novel antimicrobial substance produced by *Xenorhabdus nematophilus* (Enterobacteriaceae). *Can J Microbiol* 43:770–773.
 64. McInerney B V, Taylor WC, Lacey MJ, Akhurst RJ, Gregson RP. 1991. Biologically active metabolites from *Xenorhabdus* spp., Part 2. Benzopyran-1-one Derivatives with Gastroprotective activity. *J Nat Prod* 54:785–795.
 65. Heunis TDJ, Dicks LMT. 2010. Nanofibers offer alternative ways to the treatment of skin infections. *J Biomed Biotechnol* 2010:1–10.
 66. Nuñez-Anita RE, Acosta-Torres LS, Vilar-Pineda J, Martínez-Espinosa JC, de la Fuente-Hernandez J, Castano VM. 2014. Toxicology of antimicrobial nanoparticles for prosthetic devices. *Int J Nanomedicine* 2014:3999–4006.
 67. Sheingold BH, Hahn JA. 2014. The history of healthcare quality: The first 100 years 1860 – 1960. *Int J Africa Nurs Sci* 1:18–22.
 68. Dowdle WR. 2003. Perspectives for the elimination/eradication of diseases with vaccines, p. 354–355. *In* Quadros, CA (ed.), *Vaccines: Preventing diseases and protecting health*, 1st ed. PAHO, Washington, D.C.
 69. Hughes GA. 2005. Nanostructure-mediated drug delivery. *Nanomedicine*

- Nanotechnology, *Biol Med* 1:22–30.
70. Sparer R V., Chung S, Ringeisen CD, Himmelstein KJ. 1984. Controlled release from erodible poly(ortho ester) drug delivery systems. *J Control Release* 1:23–32.
 71. Jong WH De. 2008. Drug delivery and nanoparticles: Applications and hazards. *Int J Nanomedicine* 3:133–149.
 72. Bangham AD, Standish MM, Watkins JC. 1965. Diffusion of univalent ions across the lamellae. *J Mol Biol* 13:238–252.
 73. Bangham AD, Horne RW. 1964. Negative staining of phospholipids and their structural modification by surface-active agents as observed in the electron microscope. *J Mol Biol* 8:660–668.
 74. Allen TM, Cullis PR. 2013. Liposomal drug delivery systems: From concept to clinical applications. *Adv Drug Deliv Rev* 65:36–48.
 75. Langer R, Folkman J. 1976. Polymers for the sustained release of proteins and other macromolecules. *Nature* 263:797–800.
 76. Li JK, Wang N, Wu XS. 1998. Poly(vinyl alcohol) nanoparticles prepared by freezing-thawing process for protein/peptide drug delivery. *J Control Release* 56:117–126.
 77. Abbasi E, Aval S, Akbarzadeh A, Milani M, Nasrabadi H, Joo S, Hanifehpour Y, Nejati-Koshki K, Pashaei-Asl R. 2014. Dendrimers: synthesis, applications, and properties. *Nanoscale Res Lett* 9:247.
 78. Yatvin MB, Kreutz W, Horwitz BA, Shinitzky M. 1980. pH-Sensitive Liposomes: Possible clinical implications. *Science* 210:1253–1255.
 79. Leserman LD, Barbet J, Kourilsky F, Weinstein JN. 1980. Targeting to cells of fluorescent liposomes covalently coupled with monoclonal antibody or protein A. *Nature* 288:602–604.
 80. Klivanov AL, Maruyama K, Torchilin VP, Huang L. 1990. Amphipathic polyethyleneglycols effectively prolong the circulation time of liposomes. *FEBS Lett* 268:235–237.
 81. Barenholz Y. 2012. Doxil® - The first FDA-approved nano-drug: Lessons learned. *J Control Release* 160:117–134.
 82. Bobo D, Robinson KJ, Islam J, Thurecht KJ, Corrie SR. 2016. Nanoparticle-based medicines: A review of FDA-approved materials and clinical trials to date. *Pharm Res* 33:2373–2387.

83. Chege M, McConville A, Davis J. 2017. Microneedle drug delivery systems: Appraising opportunities for improving safety and assessing areas of concern. *J Chem Heal Saf* 24:6–14.
84. Donnelly RF, Raghu T, Singh R, Woolfson D. 2010. Microneedle-based drug delivery systems: microfabrication, drug delivery, and safety. *Drug Deliv* 17:187–207.
85. Discher BM, Won Y, Ege DS, Lee JC, Frank S, Discher DE, Hammer DA. 1999. Polymersomes: Tough vesicles made from diblock copolymers. *Science (80-)* 284:1143–1146.
86. Christian DA, Cai S, Bowen DM, Kim Y, Pajerowski JD, Discher DE. 2009. Polymersome carriers: from self-assembly to siRNA and protein therapeutics. *Eur J Pharm Biopharm* 71:463–474.
87. Rolland JP, Maynor BW, Euliss LE, Exner AE, Denison GM, Desimone JM. 2005. Direct fabrication and harvesting of monodisperse, shape-specific nanobiomaterials. *J Am Chem Soc* 127:10096–10100.
88. Percec V, Wilson DA, Leowanawat P, Wilson CJ, Hughes AD, Kaucher MS, Hammer DA, Levine DH, Kim AJ, Bates FS, Davis KP, Lodge TP, Klein ML, DeVane RH, Aqad E, Rosen BM, Argintam AO, Sienkowska MJ, Rissanen K, Nummelin S, Ropponen J. 2010. Self-Assembly of Janus dendrimers into uniform dendrimersomes and other complex architectures. *Sci New Ser* 328:1009–1014.
89. Zhao L, Seth A, Wibowo N, Zhao C-X, Mitter N, Yu C, Middelberg APJ. 2014. Nanoparticle vaccines. *Vaccine* 32:327–337.
90. Bolhassani A, Javan zad S, Saleh T, Hashemi M, Aghasadeghi MR. 2014. Polymeric nanoparticles: potent vectors for vaccine delivery targeting cancer and infectious diseases. *Hum Vaccin Immunother* 10:321–332.
91. Niikura K, Matsunaga T, Suzuki T, Kobayashi S, Yamaguchi H, Orba Y, Kawaguchi A, Hasegawa H, Kajino K, Ninomiya T, Ijiro K, Sawa H. 2013. Gold nanoparticles as a vaccine platform: Influence of size and shape on immunological responses in vitro and in vivo. *ACS Nano* 7:3926–3938.
92. Hans ML, Lowman AM. 2006. Nanoparticles for Drug Delivery, p. 637–664. *In* Gogotsi, Y (ed.), *Nanomaterials Handbook*, 1sted. Taylor and Fracis, New York.
93. Mudshinge SR, Deore AB, Patil S, Bhalgat CM. 2011. Nanoparticles: Emerging carriers for drug delivery. *Saudi Pharm J* 19:129–141.

94. Khan I, Saeed K, Khan I. 2017. Nanoparticles: Properties, applications and toxicities. Arab J Chem.
95. Salouti M, Ahangari A. 2014. Nanoparticle based drug delivery systems for treatment of infectious diseases, p. 155–192. *In* Sezer, AD (ed.), *Application of Nanotechnology in Drug Delivery*. InTech.
96. Inomata K, Nobuyuki A, Koinuma, Hideomi. 1994. Production of fullerenes by low temperature plasma chemical vapor deposition under atmospheric pressure. *Jpn J Appl Phys* 33:197–199.
97. Friedman SH, DeCamp DL, Sijbesma RP, Srdanov G, Wudl F, Kenyon GL. 1993. Inhibition of the HIV-1 protease by fullerene derivatives: model building studies and experimental verification. *J Am Chem Soc* 115:6506–6509.
98. Kalhapure RS, Suleman N, Mocktar C, Seedat N, Govender T. 2015. Nanoengineered drug delivery systems for enhancing antibiotic therapy. *J Pharm Sci* 104:872–905.
99. Mukherjee S, Ray S, Thakur R. 2009. Solid lipid nanoparticles: A modern formulation approach in drug delivery system. *Indian J Pharm Sci* 71:349.
100. Nithyapriya M, Chellaram C. 2012. Gold Nanoshells in Medicine – A Review. *Indian J Innov Dev* 1:43–45.
101. Kalele S, Gosavi SW, Urban J, Kulkarni SK. 2006. Nanoshell particles: synthesis, properties and applications. *Curr Sci* 91:1038–1052.
102. Mirkin CA, Letsinger RL, Mucic RC, Storhoff JJ. 1996. A DNA-based method for rationally assembling nanoparticles into macroscopic materials. *Nature* 382:607–609.
103. Ung T, Liz-Marzán LM, Mulvaney P. 1998. Controlled method for silica coating of silver colloids. *Langmuir* 14:3740–3748.
104. Foubert A, Beloglazova N V, Rajkovic A, Sas B, Madder A, Goryacheva IY, De Saeger S. 2016. Bioconjugation of quantum dots: Review & impact on future application. *TrAC - Trends Anal Chem* 83:31–48.
105. Sirelkhatim A, Mahmud S, Seeni A, Kaus NHM, Ann LC, Bakhori SKM, Hasan H, Mohamad D. 2015. Review on zinc oxide nanoparticles: Antibacterial activity and toxicity mechanism. *Nano-Micro Lett* 7:219–242.
106. Caminade A-M, Laurent R, Delavaux-Nicot B, Majoral J-P. 2012. “Janus” dendrimers: syntheses and properties. *New J Chem* 36:217–226.
107. Letchford K, Burt H. 2007. A review of the formation and classification of amphiphilic

- block copolymer nanoparticulate structures: micelles, nanospheres, nanocapsules and polymersomes. *Eur J Pharm Biopharm* 65:259–269.
108. Jones MC, Leroux JC. 1999. Polymeric micelles - A new generation of colloidal drug carriers. *Eur J Pharm Biopharm* 48:101–111.
 109. Kataoka K, Harada A, Nagasaki Y. 2001. Block copolymer micelles for drug delivery: Design, characterization and biological significance. *Adv Drug Deliv Rev* 47:113–131.
 110. Junghanns JUAH, Müller RH. 2008. Nanocrystal technology, drug delivery and clinical applications. *Int J Nanomedicine* 3:295–309.
 111. Rao C, Thomas P, Kulkarni G. 2007. Basics of Nanocrystals, p. 1–24. *In* *Nanocrystals: Synthesis, properties and applications*. Springer-Verlag Berlin Heidelberg, Berlin.
 112. Müller RH, Becker R, Kruss B, Peters K. 1999. Pharmaceutical nanosuspensions for medicament administration as systems with increased saturation solubility and rate of solution. US5858410 A.
 113. Müller RH, Jacobs C, Kayser O. 2001. Nanosuspensions as particulate drug formulations in therapy: Rationale for development and what we can expect for the future. *Adv Drug Deliv Rev* 47:3–19.
 114. Heller J, Domb AJ, Kumar N. 2002. Polyanhydrides and poly(ortho esters). *Adv Drug Deliv Rev* 54:887–888.
 115. Piras AM, Sandreschi S, Maisetta G, Esin S, Batoni G, Chiellini F. 2015. Chitosan Nanoparticles for the Linear Release of Model Cationic Peptide. *Pharm Res* 32:2259–2265.
 116. Soppimath KSK, Aminabhavi TMTM, Kulkarni ARAR, Rudzinski WE. 2001. Biodegradable polymeric nanoparticles as drug delivery devices. *J Control Release* 70:1–20.
 117. Nagpal K, Singh SK, Mishra DN. 2010. Chitosan nanoparticles: A promising system in novel drug delivery. *Chem Pharm Bull (Tokyo)* 58:1423–1430.
 118. Rouget C. 1859. Des substances amylacees dans le tissu des animaux. specialement les articutes (chitine). *Comp Rend* 48:792–795.
 119. Katas H, Raja MAG, Lam KL. 2013. Development of chitosan nanoparticles as a stable drug delivery system for protein/siRNA. *Int J Biomater* 2013:1–9.
 120. Pan Y, Li YJ, Zhao HY, Zheng JM, Xu H, Wei G, Hao JS, Cui F De. 2002. Bioadhesive polysaccharide in protein delivery system: Chitosan nanoparticles improve the intestinal absorption of insulin in vivo. *Int J Pharm* 249:139–147.

121. Calvo P, Remuñán-lópez C, Vila-Jato JL, Alonso MJ. 1997. Novel hydrophilic chitosan-polyethylene oxide nanoparticles as protein carriers. *J Appl Polym Sci* 63:125–132.
122. Tiyaboonchai W. 2003. Chitosan Nanoparticles: A promising system for drug delivery. *Naresuan Univ J* 11:51–66.
123. Maitra A, Ghosh P, De T, Sahoo S. 1999. Process for the preparation of highly monodispersed hydrophilicpolymeric nanoparticles of size less than 100 nm. *US* 08/779,904.
124. El-Shabouri MH. 2002. Positively charged nanoparticles for improving the oral bioavailability of cyclosporin-A. *Int J Pharm* 249:101–108.
125. Tiyaboonchai W, Limpeanchob N. 2007. Formulation and characterization of amphotericin B-chitosan-dextran sulfate nanoparticles. *Int J Pharm* 329:142–149.
126. De S, Robinson D. 2003. Polymer relationships during preparation of chitosan-alginate and poly-L-lysine-alginate nanospheres. *J Control Release* 89:101–112.
127. Chavanpatil MD, Khair A, Panyam J. 2007. Surfactant-polymer nanoparticles: A novel platform for sustained and enhanced cellular delivery of water-soluble molecules. *Pharm Res* 24:803–810.
128. Huang M, Fong CW, Khor E, Lim LY. 2005. Transfection efficiency of chitosan vectors: Effect of polymer molecular weight and degree of deacetylation. *J Control Release* 106:391–406.
129. Bozkir A, Saka OM. 2004. Chitosan Nanoparticles for Plasmid DNA Delivery: Effect of Chitosan Molecular Structure on Formulation and Release Characteristics. *Drug Deliv* 11:107–112.
130. Bhattarai N, Ramay HR, Chou SH, Zhang M. 2006. Chitosan and lactic acid-grafted chitosan nanoparticles as carriers for prolonged drug delivery. *Int J Nanomedicine* 1:181–187.
131. Van der Lubben IM, Verhoef JC, Borchard G, Junginger HE. 2001. Chitosan for mucosal vaccination. *Adv Drug Deliv Rev* 52:139–144.
132. Sahoo N, Sahoo RK, Biswas N, Guha A, Kuotsu K. 2015. Recent advancement of gelatin nanoparticles in drug and vaccine delivery. *Int J Biol Macromol* 81:317–331.
133. Kumari A, Yadav SK, Yadav SC. 2010. Biodegradable polymeric nanoparticles based drug delivery systems. *Colloids Surfaces B Biointerfaces* 75:1–18.
134. Shyni K, Hema GS, Ninan G, Mathew S, Joshy CG, Lakshmanan PT. 2014. Isolation and

- characterization of gelatin from the skins of skipjack tuna (*katsuwonus pelamis*), dog shark (*scoliodon sorrakowah*), and rohu (*labeo rohita*). Food Hydrocoll 39:68–76.
135. Elzoghby AO. 2013. Gelatin-based nanoparticles as drug and gene delivery systems: Reviewing three decades of research. J Control Release 172:1075–1091.
 136. Weber C, Coester C, Kreuter J, Langer K. 2000. Desolvation process and surface characterisation of protein nanoparticles. Int J Pharm 194:91–102.
 137. Ofokansi K, Winter G, Fricker G, Coester C. 2010. Matrix-loaded biodegradable gelatin nanoparticles as new approach to improve drug loading and delivery. Eur J Pharm Biopharm 76:1–9.
 138. Bennet D, Kim S. 2014. Application of Nanotechnology in Drug Delivery. InTech.
 139. Kim KJ, Byun Y. 1999. Preparation and characterizations of self-assembled PEGylated gelatin nanoparticles. Biotechnol Bioprocess Eng 4:210 – 214.
 140. Pounder RJ, Dove AP. 2010. Towards poly(ester) nanoparticles: recent advances in the synthesis of functional poly(ester)s by ring-opening polymerization. Polym Chem 1:260–271.
 141. Uhrich KE, Cannizzaro SM, Langer RS, Shakesheff KM. 1999. Polymeric systems for controlled drug release. Chem Rev 99:3181–3198.
 142. Vert M, Li SM, Spenlehauer G, Guerin P. 1992. Bioresorbability and biocompatibility of aliphatic polyesters. J Mater Sci Mater Med 3:432–446.
 143. Mehta R, Kumar V, Bhunia H, Upadhyay SN. 2005. Synthesis of poly(lactic acid): A review. J Macromol Sci - Polym Rev 45:325–349.
 144. Burg K. 2014. Poly (α -ester)s, p. 115–121. In Kumbar, SG, Laurencin, CT, Deng, M (eds.), Natural and synthetic biomedical polymers. Elsevier Burlington.
 145. Jamshidian M, Tehrany EA, Imran M, Jacquot M, Desobry S. 2010. Poly-Lactic Acid: Production, applications, nanocomposites, and release studies. Compr Rev Food Sci Food Saf 9:552–571.
 146. Gentile P, Chiono V, Carmagnola I, Hatton P V. 2014. An overview of poly(lactic-co-glycolic) Acid (PLGA)-based biomaterials for bone tissue engineering. Int J Mol Sci 15:3640–3659.
 147. Makadia HK, Siegel SJ. 2011. Poly Lactic-co-Glycolic Acid (PLGA) as biodegradable controlled drug delivery carrier. Polymers (Basel) 3:1377–1397.

148. Hardin CC, Knopp JA. 2013. The Krebs Cycle, p. 180–183. *In* Biochemistry - Essential Concepts. Oxford University Press.
149. Danhier F, Ansorena E, Silva JM, Coco R, Le Breton A, Préat V. 2012. PLGA-based nanoparticles: An overview of biomedical applications. *J Control Release* 161:505–522.
150. Sinha VR, Bansal K, Kaushik R, Kumria R, Trehan A. 2004. Poly- ϵ -caprolactone microspheres and nanospheres: An overview. *Int J Pharm* 278:1–23.
151. van Natta FJ, Hill JW, Carothers WH. 1934. Studies of polymerization and ring Formation. XXIII.1 ϵ -caprolactone and its polymers. *J Am Chem Soc* 56:455–457.
152. Heller J, Himmelstein KJ. 1985. Poly(ortho ester) biodegradable polymer systems. *Methods Enzymol* 112:422–436.
153. Heller J, Barr J, Ng SY, Abdellaoui KS, Gurny R. 2002. Poly(ortho esters): synthesis, characterization, properties and uses. *Adv Drug Deliv Rev* 54:1015–1039.
154. Heller J, Barr J, Ng SY, Shen HR, Schwach-Abdellaoui K, Emmahl S, Rothen-Weinhold A, Gurny R. 2000. Poly(ortho esters) - Their development and some recent applications. *Eur J Pharm Biopharm* 50:121–128.
155. Heller J. 1990. Development of poly(ortho esters): a historical overview. *Biomaterials* 11:659–665.
156. Vistnes L, Schmitt E, Ksander G, Rose E, Balkenhol W, Coleman C. 1976. Evaluation of a prototype therapeutic system for prolonged, continuous topical delivery of homosulfanilamide in the management of *Pseudomonas* burn wound sepsis. *Surgery* 7:690–696.
157. Roskos K, Tefft J, Fritzing B, Heller J. 1992. Development of a morphine-triggered naltrexone delivery system. *J Control Release* 19:145–159.
158. Segal S. 1987. A new delivery system for contraceptive steroids. *Am J Obs Gynecol* 157:1090–1092.
159. Heller J. 1993. Poly(ortho esters)Biopolymers I. *Advances in polymer Science*. Springer, Berlin, Heidelberg, Berlin, Heidelberg.
160. Ng SY, Vandamme T, Taylor MS, Heller J. 1997. Synthesis and erosion studies of self-catalyzed poly(ortho ester)s. *Macromolecules* 30:770–772.
161. Schwach-Abdellaoui K, Heller J, Gurny R. 1999. Hydrolysis and erosion studies of autocatalyzed poly(ortho esters) containing lactoyl–lactyl acid dimers. *Macromolecules* 32:301–307.

162. Schwach-Abdellaoui K, Vivien-Castioni N, Gurny R. 2000. Local delivery of antimicrobial agents for the treatment of periodontal disease of periodontal diseases. *Eur J Pharm Biopharm* 50:83–99.
163. Wang C, Ge Q, Ting D, Nguyen D, Shen H-R, Chen J, Eisen HN, Heller J, Langer R, Putnam D. 2004. Molecularly engineered poly(ortho ester) microspheres for enhanced delivery of DNA vaccines. *Nat Mater* 3:190–196.
164. Bucher J, Slade W. 1909. The anhydrides of isophthalic and terephthalic acid, p. 1319–1321. *In* *J. Am. Chem. Soc.*1.
165. Rosen HB, Chang J, Wnek GE, Linhardt RJ, Langer R. 1983. Bioerodible polyanhydrides for controlled drug delivery. *Biomaterials* 4:131–133.
166. Tamada J, Langer RS. 1992. The development of polyanhydrides for drug delivery applications. *J Biomater Sci Polym Ed* 3:315–353.
167. Kumar N, Langer RS, Domb AJ. 2002. Polyanhydrides: An overview. *Adv Drug Deliv Rev* 54:889–910.
168. Eameema M, Duvvuri LS, Khan W, Domb AJ. 2014. Polyanhydrides, p. 181–192. *In* Kumbar, SG, Laurencin, CT, Deng, M (eds.), *Natural and synthetic biomedical polymers* First. Elsevier Science.
169. Chiu Li L, Deng J, Stephens D. 2002. Polyanhydride implant for antibiotic delivery - From the bench to the clinic. *Adv Drug Deliv Rev* 54:963–986.
170. Heikkilä P, Taipale A, Lehtimäki M, Harlin A. 2008. Electrospinning of polyamides with different chain compositions for filtration application. *Polym Eng Sci* 48:1168–1176.
171. Saxena T, Karumbaiah L, Valmikinathan CM. 2014. Proteins and Poly (Amino Acids), p. 43–65. *In* Kumbar, SG, Laurencin, CT, Deng, M (eds.), *Natural and synthetic biomedical polymers*, 1st ed. Elsevier.
172. Summerhayes, C. P., Thorpe SA. 2014. Polyphosphazenes, p. 193–206. *In* Kumbar, SG, Laurencin, CT, Deng, M (eds.), *Natural and synthetic biomedical polymers* First. Elsevier.
173. Kireev V, Kolesnikov G, Raigorodskii I. 1969. Polyphosphazenes. *Russ Chem Rev* 38:667–682.
174. Stokes HN. 1897. Chloronitrides of phosphorus. *Am Chem J* 19:782–796.
175. Lakshmi S, Katti DS, Laurencin CT. 2003. Biodegradable polyphosphazenes for drug delivery applications. *Adv Drug Deliv Rev* 55:467–482.
176. Potin P, de Jaeger R. 1991. Polyphosphazenes: synthesis, structures, properties,

- applications. *Eur Polym J* 27:341–348.
177. Allcock HR, Kugel RL. 1965. Synthesis of high polymeric alkoxy- and aryloxyphosphonitriles. *J Am Chem Soc* 87:4216–4217.
 178. Allcock HR, Kugel RL, Valan KJ. 1966. Phosphonitrilic compounds. VI. High molecular weight poly(alkoxy- and aryloxyphosphazenes). *Inorg Chem* 5:1709–1715.
 179. Caliceti P, Veronese FM, Lora S. 2000. Polyphosphazene microspheres for insulin delivery. *Int J Pharm* 211:57–65.
 180. Jokerst J V, Lobovkina T, Zare RN, Gambhir SS. 2011. Nanoparticle PEGylation for imaging and therapy. *Nanomedicine* 6:715–728.
 181. Anbarasu M, Anandan M, Chinnasamy E, Gopinath V, Balamurugan K. 2015. Synthesis and characterization of polyethylene glycol (PEG) coated Fe₃O₄ nanoparticles by chemical co-precipitation method for biomedical applications. *Spectrochim Acta Part A Mol Biomol Spectrosc* 135:536–539.
 182. Cheng J, Teply BA, Sherifi I, Sung J, Luther G, Gu FX, Levy-Nissenbaum E, Radovic-Moreno AF, Langer R, Farokhzad OC. 2007. Formulation of functionalized PLGA–PEG nanoparticles for in vivo targeted drug delivery. *Biomaterials* 28:869–876.
 183. Xu J, Wong DHC, Byrne JD, Chen K, Bowerman C, Desimone JM. 2013. Future of the particle replication in nonwetting templates (PRINT) technology. *Angew Chemie - Int Ed* 52:6580–6589.
 184. Pinto Reis C, Neufeld RJ, Ribeiro AJ, Veiga F. 2006. Nanoencapsulation I. Methods for preparation of drug-loaded polymeric nanoparticles. *Nanomedicine Nanotechnology, Biol Med* 2:8–21.
 185. Astete CE, Sabliov CM. 2006. Synthesis and characterization of PLGA nanoparticles. *J Biomater Sci Polym Ed* 17:247–289.
 186. Mai Hoa LT, Chi NT, Triet NM, Thanh Nhan LN, Chien DM. 2009. Preparation of drug nanoparticles by emulsion evaporation method. *J Phys Conf Ser* 187.
 187. Desgouilles S, Vauthier C, Bazile D, Vacus J, Grossiord JL, Veillard M, Couvreur P. 2003. The design of nanoparticles obtained by solvent evaporation: A comprehensive study. *Langmuir* 19:9504–9510.
 188. Alex R, Bodmeier R. 1990. Encapsulation of water-soluble drugs by a modified solvent evaporation method. I. Effect of process and formulation variables on drug entrapment. *J Microencapsul* 7:347–55.

189. Li M, Rouaud O, Poncelet D. 2008. Microencapsulation by solvent evaporation: State of the art for process engineering approaches. *Int J Pharm* 363:26–39.
190. Hans M., Lowman A. 2002. Biodegradable nanoparticles for drug delivery and targeting. *Curr Opin Solid State Mater Sci* 6:319–327.
191. Ahamad N, Srinivasa Rao DA, Katti DS. 2017. Overview of methods of making polyester Nano- and microparticulate systems for drug delivery, *In Ravikumar, M (ed.), Handbook of polyester drug delivery systems* Reprint. CRC Press.
192. Julienne MC, Alonso MJ, Benoit JP. 1992. Preparation Of Poly (D , L-lactide / glycolide) nanoparticles of controlled particle size distribution: Application of experimental designs. *Drug Dev Ind Pharm* 18:1063–1077.
193. Torché AM, Jouan H, Le Corre P, Albina E, Primault R, Jestin A, Le Verge R. 2000. Ex vivo and in situ PLGA microspheres uptake by pig ileal Peyer’s patch segment. *Int J Pharm* 201:15–27.
194. Vrancken MN, Claeys DA. 1970. Process for encapsulating water and compounds in aqueous phase by evaporation. US3523906 A. United States of America.
195. Esfandyari-manesh M, Khoshroo K, Eskandarion S, Jafarzadeh Kashi TS, Dinarvand R, Marashi, Amin SM. 2012. Preparation and characterization of Ciprofloxacin-PLGA and minocycline-PLGA nanoparticles and comparing their antibacterial activity, p. 12–14. *In Proceedings of the 4th International Conference on Nanostructures.*
196. McCall RL, Sirianni RW. 2013. PLGA nanoparticles formed by single- or double-emulsion with vitamin E- TPGS. *J Vis Exp* 82:1–8.
197. Dillen K, Vandervoort J, Van den Mooter G, Ludwig A. 2006. Evaluation of ciprofloxacin-loaded Eudragit® RS100 or RL100 / PLGA nanoparticles. *Int J Pharm* 314:72–82.
198. Cohen-sela E, Chorny M, Koroukhov N, Danenberg HD, Golomb G. 2009. A new double emulsion solvent diffusion technique for encapsulating hydrophilic molecules in PLGA nanoparticles. *J Control Release* 133:90–95.
199. Song C., Labhasetwar V, Murphy H, Qu X, Humphrey W., Shebuski R., Levy R. 1997. Formulation and characterization of biodegradable nanoparticles for intravascular local drug delivery. *J Control Release* 43:197–212.
200. Niwa T, Takeuchi H, Hino T, Kunou N, Kawashima Y. 1993. Preparations of biodegradable nanospheres of water-soluble and insoluble drugs with D, L-lactide/glycolide copolymer by a novel spontaneous emulsification solvent diffusion

- method, and the drug release behavior. *J con* 25:89–98.
201. Kumar S, Dilbaghi N, Saharan R, Bhanjana G. 2012. Nanotechnology as emerging tool for enhancing solubility of poorly water-soluble drugs. *Bionanoscience* 2:227–250.
 202. Murakami H, Kobayashi M, Takeuchi H, Kawashima Y. 1999. Preparation of poly(DL-lactide-co-glycolide) nanoparticles by modified spontaneous emulsification solvent diffusion method. *Int J Pharm* 187:143–152.
 203. Bindschaedler C, Gurney R, Doelker E. 1988. Process for preparing a powder of water-insoluble polymer which can be redispersed in a liquid phase, the resulting powder and utilization thereof. WO8808011.
 204. Allémann E, Gurny R, Doelker E. 1992. Preparation of aqueous polymeric nanodispersions by a reversible salting-out process: influence of process parameters on particle size. *Int J Pharm* 87:247–253.
 205. Wang Y, Li P, Truong-Dinh Tran T, Zhang J, Kong L. 2016. Manufacturing techniques and surface engineering of polymer based nanoparticles for targeted drug delivery to cancer. *Nanomaterials* 6:26.
 206. Quintnar-Guerrero D, Allémann E, Fessi H, Doelker E. 1998. Preparation techniques and mechanisms of formation of biodegradable nanoparticles from preformed polymers. *Drug Dev Ind Pharm* 24:1113–1128.
 207. Mendoza-Munoz N, Quintanar-Guerrero D, Allemann E. 2012. The impact of the salting-out technique on the preparation of colloidal particulate systems for pharmaceutical applications. *Recent Pat Drug Deliv Formul* 6:236–249.
 208. Fessi H, Puisieux F, Devissaguet JP, Ammoury N, Benita S. 1989. Nanocapsule formation by interfacial polymer deposition following solvent displacement. *Int J Pharm* 55:1–4.
 209. Govender T, Stolnik S, Garnett MC, Illum L, Davis SS. 1999. PLGA nanoparticles prepared by nanoprecipitation: Drug loading and release studies of a water soluble drug. *J Control Release* 57:171–185.
 210. Schubert S, Delaney, Jr JT, Schubert US. 2011. Nanoprecipitation and nanoformulation of polymers: from history to powerful possibilities beyond poly(lactic acid). *Soft Matter* 7:1581–1588.
 211. Betancourt T, Brown B, Brannon-Peppas L. 2007. Doxorubicin-loaded PLGA nanoparticles by nanoprecipitation: preparation, characterization and in vitro evaluation. *Nanomedicine* 2:219–232.

212. Barichello JM, Morishita M, Takayama K, Nagai T. 1999. Encapsulation of hydrophilic and lipophilic drugs in PLGA nanoparticles by the nanoprecipitation method. *Drug Dev Ind Pharm* 25:471–476.
213. Quintanar-Guerrero D, Allémann E, Fessi H, Doelker E. 1998. Preparation techniques and mechanisms of formation of biodegradable nanoparticles from preformed polymers. *Drug Dev Ind Pharm* 24:1113–1128.
214. Mora-Huertas CE, Fessi H, Elaissari A. 2010. Polymer-based nanocapsules for drug delivery. *Int J Pharm* 385:113–142.
215. Miladi K, Sfar S, Fessi H, Elaissari A. 2016. Nanoprecipitation process: From particle preparation to in vivo applications, p. 17–53. *In* Vauthier, C, Ponchel, G (eds.), *Polymer Nanoparticles for Nanomedicines*. Springer International Publishing, Cham.
216. Bilati U, Allémann E, Doelker E. 2005. Development of a nanoprecipitation method intended for the entrapment of hydrophilic drugs into nanoparticles. *Eur J Pharm Sci* 24:67–75.
217. Mahalingam M, Krishnamoorthy K. 2015. Selection of a suitable method for the preparation of polymeric nanoparticles: Multi-criteria decision making approach. *Adv Pharm Bull* 5:57–67.
218. Anton N, Benoit JP, Saulnier P. 2008. Design and production of nanoparticles formulated from nano-emulsion templates-A review. *J Control Release* 128:185–199.
219. Perazzo A, Preziosi V, Guido S. 2015. Phase inversion emulsification: Current understanding and applications. *Adv Colloid Interface Sci* 222:581–599.
220. Shinoda K, Saito H. 1968. The effect of temperature on the phase equilibria and the types of dispersions of the ternary system composed of water, cyclohexane, and nonionic surfactant. *J Colloid Interface Sci* 26:70–74.
221. Sasaki Y, Kohri M, Kojima T, Taniguchi T, Kishikawa K. 2014. Preparation of polymer nanoparticles via phase inversion temperature Method using amphiphilic block polymer synthesized by atom transfer radical polymerization. *Trans Mat Soc Japan* 39:125–128.
222. Tadros TF. 2014. General classification of surfactants, p. 5–28. *In* *An introduction to surfactants*. Berlin, Germany; Boston, Massachusetts: de Gruyter.
223. Friberg SE, Corkery RW, Blute IA. 2011. Phase inversion temperature (PIT) emulsification process. *J Chem Eng Data* 56:4282–4290.

224. Izquierdo P, Esquena J, Tadros TF, Dederen C, Garcia MJ, Azemar N, Solans C. 2002. Formation and stability of nano-emulsions prepared using the phase inversion temperature method. *Langmuir* 18:26–30.
225. Bock N, Woodruff MA, Hutmacher DW, Dargaville TR. 2011. Electro spraying, a reproducible method for production of polymeric microspheres for biomedical applications. *Polymers (Basel)* 3:131–149.
226. Vonnegut B, Neubauer RL. 1952. Production of monodisperse liquid particles by electrical atomization. *J Colloid Sci* 7:616–622.
227. Zeleny J. 1914. The electrical discharge from liquid points, and a hydrostatic method of measuring the electric intensity at their surfaces. *Phys Rev* 3:69–91.
228. Taylor G. 1964. Disintegration of water drops in an electric field. *Proc R Soc A Math Phys Eng Sci* 280:383–397.
229. Nguyen DN, Clasen C, Van den Mooter G. 2016. Pharmaceutical applications of electro spraying. *J Pharm Sci* 105:2601–2620.
230. Luo C, Okubo T, Nangrejo M, Edirisinghe M. 2015. Preparation of polymeric nanoparticles by novel electro spray nanoprecipitation. *Polym Int* 64:183–187.
231. Tapia-Hernández JA, Torres-Chávez PI, Ramírez-Wong B, Rascón-Chu A, Plascencia-Jatomea M, Barreras-Urbina CG, Rangel-Vázquez NA, Rodríguez-Félix F. 2015. Micro- and Nanoparticles by Electro spray: Advances and Applications in Foods. *J Agric Food Chem* 63:4699–4707.
232. Sridhar R, Ramakrishna S. 2013. Electro sprayed nanoparticles for drug delivery and pharmaceutical applications. *Biomatter* 3:1–12.
233. Jaworek A. 2007. Micro- and nanoparticle production by electro spraying. *Powder Technol* 176:18–35.
234. Wu Y, Duong A, James L, E. B. 2012. Electro spray production of nanoparticles for drug/nucleic acid delivery, p. 224–242. *In Hashim, AA (ed.), The Delivery of Nanoparticles. InTech.*
235. Levelt Sengers J. 1979. Liquidons and gasons; controversies about the continuity of states. *Phys A Stat Mech its Appl* 98:363–402.
236. Habbay J, Hogarth J. 1879. On the solubility of solids in gases. *Proc R Soc london* 29:324–326.
237. Bhatia S. 2016. Nanoparticles types, classification, characterization, fabrication

- methods and drug delivery Applications, p. 1–225. *In* Natural Polymer Drug Delivery Systems: Nanoparticles, Plants, and Algae, 1st ed. Springer International Publishing, Cham.
238. Byrappa K, Ohara S, Adschiri T. 2008. Nanoparticles synthesis using supercritical fluid technology - towards biomedical applications. *Adv Drug Deliv Rev* 60:299–327.
239. Kankala RK, Zhang YS, Wang S Bin, Lee CH, Chen AZ. 2017. Supercritical fluid technology: An emphasis on drug delivery and related biomedical applications. *Adv Healthc Mater* 6:1–31.
240. Sekhon BS. 2010. Supercritical fluid technology: An overview of pharmaceutical applications. *Int J PharmTech Res* 2:810–826.
241. Bhardwaj L, Sharma PK, Visht S, Garg VK, Kumar N. 2010. A review on methodology and application of supercritical fluid technology in pharmaceutical industry. *Der Chem Sin* 1:183–194.
242. Ventosa N, Sala S, Veciana J, Torres J, Llibre J. 2001. Depressurization of an expanded liquid organic solution (DELLOS): A new procedure for obtaining submicron- or micron-sized crystalline particles. *Cryst Growth Des* 1:299–303.
243. Kawakatsu T, Trägårdh G, Trägårdh C. 2001. Production of W/O/W emulsions and S/O/W pectin microcapsules by microchannel emulsification. *Colloids Surfaces A Physicochem Eng Asp* 189:257–264.
244. Quintanilla-Carvajal MX, Camacho-Díaz BH, Meraz-Torres LS, Chanona-Pérez JJ, Alamilla-Beltrán L, Jiménez-Aparicio A, Gutiérrez-López GF. 2010. Nanoencapsulation: A new trend in food engineering processing. *Food Eng Rev* 2:39–50.
245. Rolland JP, Maynor BW, Euliss LE, Exner AE, Denison GM, Desimone JM. 2005. Direct fabrication and harvesting of monodisperse, shape-specific nanobiomaterials. *J Am Chem Soc* 127:10096–10100.
246. Gratton SEA, Pohlhaus PD, Lee J, Guo J, Cho MJ, DeSimone JM. 2007. Nanofabricated particles for engineered drug therapies: A preliminary biodistribution study of PRINT™ nanoparticles. *J Control Release* 121:10–18.
247. Canelas D a, Canelas D a, Herlihy KP, Herlihy KP, Desimone JM, Desimone JM. 2009. Top-down particle fabrication: control of size and shape for diagnostic imaging and drug delivery. *Wiley Interdiscip Rev Nanomedicine Nanobiotechnology* 1:391–404.
248. Lee CR, Mckenzie CA, Webster KD, Whaley R. 1991. Pegademase bovine: replacement

- therapy for severe combined immunodeficiency disease. *DICP, Ann Pharmacother* 25:1092–1095.
249. Hartsel S, Bolard J. 1996. Amphotericin B: new life for an old drug. *Trends Pharmacol Sci* 12:445–449.
250. Taylor A, Wilson KM, Murray P, Fernig DG, Lévy R. 2012. Long-term tracking of cells using inorganic nanoparticles as contrast agents: are we there yet? *Chem Soc Rev* 41:2707–2717.
251. Schweiger C. 2010. Magnetic iron oxide nanoparticles as potential contrast agents for magnetic resonance imaging.
252. Maier-Hauff K, Ulrich F, Nestler D, Niehoff H, Wust P, Thiesen B, Orawa H, Budach V, Jordan A. 2011. Efficacy and safety of intratumoral thermotherapy using magnetic iron-oxide nanoparticles combined with external beam radiotherapy on patients with recurrent glioblastoma multiforme. *J Neurooncol* 103:317–324.
253. Youngster S, Wang YS, Grace M, Bausch J, Bordens R, Wyss DF. 2002. Structure, biology, and therapeutic implications of pegylated interferon alpha-2b. *Curr Pharm Des* 8:2139–2157.
254. Rajender Reddy K, Modi MW, Pedder S. 2002. Use of peginterferon alfa-2a (40 KD) (Pegasys) for the treatment of hepatitis C. *Adv Drug Deliv Rev* 54:571–586.
255. Camardo J. 2003. The Rapamune era of immunosuppression 2003: The journey from the laboratory to clinical transplantation. *Transplant Proc* 35:18–24.
256. Rains A, Scahill L. 2004. New long-acting stimulants in children with ADHD. *J Child Adolesc Psychiatr Nurs* 17:177–179.
257. McGough JJ, Pataki CS, Suddath R. 2005. Dexamethylphenidate extended-release capsules for attention deficit hyperactivity disorder. *Expert Rev Neurother* 5:437–441.
258. Bucholz RW. 2002. Nonallograft osteoconductive bone graft substitutes. *Clin Orthop Relat Res* 395:44–52.
259. Thorwarth M, Schultze-Mosgau S, Kessler P, Wiltfang J, Schlegel KA. 2005. Bone regeneration in osseous defects using a resorbable nanoparticulate hydroxyapatite. *J Oral Maxillofac Surg* 63:1626–1633.
260. Delloye C, Cnockaert N, Cornu O. 2003. Bone substitutes in 2003: an overview. *Acta Orthop Belg* 69:1–8.
261. Murugan R, Ramakrishna S. 2005. Development of nanocomposites for bone grafting.

- Compos Sci Technol 65:2385–2406.
262. Baluch AS. 2005. Angstrom Medica: Securing FDA Approval and Commercializing a Nanomedical Device. *Nanotechnol Law Bus* 2:168–174.
263. 2009. ETEX corporation announces additional FDA clearance for equivaBone[R], the first hard setting osteoconductive and osteoinductive bone graft substitute. *Blood Wkly*.
264. Ennis B. 2008. Nanocrystalline bone graft is replaced by new bone growth. *Adv Mater Process* 166:S6.
265. Reimer P, Balzer T. 2003. Ferucarbotran (Resovist): A new clinically approved RES-specific contrast agent for contrast-enhanced MRI of the liver: Properties, clinical development, and applications. *Eur Radiol* 13:1266–1276.
266. Rodman MJ. 1991. FDA approvals: new drugs, new uses. *RN* 54:61–66.
267. Melmed GY, Targan SR, Yasothan U, Hancq D, Kirkpatrick P. 2008. Certolizumab pegol. *Nat Rev Drug Discov* 7:641–642.
268. Johnson KP. 1996. Management of relapsing/remitting multiple sclerosis with copolymer I (Copaxone). *Mult Scler* 1:325–326.
269. Sartor O. 2003. Eligard: Leuprolide acetate in a novel sustained-release delivery system. *Urology* 61:25–31.
270. Baker DE. 2002. New drugs approved by the FDA; new dosage forms and indications; agents pending FDA approval; labeling changes related to safety. *Hosp Pharm* 37:1318–1335.
271. Renaud RC, Xuereb H. 2003. From the analyst's couch: Vision impairment therapies. *Nat Rev Drug Discov* 2:425–426.
272. Curran, Monique P, McCormack PL. 2008. Methoxy polyethylene glycol-epoetin beta: A review of its use in the management of anaemia associated with chronic kidney disease. *Drugs* 68:1139–1156.
273. 2002. Boosting WBC counts during chemotherapy. *Nursing (Lond)* 32:18.
274. Foubister V. 2003. Novel candidate for treatment of haematopoietic disorders. *Drug Discov Today* 8:659–660.
275. Nagano N, Miyata S, Obana S, Ozai M, Kobayashi N, Fukushima N, Burke SK, Wada M. 2001. Sevelamer hydrochloride (Renagel), a non-calcaemic phosphate binder, arrests parathyroid gland hyperplasia in rats with progressive chronic renal insufficiency.

- Nephrol Dial Transpl 16:1870–1878.
276. LoBuono C. 2003. New acromegaly drug first to block growth hormone receptors. *Drug Topics* 147:17.
277. British T, Journal M. 1995. Therapy for all evades immune reaction. *Am J Nurs* 95:56–60.
278. Alconcel SNS, Baas AS, Maynard HD. 2011. FDA-approved poly(ethylene glycol)–protein conjugate drugs. *Polym Chem* 2:1442.
279. Annibali V, Mechelli R, Romano S, Buscarinu MC, Fornasiero A, Umeton R, Ricigliano VAG, Orzi F, Coccia EM, Salvetti M, Ristori G. 2015. IFN- β and multiple sclerosis: From etiology to therapy and back. *Cytokine Growth Factor Rev* 26:221–228.
280. Turecek PL, Romeder-Finger S, Apostol C, Bauer A, Crocker-Buqué A, Burger DA, Schall R, Gritsch H. 2016. A world-wide survey and field study in clinical haemostasis laboratories to evaluate FVIII:C activity assay variability of adynovate and obizur in comparison with advate. *Haemophilia* 22:957–965.
281. Cohen MH, Shen YL, Keegan P, Pazdur R. 2009. FDA Drug approval summary: Bevacizumab (Avastin(R)) as treatment of recurrent glioblastoma multiforme. *Oncologist* 14:1131–1138.
282. Guaglianone P, Chan K, DelaFlor-Weiss E, Hanisch R, Jeffers S, Sharma D, Muggia F. 1994. Phase I and pharmacology study of liposomal daunorubicin (DaunoXome). *Invest New Drugs* 12:103–110.
283. Forssen E. 1997. The design and development of DaunoXome for solid tumor targeting in vivo. *Adv Drug Deliv Rev* 24:133–150.
284. Chang H, Yeh M-K. 2012. Clinical development of liposome-based drug: formulation, characterization, and therapeutic efficacy. *Int J Nanomedicine* 7:49–60.
285. Glantz MJ, Jaeckle KA, Chamberlain MC, Phuphanich S, Recht L, Swinnen LJ, Maria B, LaFollette S, Schumann GB, Cole BF, Howell SB. 1999. A randomized controlled trial comparing intrathecal sustained-release cytarabine (DepoCyt) to intrathecal methotrexate in patients with neoplastic meningitis from solid tumors. *Clin Cancer Res* 5:3394–3402.
286. Silverman JA, Deitcher SR. 2013. Marqibo® (vincristine sulfate liposome injection) improves the pharmacokinetics and pharmacodynamics of vincristine. *Cancer Chemother Pharmacol* 71:555–564.

287. Iwamoto T. 2013. Clinical application of drug delivery systems in cancer chemotherapy: Review of the efficacy and side effects of approved drugs. *Biol Pharm Bulliten* 36:715–718.
288. Ma Y, Wang H, Yang Y, Logsdon CD, Ullrich SE, Hwu P, Maitra A. 2016. Recent advancements in pancreatic cancer immunotherapy. *Cancer Res Front* 2:252–276.
289. Rust D, Jameson G. 1998. The novel lipid delivery system of amphotericin B: drug profile and relevance to clinical practice. *Oncol Nurs Forum* 25:35–48.
290. Zhao K, Reiner J, Xie W. 2001. FDA New drug approvals in 2000. *Front Biotechnol Pharm* 2:329–349.
291. Gambling D, Hughes T, Martin G, Horton W, Manvelian G. 2005. A comparison of Depodur, a novel, single-dose extended-release epidural morphine, with standard epidural morphine for pain relief after lower abdominal surgery. *Anesth Analg* 100:1065–1074.
292. Ning Y, He K, Dagher R, Sridhara R, Farrel A, Justice R, Pazdur R. 2007. Liposomal Doxorubicin in combination with Bortezomib for relapsed or refractory multiple myeloma. *Oncol J* 21.
293. Vidyasagar D. 1999. Anaesthesia and intensive care in neonates and children, *In Salvo, I, Vidyasagar, D (eds.), Anaesthesia and intensive care in neonates and children*, 1st ed. Springer Milan, Milano.
294. James S, Marvin H, Martin S, Raymond J, Craig W. 2002. The safety of Estrasorb, a new topical emulsion technology for systemic delivery of estradiol. *Obstet Gynecol* 99:61.
295. 2003. Estradiol-Topical - Novavax. *Drugs R D* 4:49–51.
296. Farokhzad OC, Langer R. 6AD. Nanomedicine: Developing smarter therapeutic and diagnostic modalities. *Adv Drug Deliv Rev* 58:1456–1459.
297. Haley B, Frenkel E. 2008. Nanoparticles for drug delivery in cancer treatment. *Urol Oncol Semin Orig Investig* 26:57–64.
298. Lerner, Itzhak E, Rosenberger V, Flashner-Barak M, Drabkin A, Moldavski N. 2006. Formulations of Fenofibrate. 2006/0222707 A1. United States Pat Appl Publ. United States.
299. Till MC, Simkin MM, Maebius S. 2005. Nanotech meets the FDA: A success story about the first nanoparticulate drugs approved by the FDA. *Nanotechnol Law Bus* 2:163–167.
300. Portenoy RK, Sciberras A, Eliot L, Loewen G, Butler J, Devane J. 2002. Steady-state

- pharmacokinetic comparison of a new, extended-release, once-daily morphine formulation, avinza™, and a twice-daily controlled-release morphine formulation in patients with chronic moderate-to-severe pain. *J Pain Symptom Manage* 23:292–300.
301. McLain D. 2002. An open label dose finding trial of Tizanidine (Zanaflex™) for treatment of fibromyalgia. *J Musculoskelet Pain* 10:7–18.
 302. Gao Y, Li Z, Sun M, Guo C, Yu A, Xi Y, Cui J, Lou H, Zhai G. 2011. Preparation and characterization of intravenously injectable curcumin nanosuspension. *Drug Deliv* 18:131–142.
 303. Poor MC, Diaz DR. 2009. New developments in the treatment of schizophrenia. *Ann Am psychotherapy Assoc* 12:40–41.
 304. Zavilla CM, Skledar S, Lang MB, Gross C. 2016. Implementation of a new dantrolene formulation across a multifacility health system. *Am J Heal Pharm* 73:463–467.
 305. Rosner MH, Auerbach M. 2011. Ferumoxytol for the treatment of iron deficiency. *Expert Rev Hematol* 4:399–405.
 306. Bailie GR, Johnson CA, Mason NA. 2000. Parenteral iron use in the management of anemia in end-stage renal disease patients. *Am J Kidney Dis* 35:1–12.
 307. Bailie GR, Johnson CA, Mason NA. 2000. Parenteral iron products for anemia in end-stage renal disease: Comparative considerations. *Formulary* 35:498–513.
 308. Chertow GM, Mason PD, Vaage-Nilsen O, Ahlmén J. 2006. Update on adverse drug events associated with parenteral iron. *Nephrol Dial Transplant* 21:378–382.
 309. Johnson CA, Mason NA, Bai. 1999. Intravenous iron products. *ANNA Journal* 1 26:522–524.
 310. Auerbach M, Ballard H. 2010. Clinical use of intravenous iron: Administration, efficacy, and safety. *Hematology* 2010:338–347.
 311. Zou P, Tyner K, Raw A, Lee S. 2017. Physicochemical characterization of iron carbohydrate colloid drug products. *AAPS J* 19:1359–1376.
 312. Wang Y-XJ, Hussain SM, Krestin GP. 2001. Superparamagnetic iron oxide contrast agents: physicochemical characteristics and applications in MR imaging. *Eur Radiol* 11:2319–2331.
 313. Häfeli UO. 2004. Magnetically modulated therapeutic systems. *Int J Pharm* 277:19–24.
 314. Barbour KE, Helmick CG, Boring M, Brady TJ. 2017. Vital Signs: Prevalence of doctor-diagnosed arthritis and arthritis-attributable activity limitation — United States, 2013–

2015. *Morb Mortal Wkly Rep* 66:246–253.
315. Helmick CG, Watkins-Castillo SI. 2014. The burden of musculoskeletal diseases in the United States: prevalence, societal and economic costs. *United States bone Jt Initiat*, 3rd ed.
316. Wolford ML, Palso K, Bercovitz A, Monica L. Wolford, M.A.; Kathleen Palso, M.A.; and Anita Bercovitz, M.P.H. PD. 2015. Hospitalization for total hip replacement among inpatients aged 45 and over: United States, 2000–2010Nchs.
317. Derar H, Shahinpoor M. 2015. Recent patents and designs on hip replacement prostheses. *Open Biomed Eng J* 9:92–102.
318. Parvizi J, Zmistowski B, Berbari EF, Bauer TW, Springer BD, Della Valle CJ, Garvin KL, Mont MA, Wongworawat MD, Zalavras CG. 2011. New Definition for periprosthetic joint infection: from the workgroup of the Musculoskeletal Infection Society. *Clin Orthop Relat Res* 469:2992–2994.
319. Parvizi J, Aggarwal V, Rasouli M. 2013. Periprosthetic joint infection: Current concept. *Indian J Orthop* 47:10–17.
320. Tande AJ, Patel R. 2014. Prosthetic joint infection. *Clin Microbiol Rev* 27:302–345.
321. Song Z, Borgwardt L, Høiby N, Wu H, Sørensen TS, Borgwardt A. 2013. Prosthesis infections after orthopedic joint replacement: the possible role of bacterial biofilms. *Orthop Rev (Pavia)* 5:65–71.
322. Pulido L, Ghanem E, Joshi A, Purtill JJ, Parvizi J. 2008. Periprosthetic Joint Infection: the incidence, timing, and predisposing factors. *Clin Orthop Relat Res* 466:1710–1715.
323. Katz JN, Wright J, Wright EA, Losina E. 2009. Failures of Total Hip Replacement: A Population-Based Perspective. *Orthop J Harvard Med Sch* 9:101–106.
324. Osmon DR, Berbari EF, Berendt AR, Lew D, Zimmerli W, Steckelberg JM, Rao N, Hanssen A, Wilson WR. 2013. Diagnosis and management of prosthetic joint infection: Clinical practice guidelines by the infectious diseases Society of America. *Clin Infect Dis* 56:1–25.
325. Dominici M, Le Blanc K, Mueller I, Slaper-Cortenbach I, Marini F, Krause D, Deans R, Kreating A, Prockop D, Horwitz E. 2006. Minimal criteria for defining multipotent mesenchymal stromal cells: the International Society for Cellular Therapy position statement. *Cytotherapy* 8:315–317.
326. Peister A, Mellad JA, Larson BL, Hall BM, Gibson LF, Darwin J, Dc W, Prockop DJ. 2011.

- Adult stem cells from bone marrow (MSCs) isolated from different strains of inbred mice vary in surface epitopes , rates of proliferation , and differentiation potential Adult stem cells from bone marrow (MSCs) isolated from different strains of inbre. *Blood* 103:1662–1668.
327. Ohishi M, Schipani E. 2010. Bone marrow mesenchymal stem cells. *J Cell Biochem* 109:277–282.
328. Prockop DJ. 1997. Marrow Stromal Cells as Stem Cells for Nonhematopoietic Tissues. *Science* (80-) 276:71–74.
329. Friedenstein A, Chailakhyan R, Latsinik N, Panasyuk A, Keiliss-Borok I. 1974. Stromal cells responsible for transferring the microenvironment of the hematopoietic tissues. Cloning in vitro and retransplantation in vivo. *Transplantation* 17:331–340.
330. Castro-Malaspina H, Gay RE, Resnick G, Kapoor N, Meyers P, Chiarieri D, McKenzie S, Broxmeyer HE, Moore MAS. 1980. Characterization of human bone marrow fibroblast colony-forming cells (CFU-F) and their progeny. *Blood* 56:289–301.
331. Pittenger MF, Mackay AM, Beck SC, Jaiswal RK, Douglas R, Mosca JD. 1999. Multilineage potential of adult human mesenchymal stem cells. *Science* (80-) 284:143–149.
332. Jacobs FA, Sadie-Van Gijsen H, van de Vyver M, Ferris WF. 2016. Vanadate impedes adipogenesis in mesenchymal stem cells derived from different depots within bone. *Front Endocrinol (Lausanne)* 7:1–12.

STELLENBOSCH UNIVERSITY

Chapter 3

Characterization and cytotoxicity analysis of a novel antimicrobial
compound produced by a strain of
Xenorhabdus khoisanae

Characterization and cytotoxicity analysis of a novel antimicrobial compound produced by a strain of *Xenorhabdus khoisanae*

Elzaan Booysen^a, Hanél Sadie-Van Gijsen^b, Jonike Dreyer^a, Anton Du Preez van Staden,^c Marina Rautenbach^d, Shelly M Deane^a and Leon MT Dicks^a

Department of Microbiology, Stellenbosch University, Stellenbosch, South Africa^a; Division of Endocrinology, Department of Medicine, Stellenbosch University, Parow, South Africa^b; Department of Physiological Sciences, Stellenbosch University, Stellenbosch, South Africa^c; Department of Biochemistry, Stellenbosch University, Stellenbosch, South Africa^d

The increase in antibiotic resistance has shifted the focus towards screening microorganisms from less explored niches for novel antimicrobial compounds. In this study, we report on the isolation and purification of two xenocoumacin 2–like antibiotics and a novel broad-spectrum antimicrobial compound from a strain of *Xenorhabdus khoisanae* associated with the entomopathogenic nematode *Steinernema khoisanae*. Both antibiotics have a mass-to-charge (m/z) ratio of 407, similar to that reported for xenocoumacin 2. The larger antimicrobial compound (m/z ratio = 671) has not yet been reported. The three compounds were isolated by exposing colonies to XAD-16 beads. The hydrophobic extracts from colonies was further purified by HPLC. Fractions collected from three peaks were active against *Staphylococcus aureus* Xen 31 (methicillin-resistant) and Xen 36 (methicillin-sensitive). Further characterisation was done by UHPLC-MS (ultra-high-pressure liquid chromatography-tandem mass spectrometry) and UV-Spectrum analysis. This is the first report of xenocoumacin-like antibiotics and an antimicrobial compound with a m/z ratio of 671 produced by *X. khoisanae*. The antimicrobial compound, named rhabdin, is cytotoxic to mesenchymal stem cells (MSCs), but only at levels exceeding 3.5 mg/L. Further characterization by H^3 -NMR is in progress.

INTRODUCTION

In the early-to-mid 1900s, more than 20 novel classes of antibiotics were discovered (1, 2), but only three novel classes have entered the market since 1962 (3). Microorganisms from unique environments, and living in close symbiotic relationship with their hosts, may be a source of novel antibiotics or antibiotic-like compounds. The genus *Xenorhabdus*, classified as a member of the family Enterobacteriaceae, lives in close association with nematodes of the genus *Steinernema*, which in turn infects insects from various orders including Lepidoptera, Diptera, Orthoptera, Coleoptera and Hymenoptera (4). Once a nematode is infected with *Xenorhabdus*, the bacterial cells produce antimicrobial compounds, including antibiotics and bacteriocins to exclude other microorganisms (5). These compounds produced by *Xenorhabdus* are so successful at eradicating other microorganisms that pure cultures are isolated directly from infected nematodes. Only a few papers have been published on the antimicrobial properties of *Xenorhabdus* spp. (6–16).

The eradication of biofilm-forming bacteria, especially on prosthetic implants, is extremely difficult. *Staphylococcus aureus* is associated with 38% of prosthetic joint infections (PJIs) (17). Of these strains, 53% were methicillin-resistant (17, 18). Other pathogens include coagulase-negative staphylococci (19, 20), *Escherichia coli* and *Klebsiella pneumoniae* (17). In severe cases of PJIs, different combinations of antibiotics have to be administered intravenously for 2 to 6 weeks (21). Bactericidal antibiotics such as rifamycins, lipiarmycins, quinolones and sulfonamides that inhibit the transcription of RNA and protein synthesis, are usually used to treat prosthetic PJIs (20, 22). Of these, rifamycins have the best biofilm penetration properties (19). However, due to constant single-point mutations in the RNA polymerase gene, pathogens treated with rifamycins develop resistance rapidly (19). Rifamycins should thus always be used in combination with other antibiotics, such as levofloxacin (a fluoroquinolone). Quinolones have a different target site and inhibit the function of DNA gyrase and topoisomerase IV, thus DNA replication (23).

Treatment with an oral rifampicin- fluoroquinolone combination may be as long as 6 months, depending on the severity of the infection (21). If the infection persists, the prosthesis needs to be removed and the infected joint flushed with antibiotics (referred to as one-step revision

surgery). Patients are then usually put on a 12-week antibiotic course. Once the infection has cleared, a new prosthesis is inserted (18). In severe cases, two-step revision surgery is performed. This entails removal of the infected prosthesis and filling the area with an antibiotic-augmented cement spacer (13, 14). A new prosthesis is implanted only when the infection has been eradicated (18, 24). Apart from being a stressful experience, complications from PJIs are unpredictable, with a success rate ranging from 14 to 100% (19).

Treatment of osteoarthritis (OA), a condition affecting more than one out of four elderly people, usually involves total hip arthroplasty (THA), i.e. the insertion of a metallic prosthesis into the proximal region of the femur, replacing the femur head and neck (5, 6). Although most THAs are successful, cases of PJI caused by a bacterial biofilm forming on the prosthesis and spreading to adjacent tissue, are frequently reported (7–10). In most cases, the infection is caused by strains resistant to multiple antibiotics, including methicillin (29).

The effect of direct (as opposed to systemic) antibiotic treatment on bone formation and remodelling is largely unknown and has not been studied in depth. Bone marrow-derived mesenchymal stromal cells (bmMSCs) have traditionally been used as an *in vitro* model to study the differentiation and functions of osteoblasts (bone-forming cells). However, more recently, a distinct population of MSCs residing in the proximal end of the femur, near the hip joint, was identified and characterised (30). These proximal femur-derived mesenchymal stromal cells (pfMSCs) are phenotypically similar to bmMSCs, but functionally distinct, with decreased osteogenic potential and increased sensitivity to the cytotoxic effects of glucocorticoids (30). Given that this sensitive population of MSCs resides in the exact areas of bone tissue involved in THA, it is possible that THA failure may disproportionately affect these cells, resulting in progressive bone damage. In addition, the possible cytotoxic effects of aggressive antibiotic treatment on this MSC population may cause long-term damage to the integrity of the femoral bone, preventing full recovery from THA revision after PJI.

The discovery of new antibiotics with a broad spectrum of bactericidal activity is of paramount importance. In the present study, we describe two xenocoumacin 2-like antibiotics and a novel broad-spectrum antimicrobial compound produced by a strain of *X. khoisanae*. We also describe the effect of the broad-spectrum antimicrobial compound on bone marrow cells.

MATERIALS AND METHODS

Materials. Bacterial growth medium was sourced from Biolab Diagnostics (Midrand, South Africa), unless stated otherwise. Trifluoroacetic acid (TFA), XAD-16 beads, triethylamine, carboxymethyl resin and all constituents of osteogenic differentiation media were obtained from Sigma-Aldrich (Missouri, USA). All solvents were obtained from Merck-Millipore (St. Louis, Massachusetts, USA), unless stated otherwise. SepPak C18 Columns were obtained from Waters (Milford, Massachusetts, USA). Pierce™ BCA Protein Assay Kit (BCA) was sourced from Thermofisher Scientific (Waltham, Massachusetts, USA). Dulbecco's Modified Eagle Medium (DMEM), Penicillin/Streptomycin (Pen-Strep), trypsin and Hanks' Balanced Salt Solution were obtained from Lonza (Basel, Switzerland). Fetal bovine serum (FBS) was sourced from Biochrom (Berlin, Germany) and collagenase I (#CLS1) was sourced from Worthington Biochemical Corporation (Lakewood, USA). Cell culture dishes were obtained from NEST Biotechnology (New Jersey, USA). Sodium pentobarbitone (Eutha-naze) was sourced from Bayer (Kempton Park, Gauteng, South Africa). All mass spectrometry analysis was done with the help of the Liquid Chromatography Mass Spectrometry (LCMS) unit of the Central Analytical Facility at Stellenbosch University. Unless otherwise stipulated water, used in experiments was of analytical grade.

Bacterial growth conditions. A strain of *X. khoisanae* was isolated from a nematode-infected soil sample in the Western Cape. Soil, suspended in sterile water, was plated onto NBTA (Nutrient Agar supplemented with 0.025%, w/v bromothymol blue and 0.004%, w/v triphenyltetrazolium chloride, TTC) and incubated at 30°C for at least 48 h. Phase I cells, identified by the formation of blue colonies with the uptake of TTC and considered infective (5), were selected for further research. *Staphylococcus aureus* Xen 31 (methicillin-resistant) and *S. aureus* Xen 36 (methicillin-sensitive) were cultured in Brain Heart Infusion (BHI) broth and streaked onto BHI agar. Tubes and plates were incubated at 37°C for at least 24 h.

Isolation and purification of antimicrobial agent. *Xenorhabdus khoisanae* was cultured in Tryptic Soy Broth (TSB) for 24 h at 30°C, and then streaked out onto Tryptic Soy Agar (TSA). A single colony was transferred to 10 ml TSB, which had been treated with XAD-16 beads (5 g/10 ml) for 30 min at 4°C before autoclaving for 15 min at 121°C, and vortexed.

The cell suspension was then mixed with 5 g sterile XAD-16 beads, plated out onto TSA treated with XAD-16 beads (2%, w/v, agar; 150mm diameter plates) and incubated at 26°C for 96 h. The XAD-16 beads were removed from the surface of the agar, using a sterile metal scraper and suspended in double-distilled water (ddH₂O). The beads were washed with 30% (v/v) ethanol (25 ml/5 g beads).

Hydrophobic compounds were eluted from the XAD-16 beads, using 80% (v/v) isopropanol containing 0.1% (v/v) TFA (80% ISO-TFA; 40 ml/5 g beads). Isopropanol was removed by evaporation under vacuum using a rotary evaporator (Rotavapor R-114, Büchi) connected to a water bath (Waterbath B-480, Büchi), and compounds were concentrated by freeze-drying. The freeze-dried crude extract was suspended in ddH₂O and tested for antimicrobial activity against *S. aureus* Xen 31 and *S. aureus* Xen 36, respectively. Overnight cultures of the two strains (300 µl each) were inoculated into 30 ml melted BHI Agar (1%, v/v, agar, cooled to 40°C), swirled and plated out. Wells were made into the solidified agar with a sterile glass Pasteur pipette (5 mm in diameter) and filled with 20 µl aliquots of each fraction. Plates were incubated at 37°C for 24 h. A clear zone surrounding the well indicated antimicrobial activity.

The hydrophobic crude extract was injected onto a Discovery BIO Wide Pore C18 HPLC column (10 µm, 250 x 10 mm, Sigma-Aldrich). The chromatographic system comprised of two Waters 510 pumps, controlled by MAXIMA software. Injections were controlled manually. Absorbance were taken with a Waters 440 detector at 254 nm. An increasing linear gradient of 10% to 100% of solution B in solution A over 12 min (Solution A: de-ionized water containing 0.1% TFA, v/v, and solution B: acetonitrile containing 0.1% TFA, v/v) was applied (Table S1). Fractions collected were concentrated by freeze-drying and antimicrobial activity confirmed as described elsewhere. Freeze-dried samples were suspended in sterile water and the protein content determined using the BCA protein assay according to the manufacturer's instructions. The HPLC program used is shown in supplementary Table S1.

Characterization. The net charge of the antimicrobial molecules eluted from the C18 HPLC column was determined using the method described by Yadav and co-workers (38), but slightly modified. Carboxymethyl resin was swollen in ddH₂O, packed into a column and activated with 2% (v/v) acetic acid. The column was washed with five volumes ddH₂O and the

resin charged using five volumes 2% (v/v) triethylamine (TEA). Three millilitres (10 mg/ml) of the active fractions were loaded onto the packed column. Anionic molecules were eluted using one volume 2% TEA, followed by three volumes of ddH₂O to collect all neutral molecules. Cationic molecules were eluted using 3 to 5 ml of 2% TEA. The antimicrobial activity of all fractions was tested as described elsewhere.

Active fractions collected from the HPLC were analysed using a Waters Quadrupole Time-of-Flight Synapt G2 (Waters Corporation, Milford, USA) mass spectrometer. Ultra-high-pressure liquid chromatography-tandem mass spectrometry (UHPLC-MS/MS) was used to record high-resolution mass spectra. For direct mass analysis, 3 µl of the sample (250 µg/ml, dissolved in 50% acetonitrile) was injected into a Z spray ionization source, and for UHPLC-MS analysis, 3 µl of the sample was injected and separated on an UPLC C18 column (Acquity UPLC HSS T3, 1.8 µm particle size, 2.1 x 150 mm, Waters Corporation, Milford, USA). The sample was separated using an increasing linear gradient of 30% to 60% solution B in solution A over 9 min (solution A: 0.1% formic acid and solution B: acetonitrile). The flow rate was 0.3 ml/min (Table S2). A capillary voltage of 2.5 kV, cone voltage of 15 V and source temperature of 120°C were used for both direct Electrospray Ionization mass spectrometry (ESI-MS) and UHPLC-MS analyses. All data obtained were analysed using Masslynx software version 4.1 (Waters Corporation, Milford, USA). The novel antimicrobial compound, observed as peak C3 on HPLC (Fig 1), was provisionally labelled as rhabdin.

Determination of MIC (minimum inhibitory concentration). Freeze-dried HPLC-purified rhabdin was dissolved in sterile ddH₂O and the concentration was determined using the BCA protein assay according to the manufacturer's instructions. A micro-broth dilution assay, described by Andrews (31), was used to determine the MIC of rhabdin. *Staphylococcus aureus* Xen 31 and *S. aureus* Xen 36 were used as indicator strains. Overnight culture of the two strains were each adjusted to an optical density (OD) of 0.11 (600 nm). Different concentrations of the antimicrobial compound were added to each strain, to obtain a final volume of 200 µl and OD of 0.1, and changes in growth observed by recording absorbance readings at 600 nm, immediately after addition, and 6 h and 24 h later.

Isolation and maintenance of MSC. Ethical clearance to use rats in preparing MSC was obtained

from the Research Ethics Committee: Animal Care and Use of Stellenbosch University (clearance number: SU-ACUD15-00012). The rats (male Wistar, 12 weeks old, with an average body mass of 250 g) were housed at the Stellenbosch University Animal Facility and kept according to the guidelines of the South African Medical Research Council. They were fed *ad libitum* on standard laboratory chow and sacrificed with an intraperitoneal injection of sodium pentobarbitone (12 mg/kg body mass).

Isolation of pfMSCs and bmMSCs was performed as described by Jacobs and co-workers (30). Femora were surgically removed and cleaned from muscle tissue using sterile gauze. The proximal regions of the femora were removed with sterile surgical side cutters, cut into 1 mm³ fragments and digested in Hanks' Balanced Salt Solution containing 0.075% (w/v) collagenase I and 1.5% (w/v) bovine serum albumin for 1 h at 37°C. The denuded bone fragments were washed five times with DMEM, seeded into a culture dish with isolation media (DMEM containing 1%, v/v, Pen-Strep, and 20%, v/v, FBS) and incubated at 37°C for 24h. The bone fragments were then washed with sterile phosphate-buffered saline (PBS), retained in the dish and submerged in standard growth media (SGM: DMEM containing 1%, v/v, Pen-Strep and 10%, v/v, FBS) for 7 to 10 days to allow migration of pfMSC from the fragments. bmMSCs were flushed from bone marrow cavities with 9 ml (3 ml per flush) cell isolation media collected in a cell culture dish (100 mm diameter). pfMSCs and bmMSCs were cultured at 37°C for 24 h in 95% humidified air and in the presence of 5% CO₂. Sterile PBS at 37°C was used to remove non-adherent tissue and the media was replaced with SGM.

Both cell types (pfMSCs and bmMSCs) were cultured to 80% confluence and then disaggregated with 1 ml 0.5% (w/v) trypsin and sub-cultured at a ratio of 1:4. All cell cultures were expanded to passage 3 before being used for further experiments. Cell growth media and treatments were replaced every 2-3 days. Cells were maintained at 37°C in 95% humidified air containing 5% CO₂ and were isolated as described by Jacobs and co-workers (30).

Cytotoxicity of antimicrobial compounds. MSCs at passage 3 were seeded into 12- well plates for crystal violet staining or 96-well plates for the MTT conversion assay, and grown until post-confluence in SGM. For crystal violet staining, cells were treated with increasing concentrations of rhabdin (1xMIC = 3.5 mg/l; 2.5xMIC = 8.75 mg/l; 4xMIC = 14.0 mg/l) for 7 days, fixed with 70%

(v/v) ethanol, stained for 5 min with 0.01 % (w/v) crystal violet and washed three times with PBS. The cells were destained with 75% (v/v) ethanol and absorbance measured at 570 nm. For the MTT conversion assay, cells were treated as described for crystal violet staining, with a final volume of 100 μ l media per well. The methodology for the assay was adapted from the protocol for the Sigma-Aldrich *in vitro* Toxicology Assay Kit (MTT-based, #TOX1). After 7 days of treatment with rhabdin, 10 μ l of 5 mg/ml MTT stock solution (Sigma-Aldrich #M2128) dissolved in DMEM, was added to each well and the plates incubated for 2h at 37°C in the dark. The colour reaction was stopped by adding 100 μ l solubilization solution (10%, v/v, Triton X-100 diluted with 0.1 N HCL in anhydrous isopropanol) to each well. Samples were incubated on a plate shaker to dissolve the colour product, and solubilization was further aided by repeated mixing with a pipette. Colour development was quantified spectrophotometrically at 570 nm to determine cell viability. Background absorbance was determined at 690 nm, and subtracted from the A_{570} values. A combination of cycloheximide (10 μ g/ml) and tumour necrosis factor- α (TNF- α) (5 ng/ml) was used as the positive control for cytotoxicity in bmMSCs, while 1 μ M dexamethasone was used as the positive control for cytotoxicity in pfMSCs, as reported previously (30). All experiments were performed with quadruplicate biological repeats.

MSC differentiation. For osteoblastic differentiation, bmMSCs and pfMSCs at passage 3 were plated in 12-well culture plates and cultured in SGM until post-confluence. Differentiation was induced with osteogenic media (OM: SGM supplemented with 50 μ M ascorbic acid, 10 mM β -glycerolphosphate and 10 nM dexamethasone) as described by Jacobs and co-authors (30). Differentiating cells were treated with increasing concentrations of rhabdin as described elsewhere, and results recorded after 7 days (bmMSCs) and 21 days (pfMSCs). The mineralized extracellular matrix of cells was stained with Alizarin Red S (ARS: Amresco, USA). Cells were washed with PBS, fixed with 70% (v/v) ethanol at 25°C for 5 min, rinsed twice with water and subsequently stained with 40 mM ARS (pH 4.0 - 4.1). The bmMSCs were stained for 2-4 hours, after which excess stain was removed. The wells were washed three times with water, once with PBS and an additional three times with water. Bound stain was extracted using 10% (w/v) cetylpyridinium chloride (CPC) dissolved in 10 mM Na_2HPO_4 (pH 7.0) and quantified spectrophotometrically at 562 nm. The pfMSCs were stained overnight with ARS and washed as described for bmMSCs. As pfMSCs have an impaired mineralization response compared to bmMSCs (30), staining was quantified using image analysis, which is more sensitive

than CPC extraction. Stained culture wells were visualized by light microscopy at 10x magnification using an Olympus CKX41 microscope. For analysis of each well, four random images (one in each quadrant) were photographed. As all experiments were performed in triplicate wells, this resulted in 12 images being captured for each experimental condition per independent experiment. Image analysis was performed using ImageJ image analysis software (version 1.51 J8). Images were converted into red-green-blue stacks and analyses were performed in the green channel. The threshold value (T=90) was set to exclude any non-specific background staining and remained unchanged throughout. For each image, the percentage area stained was recorded and an average of the percentage area stained for the 12 images per condition was calculated.

Statistical analysis. GraphPad Prism (version 5.01) was used for all statistical analyses and data were expressed as average \pm standard deviation. One-way ANOVA and Dunnett's *post hoc* test were used to analyse the data. When $P < 0.05$, the difference was considered to be statistically significant and indicated with an *.

RESULTS

Isolation, purification and MIC of antimicrobial compounds. Hydrophobic compounds extracted from the *X. khoisanae* culture separated into seven peaks when loaded onto the Discovery BIO Wide Pore C18 HPLC column (HPLC, Waters), as shown in **Fig 1**. Fractions from peaks C2, C3 and C4 were active against *S. aureus* Xen 31 and Xen 36. The MIC of fraction C3, as determined against both indicator strains, was 3.5 mg/l.

Characterization of novel antibiotic. Antimicrobial compounds collected from peaks C2, C3 and C4 (**FIG 1**) were positively charged. Separation by UHPL-MS and UV-Spectrum analysis revealed the presence of an antimicrobial compound with an m/z value of 407 in peaks C2 and C4 (**FIG 2A** and **C**). The fragmentation patterns of the antimicrobial compound in the two peaks were similar, yielding m/z values of 250, 232 and 158 (**FIG 1S**). The UV- Spectra of C2 and C4 were also similar, with a UV-max of 245 nm and 314 nm (not shown). The variation in hydrophobicity suggests that peaks C2 and C4 are two isomers of the same antimicrobial compound. The m/z

value of the antimicrobial compound in peaks C2 and C4 (407 m/z), fragmentation pattern and UV-Spectra are similar to that reported for xenocoumacin 2 (7). The antimicrobial compound from peak C3 contained a different parent ion, with a m/z of 671.413 (**FIG 2**) and a UV-max of 239 nm and 296 nm (not shown). MS-MS analysis of the antimicrobial compound in peak C3 indicated the presence of four fragments (473.275 m/z , 350.199 m/z , 268.227 m/z and 144.080 m/z , **FIG 3**). Further research was conducted on the compound from peak C3, labelled as rhabdin.

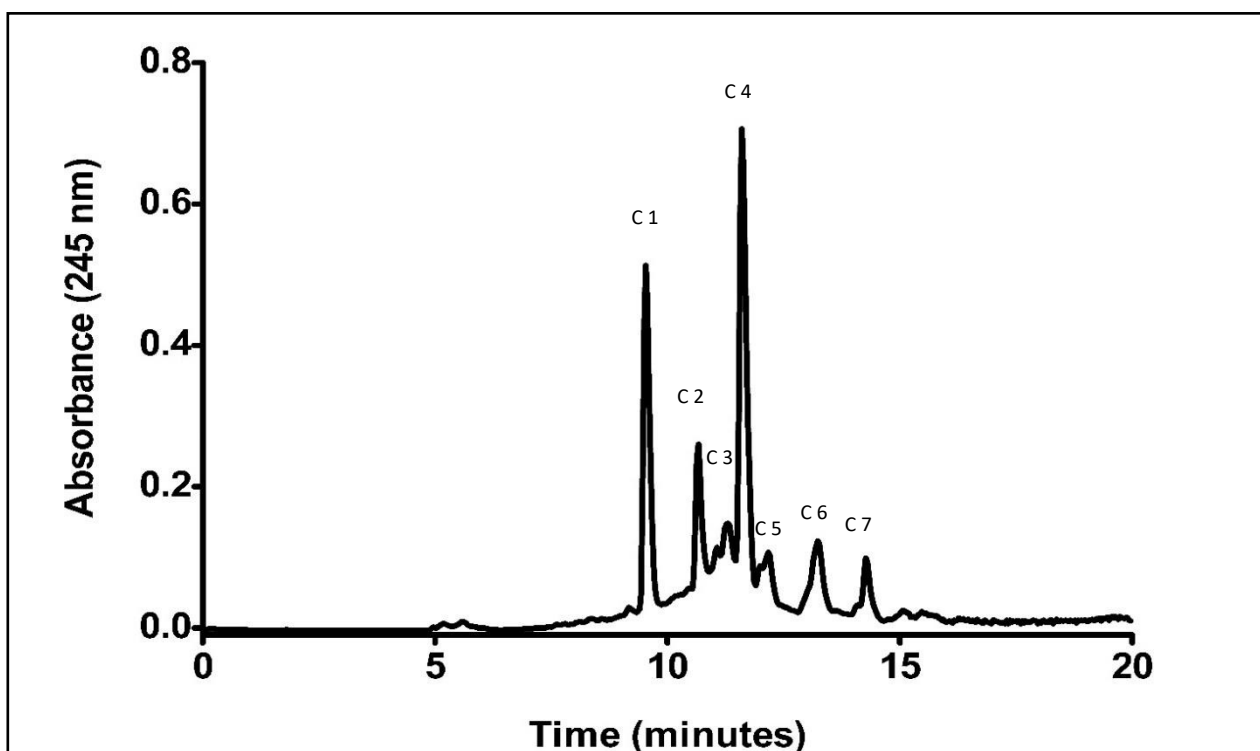


FIG 1: The chromatogram elution profile of the antimicrobial compounds isolated from a strain of *X. khoisanae*. The crude antimicrobial eluent was loaded onto a Discovery BIO Wide Pore C18 HPLC column and separated using a linear gradient of solution B in solution A from 10% to 100% over 12 min (Table S1). Seven peaks were collected, but only three peaks had antibacterial activity (Peak C 2,

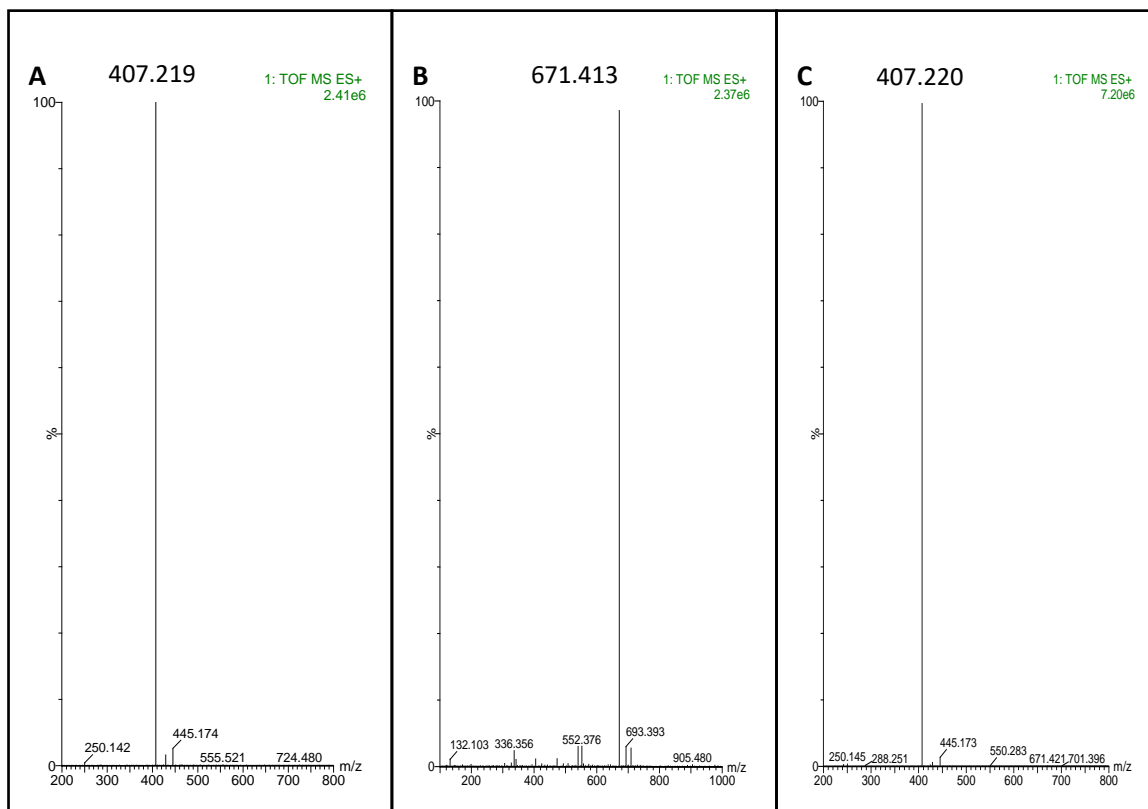


FIG 2: The LCMS spectrograms of peak C2, C3 and C4 (refer to the HPLC chromatogram in **FIG 1**). The m/z $[M + H^+]$ is shown above each peak. The main component present in peak C2 has a m/z $[M + H^+]$ of 407.219 (panel A); in peak C3 has a m/z $[M + H^+]$ of 671.413 (panel B) and in peak C4 has a m/z $[M + H^+]$ of 407.220 (panel C).

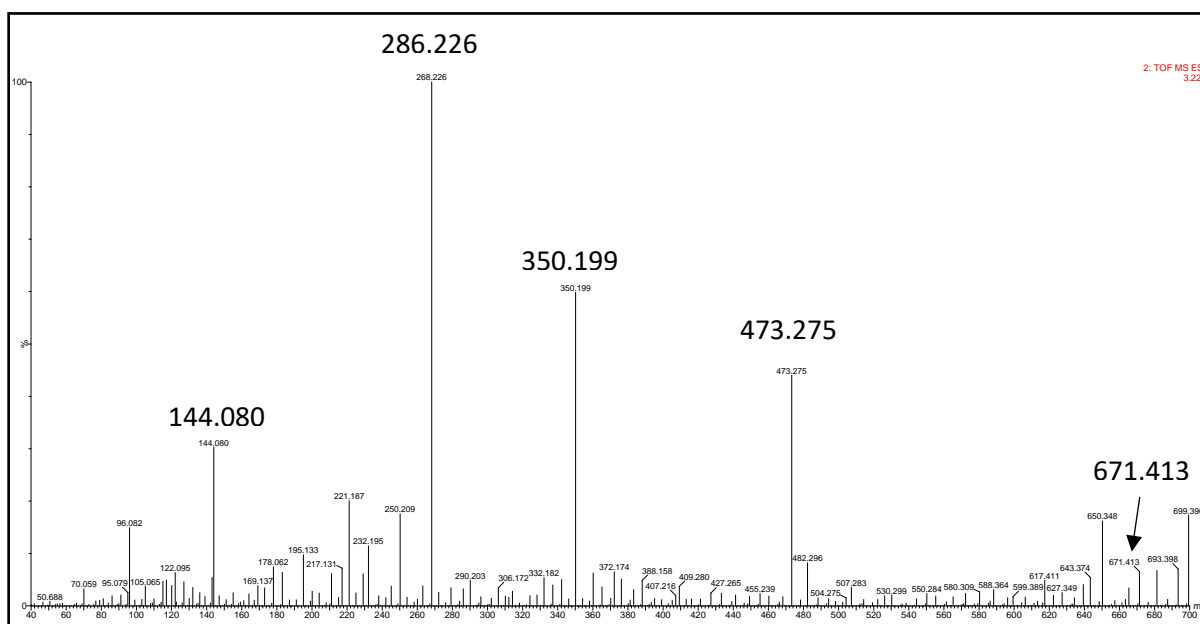


FIG 3: The MS/MS fragmentation pattern of C3 ($m/z = 671.413$). Four main fragments formed, with m/z ratios of 473.275, 350.199, 268.226 and 144.080.

Cytotoxicity. The cytotoxicity of rhabdin to rat MSCs was evaluated via crystal violet staining and the MTT conversion assay. Crystal violet stains all the cells present in the well (dead and alive), and therefore the MTT conversion assay was employed as a more sensitive indicator of cell viability and metabolic activity. At concentrations of 4 x MIC and 2.5 x MIC, rhabdin was cytotoxic to bmMSCs, while concentrations of 1 x MIC and lower (data not shown) were well tolerated by these cells (**FIG 4A**). The pfMSCs were more sensitive to rhabdin, with even 1 x MIC being cytotoxic to the cells (**FIG 4B**). The MTT assay (**FIG 5**) mostly supported the crystal violet staining results, with only a slight decrease observed in the metabolic activity for bmMSCs in the presence of 1 x MIC rhabdin (**FIG 5A**).

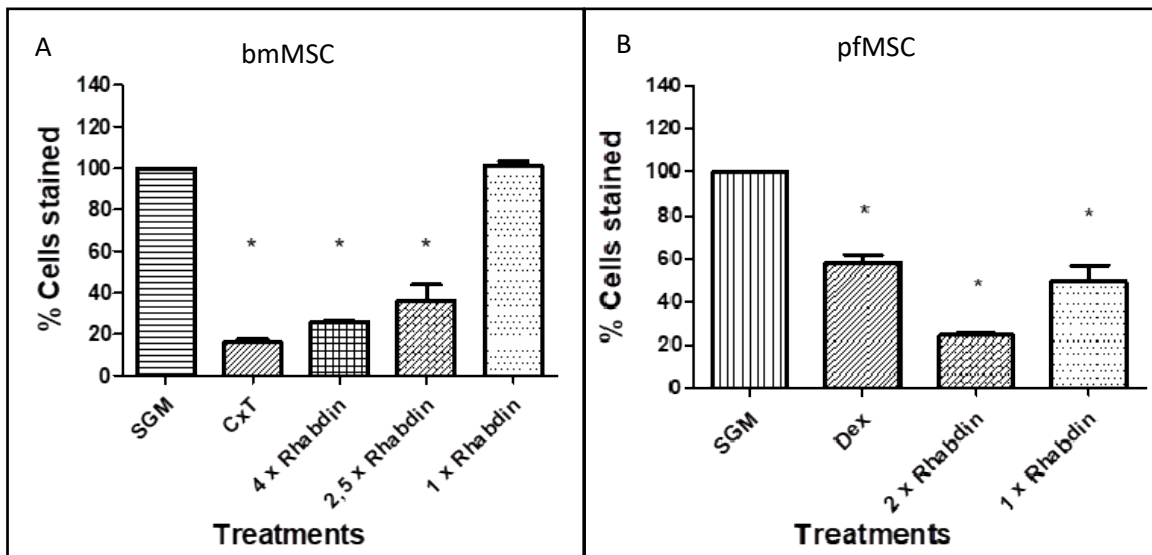


FIG 4: The effect of rhabdin on the cell culture density of bmMSCs (left panel) and pfMSCs (right panel). Cells in SGM were treated for 7 days with various concentrations of rhabdin as indicated and expressed as fold-MIC. Positive controls for cytotoxicity were 10 $\mu\text{g}/\text{ml}$ cycloheximide together with 5 ng/ml TNF α (CxT) for bmMSCs and 1 μM dexamethasone (Dex) for pfMSCs. The cultures were subsequently stained with crystal violet, the stain was extracted and quantified spectrophotometrically at 570 nm. Values for control (SGM-treated) wells were set as 100%. The graph represents the data of $n = 2$ each for 4 x MIC and 2.5 x MIC of rhabdin. The rest of the data represents $n = 4$. A *post hoc* Dunnet test was done with SGM as control. Statistical significance ($p < 0.05$) is indicated with *.

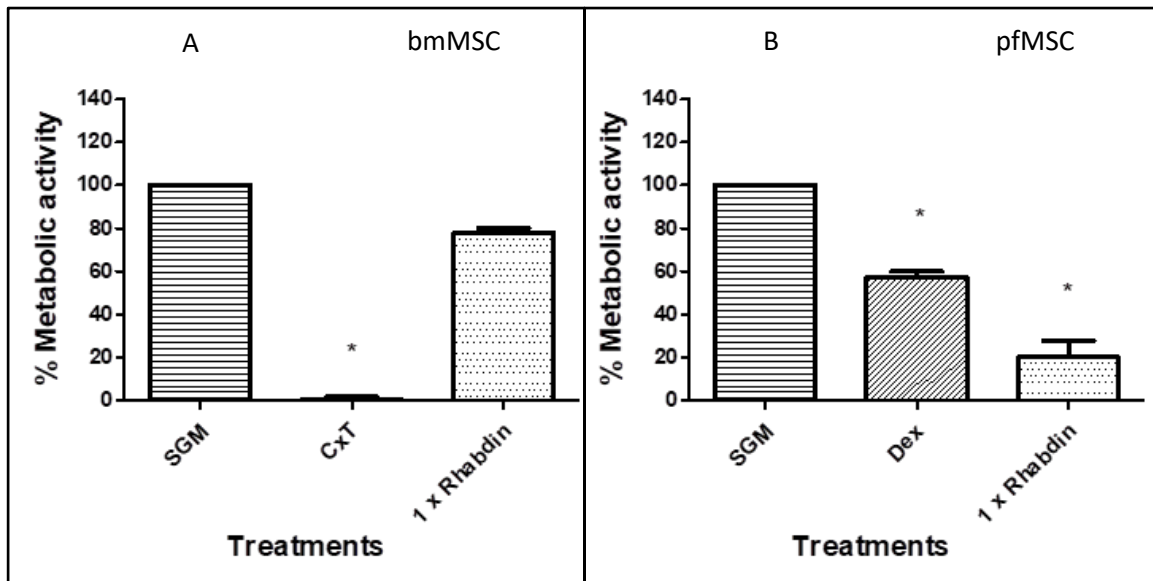


FIG 5: The effects of rhabdin on the metabolic activity of bmMSCs (left panel) and pfMSCs (right panel). Cells in SGM were treated for 7 days with various concentrations of rhabdin expressed as fold-MIC. Positive controls for cytotoxicity were 10 $\mu\text{g/ml}$ cycloheximide and 5 ng/ml $\text{TNF}\alpha$ (CxT) for bmMSCs and 1 μM dexamethasone (Dex) for pfMSCs. Cell viability was measured via an MTT conversion assay and intensity of the colour product was measured at 570 nm. Values for control (SGM-treated) cells were set as 100%. No data is available for 4 x MIC and 2.5 x MIC rhabdin since complete cell death occurred within 24h. The graph represents data of $n = 4$. A *post hoc* Dunnett test was done with SGM as control. Statistical significance ($p < 0.05$) is indicated with *.

The effects of rhabdin on the osteoblastic differentiation of MSCs. ARS stain was used to visualize the mineralized extracellular matrix that forms during osteoblast differentiation. The extracellular matrix of bmMSCs was completely mineralized after 7 days of OM treatment, while pfMSCs formed individual mineralized nodules after 21 days of OM treatment. Rhabdin at 1 x MIC appeared to induce a slight increase in mineralization in bmMSCs, although in 2 out of 7 bmMSCs isolates tested, rhabdin at 1 x MIC was toxic in the presence of OM (**FIG 6A**). Rhabdin at concentrations of 1 x MIC and upwards was cytotoxic to OM-treated pfMSCs, consistent with our observations in undifferentiated pfMSCs (**FIG 4**, data not shown for osteoblastic differentiation of pfMSCs).

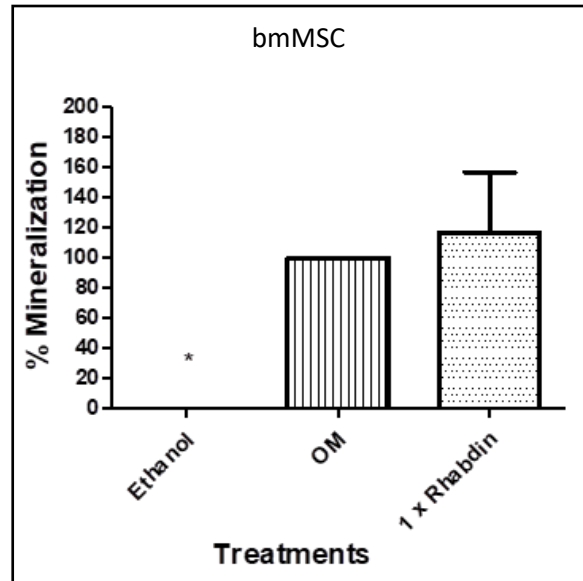


FIG 6: The effect of rhabdin on osteoblastic differentiation of bmMSCs. The ARS stain was extracted and quantified spectrophotometrically. Cells treated with control media (SGM plus 0.1%, v/v, ethanol) did not form any mineral deposits. The graph represents data of $n = 7$. All data were compared to OM, which was set as 100%. Statistical significance ($p < 0.05$) is indicated with an *.

DISCUSSION

In the present study, we describe the purification and partial characterization of a novel antimicrobial compound, provisionally labelled rhabdin, isolated from *X. khoisanae*, and with activity against methicillin-resistant and methicillin-sensitive strains of *S. aureus*. As these organisms are most often the cause of antibiotic-resistant PJI after THA surgery (28), it is imperative that new infection control strategies are developed. However, the effects of aggressive antibiotic treatment on the surrounding bone tissue need to be taken into account when such strategies are considered.

Xenorhabdus spp. are known to produce a wide variety of antimicrobial agents (7–10, 12, 32, 33). Although most antimicrobial compounds produced by *Xenorhabdus* bacteria are small molecules like indole derivatives, iodinine, phenethylamides and benzylideneacetone, some more complex compounds have been identified, including xenorhabdins, xenoroxides and xenocoumacins (33). The first *Xenorhabdus* antibiotic, produced by *X. bovienii*, was described by Paul *et al.* in 1981 (34). This was followed by the discovery of xenorhabdins and

xenocoumacins by McInerney *et al.* in 1991 (7, 8). Xenocoumacins are benzopyran-1-one derivatives, produced by a polyketide synthase (PKS) / nonribosomal peptide synthase (NRPS) system and are known to form one of two fragments with a m/z ratio of 250 or 268, respectively (35). The first xenocoumacin was isolated from *X. nematophilia* A11, with six different xenocoumacins that are known to date. Xenocoumacins 1 and 2 are produced by *X. miraniensis* and *X. nematophilia*, while xenocoumacins 3 to 6 are produced by *X. nematophilia* and *X. kzodoii* (35). This is the first article to report xenocoumacin 2 production by *X. khoisanae*. A second antimicrobial compound, produced by the *X. khoisanae* strain, was also identified (m/z [M + H⁺] 671.413) and provisionally labelled as rhabdin. This antimicrobial had a somewhat similar, yet distinct, fragmentation profile as the xenocoumacins, indicating that rhabdin might be part of the same family as the xenocoumacins, but further studies are required to determine the structure of rhabdin.

Despite their recognized antibacterial activity, little is known about the cytotoxicity of antibiotics produced by *Xenorhabdus* spp. As a first step in evaluating the possible effects of rhabdin on bone tissue, we assessed the cytotoxic and anti-osteoblastic effects of rhabdin on cultured bmMSCs and pfMSCs. Rhabdin was found to be cytotoxic at 1 x MIC in pfMSCs, and at 2 x MIC in bmMSCs, but had no anti-osteoblastic effects at 1 x MIC in bmMSCs. We observed a minor discrepancy in the actions of 1 x MIC on bmMSCs between the crystal violet staining and the MTT conversion assay, with 1 x MIC resulting in a slight loss of metabolic activity as quantified with the MTT conversion assay, but not resulting in a loss of crystal violet staining. This is likely due to 1 x MIC rhabdin causing a decrease in metabolic activity in bmMSCs, but not sufficiently so to result in cell death. This notion is supported by the observation that 1 x MIC, did not have anti-osteoblastic effects, in the majority of bmMSCs isolates tested. However, our results in pfMSCs indicate that rhabdin is unlikely to be safe to use as infection control to treat PJI, although this needs to be confirmed in an *in vivo* system. In addition, consistent with earlier published findings on sensitivity to glucocorticoids (30), pfMSCs were more sensitive than bmMSCs to the cytotoxic effects of rhabdin. Rhabdin at 1 x MIC induced a small (but not statistically significant) increase in mineralization in OM-treated bmMSCs. While an increase in local osteoblast function may contribute to bone strength and reduce the chance of osteoporosis after THA, it can also cause calcification of the joint, which may ultimately result in stiff joints and THA failure (36, 37). *In vivo* studies which include gene

expression analyses will help to shed light on the effects of rhabdin on bmMSCs and bone tissue.

It is noteworthy that rhabdin exerts its cytotoxic effects on cultured mammalian cells at concentrations between 1 x MIC and 2 x MIC, while lower concentrations (0.25 x MIC) were found not to be cytotoxic (results not shown). From these observations, we can speculate that the cytotoxic and antimicrobial effects of rhabdin are mediated via a mechanism common to eukaryotic and prokaryotic cells.

To conclude, our results indicate that our strain of *X. khoisanae* produces two types of antibacterial compounds, namely xenocoumacin 2 and a novel compound with a m/z ratio of 671. This was the first study to report on the antimicrobial activity of *X. khoisanae* secondary metabolites. Further studies including H^3 -NMR are needed to determine the specific structure of rhabdin. Such studies may also pave the way for the identification or synthesis of *Xenorhabdus* antimicrobials with potent antimicrobial activity but no cytotoxicity against mammalian cells. While rhabdin was toxic to cultured bone-derived MSCs, this may be a cell-specific effect and warrants further investigation.

ACKNOWLEDGEMENTS

We thank FraunHofer and the South African National Research Foundation for the financial support and funding of this research. Neither FraunHofer nor the South African National Research Foundation had any role in the design of the study, collection and interpretation of data or the decision to submit the work for publication. We thank Marietjie Stander and her team for assistance with UHPLC-MS and ESI-MS.

FUNDING INFORMATION

This work, including the efforts of Leon Dicks, was funded by FraunHofer and the South African National Research Foundation.

REFERENCES

1. Coates ARM, Halls G, Hu Y. 2011. Novel classes of antibiotics or more of the same? *Br J Pharmacol* 163:184–194.
2. Powers JH. 2004. Antimicrobial drug development – the past, the present, and the future. *Clin Microbiol Infect* 10:23–31.
3. Butler MS, Buss AD. 2006. Natural products — The future scaffolds for novel antibiotics? *Biochem Pharmacol* 71:919–929.
4. Thomas G, Poinar J. 1979. *Xenorhabdus* gen. nov., a genus of entomopathogenic, nematophilic bacteria of the family *Enterobacteriaceae*. *Int J Syst Bacteriol* 29:352–360.
5. Dreyer J, Malan AP, Dicks LMT. 2017. Three novel *Xenorhabdus* – *Steinernema* associations and evidence of strains of *X. khoisanae* switching between different clades. *Curr Microbiol* 74:938–942.
6. Chen G. 1983. Effect of antibiotics produced by *Xenorhabdus* spp. on soil bacteria. Nanjing Forestry University.
7. McInerney B V, Taylor WC, Lacey MJ, Akhurst RJ, Gregson RP. 1991. Biologically active metabolites from *Xenorhabdus* spp., Part 2. Benzopyran-1-one derivatives with gastroprotective activity. *J Nat Prod* 54:785–795.
8. McInerney B V, Gregson RP, Lacey MJ, Akhurst RJ, Lyons GR, Rhodes SH, Smith DRJ, Engelhardt LM, White H. 1991. Biologically active metabolites from *Xenorhabdus* spp., Part 1. Dithiopyrrolone derivatives with antibiotic activity. *J Nat Prod* 54:774–784.
9. Sundar L, Chang FN. 1993. Antimicrobial activity and biosynthesis of indole antibiotics produced by *Xenorhabdus nematophilus*. *J Gen Microbiol* 139:3139–3148.
10. Li J, Chen G, Webster JM. 1997. Nematophin, a novel antimicrobial substance produced by *Xenorhabdus nematophilus* (*Enterobacteriaceae*). *Can J Microbiol* 43:770–773.
11. Li J, Hu K, Webster JM. 1998. Antibiotics from *Xenorhabdus* spp. and *Photorhabdus* spp. (*Enterobacteriaceae*). *Chem Heterocycl Compd* 34:1331–1339.
12. Lang G, Kalvelage T, Peters A, Wiese J, Imhoff JF. 2008. Linear and cyclic peptides from the entomopathogenic bacterium *Xenorhabdus nematophilus*. *J Nat Prod* 71:1074–1077.
13. Park D, Ciezki K, van der Hoeven R, Singh S, Reimer D, Bode HB, Forst S. 2009. Genetic analysis of xenocoumacin antibiotic production in the mutualistic bacterium *Xenorhabdus nematophila*. *Mol Microbiol* 73:938–949.

14. Fuchs SW, Proschak A, Jaskolla TW, Karas M, Bode HB. 2011. Structure elucidation and biosynthesis of lysine-rich cyclic peptides in *Xenorhabdus namtophila*. *Org Biomol Chem* 9:3130–3132.
15. Xiao Y, Meng F, Qiu D, Yang X. 2012. Two novel antimicrobial peptides purified from the symbiotic bacteria *Xenorhabdus budapestensis* NMC-10. *Peptides* 35:253–260.
16. Zhou Q, Grundmann F, Kaiser M, Schiell M, Gaudriault S, Batzer A, Kurz M, Bode HB. 2013. Structure and biosynthesis of xenoamicins from entomopathogenic *Xenorhabdus*. *Chem Eur J* 19:16772–16779.
17. Pulido L, Ghanem E, Joshi A, Purtill JJ, Parvizi J. 2008. Periprosthetic joint infection. *Clin Orthop Relat Res* 466:1710–1715.
18. Parvizi J, Aggarwal V, Rasouli M. 2013. Periprosthetic joint infection: Current concept. *Indian J Orthop* 47:10–17.
19. Ma Z, Lynch AS. 2016. Development of a dual-acting antibacterial agent (TNP-2092) for the treatment of persistent bacterial infections. *J Med Chem* 59:6645–6657.
20. Moran E, Byren I, Atkins BL. 2010. The diagnosis and management of prosthetic joint infections. *J Antimicrob Chemother* 65:45–54.
21. Osmon DR, Berbari EF, Berendt AR, Lew D, Zimmerli W, Steckelberg JM, Rao N, Hanssen A, Wilson WR. 2013. Diagnosis and management of prosthetic joint infection: Clinical practice guidelines by the infectious diseases Society of America. *Clin Infect Dis* 56:1–25.
22. Song Z, Borgwardt L, Høiby N, Wu H, Sørensen TS, Borgwardt A. 2013. Prosthesis infections after orthopedic joint replacement : the possible role of bacterial biofilms. *Orthop Rev (Pavia)* 5:65–71.
23. Drlica K, Zhao X. 1997. DNA gyrase, topoisomerase IV, and the 4-quinolones. *Microbiol Mol Biol Rev* 61:377–392.
24. Wolf M, Clar H, Friesenbichler J, Schwantzer G, Bernhardt G, Gruber G, Glehr M, Leithner A, Sadoghi P. 2014. Prosthetic joint infection following total hip replacement : results of one-stage versus two-stage exchange. *Int Orthop* 38:1363–1368.
25. Siopack JS, Jergesen HE. 1995. Total hip arthroplasty. *West J Med* 162:243–249.
26. Knight SR, Aujla R, Biswas SP. 2011. Total Hip Arthroplasty - over 100 years of operative history. *Orthop Rev (Pavia)* 3:72–74.
27. Pivec R, Johnson AJ, Mears SC, Mont MA. 2012. Hip arthroplasty. *Lancet* 380:1768–

1777.

28. Lentino JR. 2003. Prosthetic joint infections: bane of orthopedists, challenge for infectious disease specialists. *Clin Infect Dis* 36:1157–1161.
29. Høiby N, Bjarnsholt T, Givskov M, Molin S, Ciofu O. 2010. Antibiotic resistance of bacterial biofilms. *Int J Antimicrob Agents* 35:322–332.
30. Jacobs FA, Sadie-Van Gijsen H, van de Vyver M, Ferris WF. 2016. Vanadate impedes adipogenesis in mesenchymal stem cells derived from different depots within bone. *Front Endocrinol (Lausanne)* 7:1–12.
31. Andrews JM. 2001. Determination of minimum inhibitory concentrations. *J Antimicrob Chemother* 48:5–16.
32. Akhurst R. 1982. Antibiotic Activity of *Xenorhabdus* spp., bacteria symbiotically associated with insect pathogenic nematodes of the families *Heterorhabditidae* and *Steinernematidae*. *J Gen Microbiol* 128:3061–3065.
33. Bode HB. 2009. Entomopathogenic bacteria as a source of secondary metabolites. *Curr Opin Chem Biol* 13:224–230.
34. Paul V, Frautschy S, Fenical W, Nelson K. 1981. Antibiotics in microbial ecology: isolation and structural assignment of several new antibacterial compounds from the insect-symbiotic bacteria *Xenorhabdus* spp. *J Chem Ecol* 7:589–597.
35. Reimer D, Luxenberger E, Brachmann AO, Bode HB. 2009. A new type of pyrrolidine biosynthesis is involved in the late steps of xenocoumacin production in *Xenorhabdus nematophila*. *ChemBioChem* 10:1997–2001.
36. Orriss IR, Arnett TR, George J, Witham MD. 2016. Allopurinol and oxypurinol promote osteoblast differentiation and increase bone formation. *Exp Cell Res* 342:166–174.
37. MacMullan PA, McCarthy GM. 2010. The meniscus, calcification and osteoarthritis: a pathologic team. *Arthritis Res Ther* 12:116–117.

SUPPLEMENTARY INFORMATION

TABLE S1: The elution program used to purify the crude antimicrobial isolated from a *X. khoisanae* strain using HPLC. A: 0.1% TFA prepared with analytical grade water. Solution B: 90% acetonitrile in 0.1 % TFA (vol/vol/vol).

Time	A%	B%	Walters Curve
0	90%	10%	-
0,5	90%	10%	-
12,5	0%	100%	6
14	0%	100%	-
20	90%	10%	6
25	90%	10%	-

TABLE S2: The elution program used to analyse the active fractions collected from the HPLC. Solution A: 0.1% (v/v) formic acid prepared with analytical grade water. Solution B: 90% acetonitrile in 0.1 % formic acid (vol/vol/vol)

Time	A%	B%	Walters Curve
0	100%	0%	-
0,5	100%	0%	-
1	70%	30%	6
10	40%	60%	6
15	20%	80%	6
15,1	100%	0%	-
20	100%	0%	-

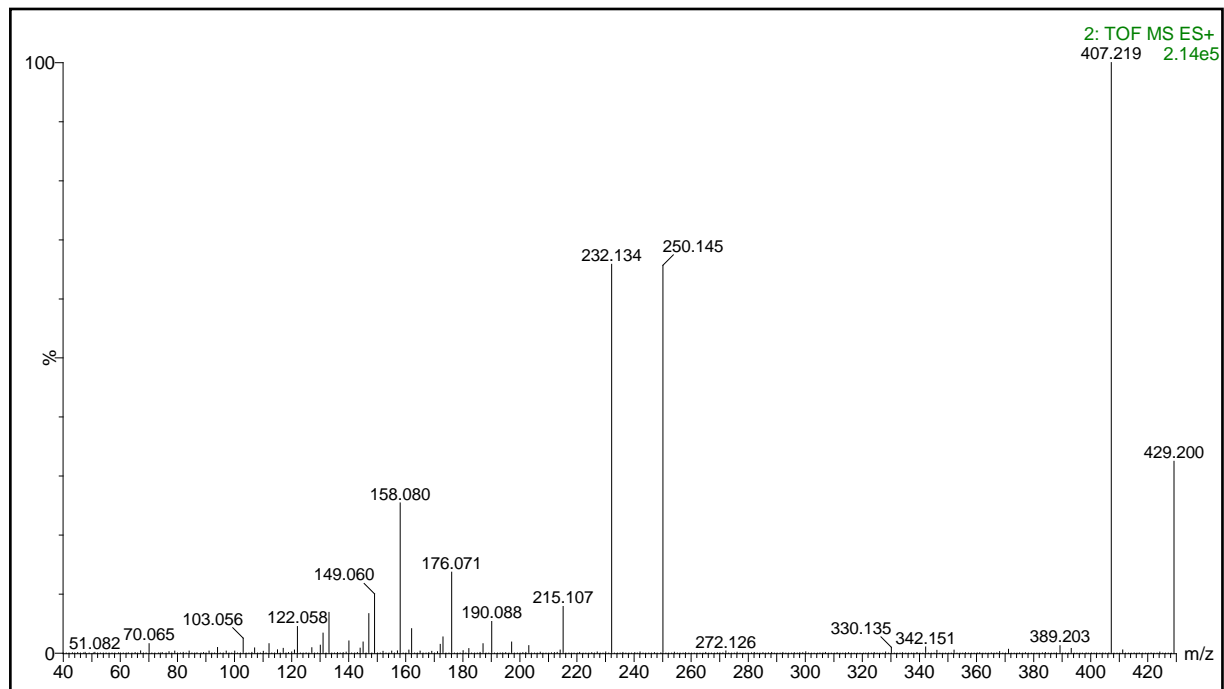


FIG S1: The MS/MS fragmentation pattern of C2 and C4 ($m/z = 407.219$). The parent ion in both peak C2 and C4 has a m/z of 407 and forms the same fragmentation pattern. Three main fragments formed namely 250.145, 232.134, 158.080.

STELLENBOSCH UNIVERSITY

Chapter 4

Evaluation of the osteogenic and cytotoxicity effects of vancomycin on rat-derived mesenchymal stem cells

Evaluation of the osteogenic and cytotoxicity effects of vancomycin on rat-derived mesenchymal stem cells

Elzaan Booysen ^a, Hanél Sadie-Van Gijsen^b, Shelly M Deane^a, Leon MT Dicks^a

Department of Microbiology, Stellenbosch University, Stellenbosch, South Africa^a; Division of Endocrinology, Department of Medicine, Stellenbosch University, Parow, South Africa^b

Periprosthetic joint infections (PJI) are the major cause for total hip arthroplasty (THA) failures. In the majority of PJI cases, methicillin-resistant *Staphylococcus aureus* (MRSA) is the causative agent. Traditionally, MRSA is treated with vancomycin, a glycopeptide, that is administered directly to the infected tissue or intravenously. The effect of applying vancomycin directly to bone tissue has not been studied in depth. In this study, we report on the cytotoxicity and osteogenic effects of vancomycin on rat-derived mesenchymal stem cells (MSCs). Two populations of MSCs were isolated from rat femora, i.e. bone marrow-derived mesenchymal stem cells (bmMSCs) and proximal femur-derived mesenchymal stem cells (pfMSCs). The cells were exposed to increasing concentrations of vancomycin, based on the minimum inhibitory concentration (MIC) of vancomycin against *S. aureus* Xen 31 (MRSA) and *S. aureus* Xen 36. High doses of vancomycin induced osteogenic differentiation in bmMSCs and had no cytotoxic side effects on bmMSCs. The pfMSCs were more sensitive and vancomycin caused a slight decrease in metabolic activity, as well as a decrease in osteogenic differentiation at 1 µg/ml and 5 µg/ml. These results suggest that directly applying vancomycin to an infected hip joint will not have any long-term detrimental effects, since the pfMSC population should recover after vancomycin cessation.

INTRODUCTION

The three major load bearing joints in the human body are the ankle, knee and hip (1). The human hip joint has a complex anatomical structure and is responsible for carrying the weight

of the upper body. During daily activity, the hip joint may experience loading forces up to 7 times the body weight of the individual. This places the hip joint under immense mechanical pressure and is most likely the main cause for osteoarthritis (OA) in the joint (2). OA affects more than 25% of elderly people and is therefore a major cause of disability in this population group (3, 4).

Currently, the only treatment available for severe hip OA is total hip arthroplasty (THA) (5). A metal prosthesis is inserted into the proximal region of the femur, replacing the proximal femur head and neck (6). Although THA is considered the most successful orthopaedic procedure of the past 120 years, and although advances in the field have significantly improved the risk profile associated with this procedure over the past five decades, complications still do occur (7–9). Periprosthetic joint infection (PJI) is the main cause for THA revision surgeries and is defined as bacterial contamination of the joint prosthesis and infection of the adjacent tissue (10). Most, if not all, PJI are caused by bacteria capable of forming biofilms (5). Many strains of these bacteria are resistant to a number of antibiotics (11), and treating PJI is therefore extremely difficult.

The most common bacterial infections after THA are Gram-positive cocci. *Staphylococcus aureus* was isolated in 38% of all cases and 53% of the strains were methicillin-resistant (12). Failed treatment of PJI with conventional antibiotic regimes places an immense burden on medical professionals. Conventional treatments include intravenous administration of antibiotics for a maximum of 2 weeks, while aggressive treatment includes removal of the infected prosthesis and flushing of the infected joint (one-step revision surgery), followed by another 12 weeks on antibiotics. Once the infection has been cleared, a new prosthesis is inserted (13). In severe cases, a surgeon can opt for a two-step revision surgery. This entails initial removal of the infected prosthesis and insertion of an antibiotic-augmented cement spacer, followed by the implantation of a new prosthesis once the bacterial infection has been eradicated (13, 14). Both one-step and two-step revision surgeries can result in prolonged immobility, hospitalization and morbidity. The cost of treatment of a single episode of PJI can escalate to USD 50,000 or more (9). The increase in antibiotic resistance among hospital acquired infections, like PJI, have also increased the risk of failing to successfully treat PJI (15,

16). It is therefore clear that PJI presents a major challenge from both a health-care and economic perspective (17).

Traditionally, methicillin-resistant *Staphylococcus* infections are treated with vancomycin (18). Vancomycin is either administered intravenously or directly to the infected site, by means of antibiotic-loaded cement spacers (19–21). The effect of direct (as opposed to systemic) vancomycin treatment on bone formation and remodelling is largely unknown. The effect of pharmaceutical drugs on bone formation and remodelling is traditionally evaluated *in vitro* with bone-marrow derived mesenchymal stem cells (bmMSCs). Recently, Jacobs and co-authors (22) reported on a second mesenchymal stem cell population in the femur, isolated from the proximal end of a femur. Although these proximal femur mesenchymal stem cells (pfMSCs) are phenotypically similar to bmMSCs, they are functionally distinct, with increased glucocorticoid sensitivity and a reduced osteoblastic differentiation potential. Since pfMSCs are located at the proximal end of femurs, this is also the exact area of tissue in contact with the prosthesis. Thus, direct application of vancomycin to pfMSCs could directly affect the success of THA revision surgeries. In the present study, we evaluate the cytotoxic and osteogenic effects of vancomycin on rat-derived mesenchymal stem cells.

MATERIALS AND METHODS

Materials. Bacterial growth medium was sourced from Biolab Diagnostics (Midrand, South Africa), unless stated otherwise. All constituents of osteogenic differentiation media were obtained from Sigma-Aldrich (Missouri, USA). Dulbecco's Modified Eagle Medium (DMEM), Penicillin/Streptomycin (Pen-Strep), trypsin and Hanks' Balanced Salt Solution were obtained from Lonza (Basel, Switzerland). Fetal bovine serum (FBS) was sourced from Biochrom (Berlin, Germany) and collagenase I (#CLS1) was sourced from Worthington Biochemical Corporation (Lakewood, USA). Cell culture dishes were obtained from NEST Biotechnology (New Jersey, USA). Sodium pentobarbitone (Eutha-naze) was sourced from Bayer (Kempton Park, Gauteng, South Africa).

Determination of MIC (minimum inhibitory concentration). A micro-broth dilution assay, described by Andrews (23), was used to determine the MIC of vancomycin. *Staphylococcus aureus* Xen 31 and *S. aureus* Xen 36 were used as indicator strains. Indicator strains from an overnight culture, cultivated at 37°C, were streaked out onto Brain Heart Infusion (BHI) agar and incubated for 24 h at 37°C. A singly colony was inoculated into BHI broth and incubated for 18 h at 37°C. Overnight culture of the two strains were both adjusted to an optical density (OD) of 0.1 (600 nm). Different concentrations of vancomycin were added to each strain (final volume of 200 µl) and changes in growth observed by recording absorbance readings at 600 nm, immediately after addition, and 6 h and 24 h later.

Isolation and maintenance of MSC. Ethical clearance, clearance number: SU-ACUD15- 00012, to conduct experiments involving animals was granted by the Research Ethics Committee: Animal Care and Use of Stellenbosch University as part of a parent study group led by Prof William Ferris of the Department of Medicine, Stellenbosch University. The cells were isolated from Wistar rats' femora and used for various sub-projects of this parent study. Adult Wistar rats (male, 12 weeks old, with an average body mass of 250 g) were fed *ad libitum* on standard laboratory chow and housed at the Stellenbosch University Animal Facility. Rats were kept according to the guidelines of the South African Medical Research Council.

Isolated mesenchymal stem cells (MSCs) were maintained at 37°C in 95% humidified air and in the presence of 5% CO₂. Isolation was performed as described by Jacobs and co- authors (22). Femora of rats, sacrificed with an intraperitoneal injection of sodium pentobarbitone (12 mg/kg body mass), were surgically removed and cleaned from any residual muscle tissue using sterile gauze. Proximal regions of the femora were removed with sterile side cutters, cut in 1 mm³ fragments and digested in Hanks' Balanced Salt solution containing 0.075% (w/v) collagenase I and 1.5% bovine serum albumin for an hour at 37°C. The denuded bone fragments were washed five times with DMEM, seeded into a culture dish (Ø100), immersed with isolating medium and incubated overnight at 37°C in 95% humidified air containing 5% CO₂. This was followed by rinsing the bone fragments with warm sterile phosphate-buffered saline (PBS ;37°C). The fragments were submerged in standard growth medium (SGM: DMEM containing 1% Pen-Strep and 10% FBS) for 7 to 10 days to allow migration of pfMSCs from the fragments. bmMSCs were flushed from the femora bone marrow cavities with cell isolation

medium (DMEM containing 1% Pen-Strep and 20% FBS), collected in a cell culture dish (\varnothing 100) and cultured at 37°C for 24 h in the presence of 5% CO₂ and 95% humidified air. Non-adherent material was removed after 24 h using warm sterile PBS (37°C) and the adherent cells submerged in SGM. Isolated cells were cultured to 80% confluence and disaggregated with 1 ml 0.5% (w/v) trypsin added to 9 ml cells and sub-cultured at a ratio of 1:4. Cells were expanded to passage 3 before being used for further experiments and SGM with and without treatment compounds were replaced every 2-3 days.

Cytotoxicity of vancomycin. Isolated MSCs at passage 3 were seeded into 12-well plates for crystal violet staining or 96-well plates for the MTT conversion assay, and grown until post-confluence in SGM. A combination of cycloheximide (10 µg/ml) and tumour necrosis factor- α (TNF- α ; 5 ng/ml) was used as the positive control for cytotoxicity in bmMSCs, while 1 µM dexamethasone (Dex) was used as the positive control for cytotoxicity in pfMSCs, as reported previously (22). For crystal violet staining, cells were treated with increasing concentrations of vancomycin (1 x MIC= 5 mg/ml; 4 x MIC = 20 mg/ml) as determined by the MIC, described elsewhere. Cells were cultured for 7 days, replacing media and treatments every 2-3 days, fixed with 70% (v/v) ethanol, stained for 5 min with 0.01% (w/v) crystal violet solution and rinsed three times with PBS. Crystal violet was extracted with 75% (v/v) ethanol and absorbance measured at 570 nm.

For the MTT conversion assays, cells were treated as described for crystal violet staining, with a final volume of 100 µl per well. The methodology for the assay was adapted from the protocol for the Sigma-Aldrich *in vitro* Toxicology Assay Kit (MTT-based, #Tox1). After 7 days of treatment with vancomycin, 10 µl of 5 mg/ml MTT stock solution (Sigma-Aldrich #M2128), dissolved in DMEM, was added to each well. The plates were incubated for 2h at 37°C in the dark and the colour reaction stopped by adding 100 µl of solubilization solution (10% Triton X-100 diluted with 0.1 N HCL in anhydrous isopropanol) to each well. Solubilization was aided by incubating the 96-well plate on a plate shaker and repeated mixing with a pipette. Colour development was quantified spectrophotometrically at 690 nm (background absorbance) and 570 nm, respectively. The absorbance values of the background (690 nm) were subtracted from the A₅₇₀ values. All experiments were performed with quadruplicate biological repeats and triplicate technical repeats.

MSC differentiation. Isolated MSCs at passage 3 were plated in 12-well culture plates and cultures in SGM until post-confluence as described elsewhere. Osteoblastic differentiation was induced with osteogenic media (OM: SGM supplemented with 50 μ M ascorbic acid, 10 mM β -glycerolphosphate and 10 nM dexamethasone) as described by Jacobs and co-authors (22). Cells were treated with vancomycin as described elsewhere. Differentiation was evaluated by staining with Alizarin Red S stain (ARS: Amresco, USA) after 7 days (bmMSC) or 21 days (pfMSC). Before staining with 40mM ARS (pH 4.0 – 4.1), cells were washed with sterile pre-warmed PBS, fixed for 5 min at 25 °C with 70% (v/v) ethanol and rinsed twice with sterile water. After staining for 2 to 4 hours (bmMSC), the excess stain was removed and cells were washed in triplicate with water, once with PBS and an additional three times with water. Bound stain was extracted using 10% (w/v) cetylpyridinium chloride (CPC) dissolved in 10 mM Na_2HPO_4 (pH 7.0) and quantified spectrophotometrically at 562 nm. pfMSCs were stained overnight with ARS and washed, as described for bmMSC. Since pfMSCs have reduced osteogenic potential, staining was quantified using image analysis. Images were captured using an Olympus CKX41 microscope (CKX41, CxhN 10x0.25 PhP objective), fitted with a Canon EOS 600D camera at 10x magnification. Four random images (one in each quadrant) were taken of each well, resulting in 12 images per treatment since experiments were performed in triplicate. Images were analysed with ImageJ software (version 1.51 J8) and converted into red-green-blue stacks. Analyses were performed in the green channel. A threshold value of T=90 was used to exclude non-specific background staining and remained unchanged throughout. The percentage area stained was recorded and the average for the 12 images per condition was calculated.

Statistical analysis. GraphPad Prism (version 5.01) was used for all statistical analyses and data were expressed as average \pm SD. One-way ANOVA and Dunnett's *post hoc* test were used to analyse the data. When $p < 0.05$, the difference was considered to be statistically significant and indicated with an *.

RESULTS AND DISCUSSION

Vancomycin is commonly used to treat MRSA infections. MRSA has been found to be the major causative agent in PJI (12). The MIC of vancomycin against *S. aureus* Xen 31 (MRSA) and Xen 36

was 5 µg/ml and 1 µg/ml, respectively. This indicates that *S. aureus* Xen 31 has reduced susceptibility for vancomycin.

Vancomycin, a glycopeptide, inhibits cell wall synthesis by binding to the terminal D-Ala-D-Ala dipeptide of peptidoglycan units (24). The effect of directly applying vancomycin on bone tissue has not been studied in depth. In the present study, we evaluated the cytotoxicity and anti-osteogenic effects of vancomycin, a glycopeptide, on two populations of rat femora derived MSCs, the bmMSCs and pfMSCs. The cytotoxicity of vancomycin to rat MSCs was evaluated via crystal violet staining and the MTT conversion assay. Both methods are used since crystal violet stains all cells present in a well (dead and alive), while the MTT conversion assay is more sensitive and is used to indicate metabolic activity and cell viability.

High doses of vancomycin had no cytotoxic effects on bmMSCs, (**Fig 1A**) and no significant difference was observed between the cells treated with 1 x MIC and 4 x MIC vancomycin. The same applies for pfMSCs (**Fig 1B**), since only Dex treated cells were significantly different from SGM treated cells. A slight increase in cell density is observed for pfMSCs treated with 1 x MIC vancomycin, but this increase is not significant. The MTT conversion assay (**Fig 2**) supports the crystal violet staining data, with no cytotoxic effects observed for bmMSCs and pfMSCs treated with the highest dose of vancomycin (4 x MIC). These results indicate that directly administering vancomycin to an infected hip joint will not have a detrimental effect on the MSC populations present near the joint.

Osteoblastic differentiation was evaluated by staining the mineralized extracellular matrix with ARS. The bmMSCs were fully differentiated after 7 days of treatment with OM, while pfMSCs formed individual mineralized nodules after 21 days of OM treatment. The osteoblastic differentiation results correspond with results obtained by Jacobs and co-authors (22). Osteoblastic differentiation in bmMSCs increased slightly, but not significantly, when treated with 4 x MIC vancomycin (**Fig 3A**). In contrast, pfMSCs treated with vancomycin showed significantly reduced osteoblastic differentiation (**Fig 3B**). This indicates that direct application of vancomycin to an infected hip joint will halt osteoblastic differentiation, but since vancomycin is not cytotoxic to pfMSCs, osteoblastic differentiation of these cells will continue once vancomycin treatment is halted.

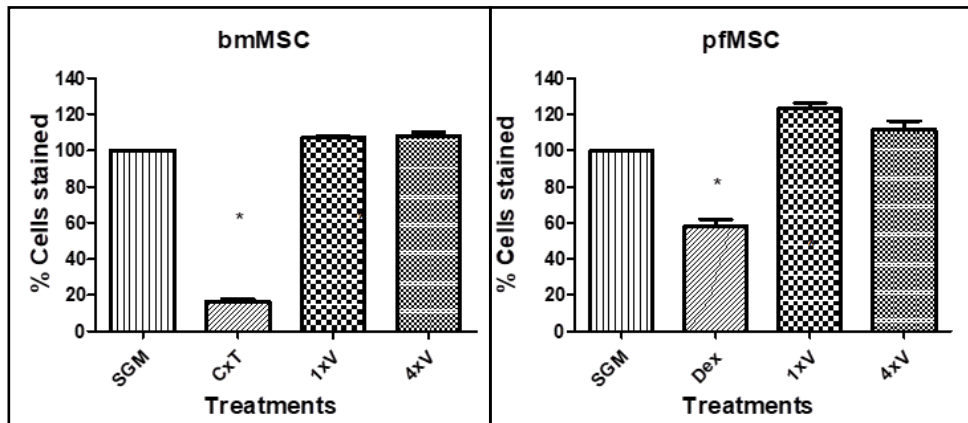


FIG 1: The effect of vancomycin on bmMSCs (left panel) and pfMSCs (right panel) densities. Cells in SGM were treated for 7 days with different concentrations of vancomycin, as indicated and expressed as fold-MIC. Positive controls for cytotoxicity were 10 $\mu\text{g/ml}$ cycloheximide together with 5 ng/ml TNF α (CxT) for bmMSCs and 1 μM dexamethasone (Dex) for pfMSCs. The cells were stained with crystal violet, the stain was extracted and quantified spectrophotometrically at 570 nm. Values for control (SGM-treated) wells were set as 100%. The graph represents data of $n = 4$. A *post hoc* Dunnet test was done with SGM as control. Statistical significance ($p < 0.05$) is indicated with *.

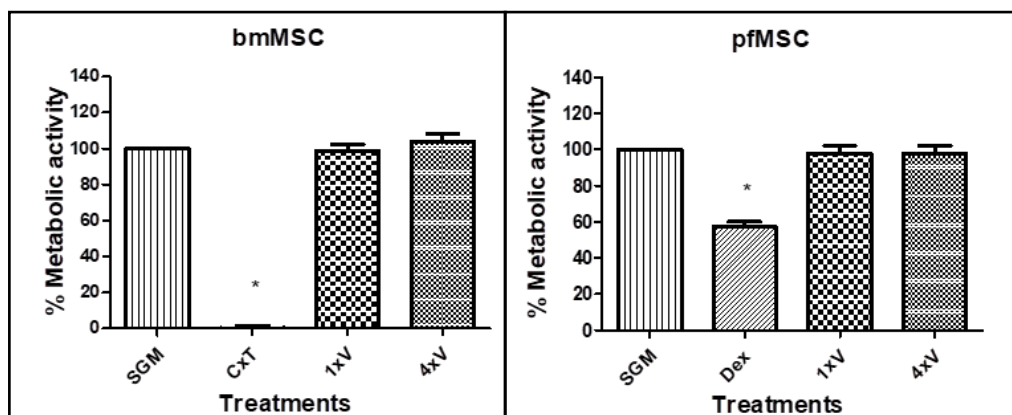


FIG 2: The effect of vancomycin on the metabolic activity of bmMSCs (left panel, A) and pfMSCs (right panel, B). Cells in SGM were treated for 7 days with different concentrations of vancomycin expressed as fold-MIC. Positive controls for cytotoxicity were 10 $\mu\text{g/ml}$ cycloheximide and 5 ng/ml TNF α (CxT) for bmMSCs and 1 μM dexamethasone (Dex) for pfMSCs. Cell viability was measured via an MTT conversion assay and intensity of the colour product was measured at 570 nm. Values for control (SGM-treated) cells were set as 100%. The graph represents data of $n = 4$. A *post hoc* Dunnet test was done with SGM as control. Statistical significance ($p < 0.05$) is indicated with *.

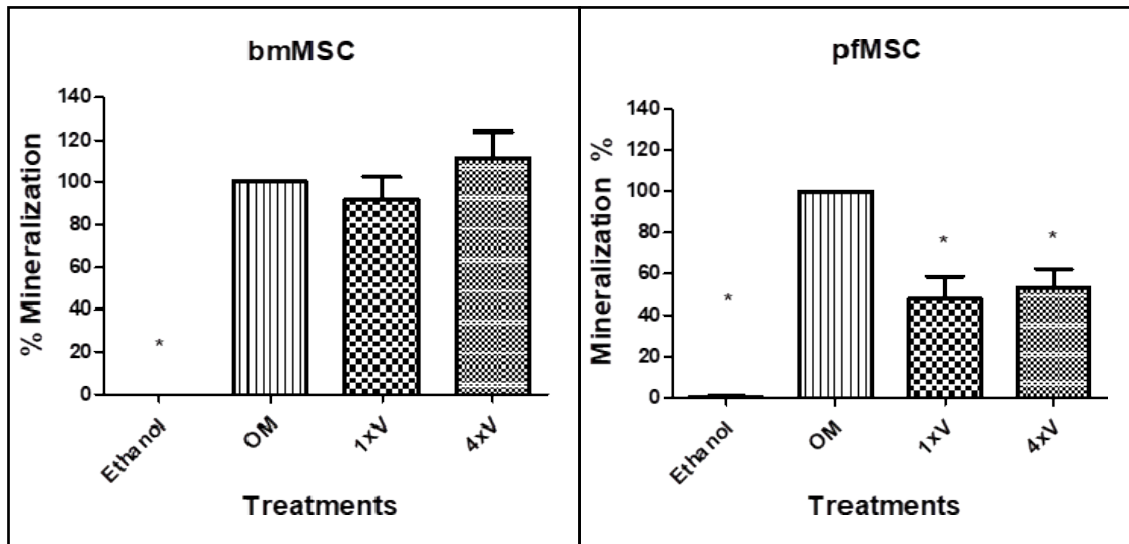


FIG 3: The effect of vancomycin on the osteoblastic differentiation of bmMSC (left panel, A) and pfMSC (right panel, B). Cells were treated with increasing concentrations of vancomycin. The formation of mineralized extracellular matrix was evaluated after 7 days (bmMSCs) or 21 days (pfMSCs). Cells treated with control media (SGM plus 0.1%, v/v, ethanol) did not form any mineralized deposits. The graph represents $n = 7$. All data were compared to OM, which was set as 100%. Statistical significance ($p < 0.05$) is indicated with an *.

CONCLUSION

Directly applying high doses of vancomycin to infected bone tissue in an effort to eradicate a persistent PJI may spare the surrounding bone tissue. Vancomycin exhibited mild anti-osteoblastic effects in differentiating pfMSCs, which may cause local loss of bone mineral density at vancomycin-treated sites, but we hypothesize that the absence of cytotoxicity of vancomycin on undifferentiated pfMSCs could result in the population of pfMSCs surrounding the affected area remaining intact, which will contribute to repair of the bone tissue upon cessation of vancomycin treatment.

REFERENCES

1. Kujala UM, Kaprio J, Sarna S. 1994. Osteoarthritis of weight bearing joints of lower limbs in former élite male athletes. *Br Med J* 308:231–234.
2. Crowninshield RD, Johnston RC, Andrews JG, Brand RA. 1978. A biomechanical investigation of the human hip. *J Biomech* 11:75–85.
3. Sato T, Sato N. 2015. Clinical relevance of the hip joint: Part I - Review of the anatomy of the hip joint. *Int Musculoskelet Med* 37:141–145.
4. Zhang Y, Jordan JM. 2010. Epidemiology of Osteoarthritis. *Clin Geriatr Med* 26:355–369.
5. Song Z, Borgwardt L, Høiby N, Wu H, Sørensen TS, Borgwardt A. 2013. Prosthesis infections after orthopedic joint replacement: the possible role of bacterial biofilms. *Orthop Rev (Pavia)* 5:65–71.
6. Siopack JS, Jergesen HE. 1995. Total hip arthroplasty. *West J Med* 162:243–249.
7. Knight SR, Aujla R, Biswas SP. 2011. Total Hip Arthroplasty - over 100 years of operative history. *Orthop Rev (Pavia)* 3:72–74.
8. Pivec R, Johnson AJ, Mears SC, Mont MA. 2012. Hip arthroplasty. *Lancet* 380:1768–1777.
9. Lentino JR. 2003. Prosthetic joint infections: bane of orthopedists, challenge for infectious disease specialists. *Clin Infect Dis* 36:1157–1161.
10. Tande AJ, Patel R. 2014. Prosthetic joint infection. *Clin Microbiol Rev* 27:302–345.
11. Høiby N, Bjarnsholt T, Givskov M, Molin S, Ciofu O. 2010. Antibiotic resistance of bacterial biofilms. *Int J Antimicrob Agents* 35:322–332.
12. Pulido L, Ghanem E, Joshi A, Purtill JJ, Parvizi J. 2008. Periprosthetic Joint Infection: the incidence, timing, and predisposing factors. *Clin Orthop Relat Res* 466:1710–1715.
13. Parvizi J, Aggarwal V, Rasouli M. 2013. Periprosthetic joint infection: Current concept. *Indian J Orthop* 47:10–17.
14. Wolf M, Clar H, Friesenbichler J, Schwantzer G, Bernhardt G, Gruber G, Glehr M, Leithner A, Sadoghi P. 2014. Prosthetic joint infection following total hip replacement: results of one-stage versus two-stage exchange. *Int Orthop* 38:1363–1368.
15. Siljander MP, Sobh AH, Baker KC, Baker EA, Kaplan LM. 2018. Multidrug-resistant organisms in the setting of periprosthetic joint infection - diagnosis, prevention, and treatment. *J Arthroplasty* 33:185–194.

16. Ravi S, Zhu M, Luey C, Young SW. 2016. Antibiotic resistance in early periprosthetic joint infection. *Orthop Surg* 86:1014–1018.
17. Parvizi J, Alijanipour P, Barberi EF, Hickok NJ, Phillips SK, Shapiro IM, Schwarz EM, Stevens MH, Wang Y, Shirliff ME. 2015. Novel developments in the prevention, diagnosis, and treatment of periprosthetic joint infections. *J Am Acad Orthop Surg* 23:32–43.
18. Kirby A, Graham R, Williams NJ, Wootton M, Broughton CM, Alanazi M, Anson J, Neal TJ, Parry CM. 2010. *Staphylococcus aureus* with reduced glycopeptide susceptibility in Liverpool, UK. *J Antimicrob Chemother* 65:721–724.
19. Gu H, Ho PL, Tong E, Wang L, Xu B. 2003. Presenting vancomycin on nanoparticles to enhance antimicrobial activities. *Nano Lett* 3:1261–1263.
20. Zakeri-milani P, Loveymi BD, Jelvehgari M, Valizadeh H. 2013. The characteristics and improved intestinal permeability of vancomycin PLGA-nanoparticles as colloidal drug delivery system. *Colloids Surfaces B Biointerfaces* 103:174–181.
21. Lotfipour F, Abdollahi S, Jelvehgari M, Valizadeh H, Hassan M, Milani M. 2013. Study of antimicrobial effects of vancomycin loaded PLGA nanoparticles against *Enterococcus* clinical isolates. *Drug Res (Stuttg)* 64:348–352.
22. Jacobs FA, Sadie-Van Gijsen H, van de Vyver M, Ferris WF. 2016. Vanadate impedes adipogenesis in mesenchymal stem cells derived from different depots within bone. *Front Endocrinol (Lausanne)* 7:1–12.
23. Andrews JM. 2001. Determination of minimum inhibitory concentrations. *J Antimicrob Chemother* 48:5–16.
24. Fair RJ, Tor Y. 2014. Antibiotics and bacterial resistance in the 21st century. *Perspect Medicin Chem* 6:25–64.

STELLENBOSCH UNIVERSITY

Chapter 5

Antibacterial activity of vancomycin encapsulated in poly(DL-lactide-co-glycolide) nanoparticles

Antibacterial activity of vancomycin encapsulated in poly(DL-lactide-co-glycolide) nanoparticles

Elzaan Booysen^a, Martin Bezuidenhoudt^b, Anton Du Preez van Staden^c, Dimitri Dimitrov^b, Shelly M Deane^a, Leon MT Dicks^a

Department of Microbiology, Stellenbosch University, Stellenbosch, South Africa^a,
Department of Industrial Engineering, Stellenbosch University, Stellenbosch, South Africa^b,
Department of Physiological Science, Stellenbosch University, Stellenbosch, South Africa^c

Vancomycin is often used to treat infections caused by β -lactam-resistant bacteria. However, methicillin-resistant strains of *Staphylococcus aureus* (MRSA) acquired resistance to vancomycin, rendering it less effective in the treatment of serious infections. In the search for novel antibiotics, alternative delivery mechanisms have also been explored. In this study, we report on the encapsulation of vancomycin in PLGA [poly(DL-lactide-co-glycolide)] nanoparticles by electrospraying. The nanoparticles were on average 247 nm in size with small bead formations on the surface. Clusters of various sizes were visible under the SEM (scanning electron microscope). Vancomycin encapsulated in PLGA (VNP) was more effective in inhibiting the growth of *S. aureus* Xen 31 (MRSA) and *S. aureus* Xen 36 than unencapsulated vancomycin. Encapsulated vancomycin had a minimum inhibitory concentration (MIC) of 1 $\mu\text{g/ml}$ against MRSA compared to 5 $\mu\text{g/ml}$ of free vancomycin. At least 70% (w/w) of the vancomycin was encapsulated. Thirty percent of the vancomycin was released within the first 144 h, followed by slow release over 10 days. Vancomycin encapsulated in PLGA nanoparticles may be used to treat serious infections.

INTRODUCTION

Nanomedicine is a rapidly expanding field, with the main focus on developing nanosized colloidal drug delivery vehicles. Nanoparticles, microparticles and nanofibers of various shapes are produced from polymers, metals (e.g. silver) and fatty acids (1). Polymeric

nanoparticles are well known for their ability to enhance the efficacy of drugs and improve drug circulation *in vivo* (2). The majority of polymer nanoparticles are constructed from biodegradable poly(ester) polymers, such as poly(lactide), poly(glycolide) and PLGA (3–5). The ease at which the hydrophobic characteristics of PLGA are manipulated, and the fact that it has been classified as safe, render this type of polymer ideal for the development of colloidal drug delivery systems (6).

Antibiotics that are toxic at concentrated levels, poorly soluble, temperature sensitive or degraded by proteolytic enzymes can now be delivered to infected areas in a protected (encapsulated) form. This allows pharmaceutical industries to explore the use of “outdated” antibiotics. Nanoantibiotics utilize slow release of the drug from the particle to extend the time period between administration and this improves patient compliance since less hospital visits are needed (7, 8).

In 2007, a group of researchers led by Daniel Lim showed that antibiotics associated with nanoparticles had enhanced antimicrobial activity against resistant bacterial strains (9, 10). The first nanoantibiotic approved by the FDA was Abelcet[®], a liposomal amphotericin B lipid complex used to treat fungal infections (11). Other researchers have followed their lead with encapsulation of ciprofloxacin, minocycline, ampicillin, polymyxin B and many more in various nanoparticle compositions (12–20).

Since vancomycin is commonly used to treat MRSA, the recent discovery of vancomycin-resistant MRSA by Andrew Kirby shocked the medical industry (21). This resulted in numerous research groups investing time and money in the encapsulation of vancomycin in nanoparticles.

Various techniques have been reported for encapsulating vancomycin in PLGA nanoparticles. In the majority of reports, vancomycin-loaded nanoparticles were fabricated using the double-solvent evaporation emulsification method (DSEE) (6, 22, 23). Disadvantages associated with DSEE are a low encapsulation efficiency and difficulty in controlling the size distribution of nanoparticles. In the present study, vancomycin is encapsulated in PLGA nanoparticles fabricated by electrospraying to enhance the activity of vancomycin against *S. aureus* Xen 31

and *S. aureus* Xen 36.

MATERIALS AND METHODS

Materials. Poly (DL-lactide-co-glycolide) (PLGA) was sourced from Evonik (Germany). Dimethylformamide (DMF) was acquired from Merck-Millipore (USA) and the Pierce™ BCA Protein Assay Kit (BCA) was obtained from Thermofisher Scientific (USA). Dimethyl sulfoxide, D- α Tocopherol polyethylene glycol 1000 succinate (Vitamin E) and vancomycin hydrochloride was acquired from Sigma-Aldrich (Germany). Acetonitrile was sourced from Microsep (Germany) and bacterial growth medium was sourced from Biolab Diagnostics (South Africa), unless stated otherwise. All ultra- high-pressure liquid chromatography (UHPLC) analysis was done with the help of the Liquid Chromatography Mass Spectrometry (LCMS) unit of the Central Analytical Facility at Stellenbosch University. Unless stipulated otherwise all water used in experiments was of analytical grade quality.

Production of nanoparticles. Vancomycin was encapsulated in PLGA nanoparticles to ensure slow and steady release of the antibiotic. A protocol adapted from Van Staden was used to produce the nanoparticles (24). PLGA was dissolved in DMF (15% w/v), and vancomycin dissolved in DMSO (50 mg/ml), was added to the solution to yield a final concentration of 5 mg/ml. The organic and aqueous phases were emulsified on a magnetic stirrer at 200 rpm. DMSO, without vancomycin, was added for un-associated nanoparticles (CNP). A sterile glass Pasteur pipette and high voltage supply was used to produce the nanoparticles (**FIG 1**). The anode was connected to a glass collector and the cathode inserted into the polymer solution. A constant potential difference of 15 kV was applied to the polymer solution and -5kV to the collector. The relative humidity was kept below 30% and the temperature at 25°C. Nanoparticles were scraped off the glass collector and stored for future use.

Drug loading capacity and efficiency. Five milligrams of nanoparticles was dispersed in 5 ml DMF and incubated overnight on a rotating wheel at 37°C. Samples were centrifuged at 1000 x g for 30 minutes (Sigma 3-18K, Scientific equipment specialists, USA) and the concentration of encapsulated vancomycin determined using a modification of the UHPLC

protocol described by Baranowska and co-authors (25). An increasing linear gradient of 10% to 90% solution B in solution A over 30 seconds (Solution A: de-ionized water containing 0,1% TFA, v/v and solution B: acetonitrile containing 0.1% TFA, v/v) was applied. Absorbance readings were taken at 280 nm. The drug loading capacity (DLC) and encapsulation efficiency (EE) of the nanoparticles were determined using the following equations:

$$DLC = \frac{\text{Mass of antimicrobial in sample}}{\text{Total mass of sample}} \times 100 \quad (1)$$

$$EE = \frac{\text{Mass of vancomycin in sample}}{\text{Mass of initial vancomycin added to PLGA solution}} \times 100 \quad (2)$$

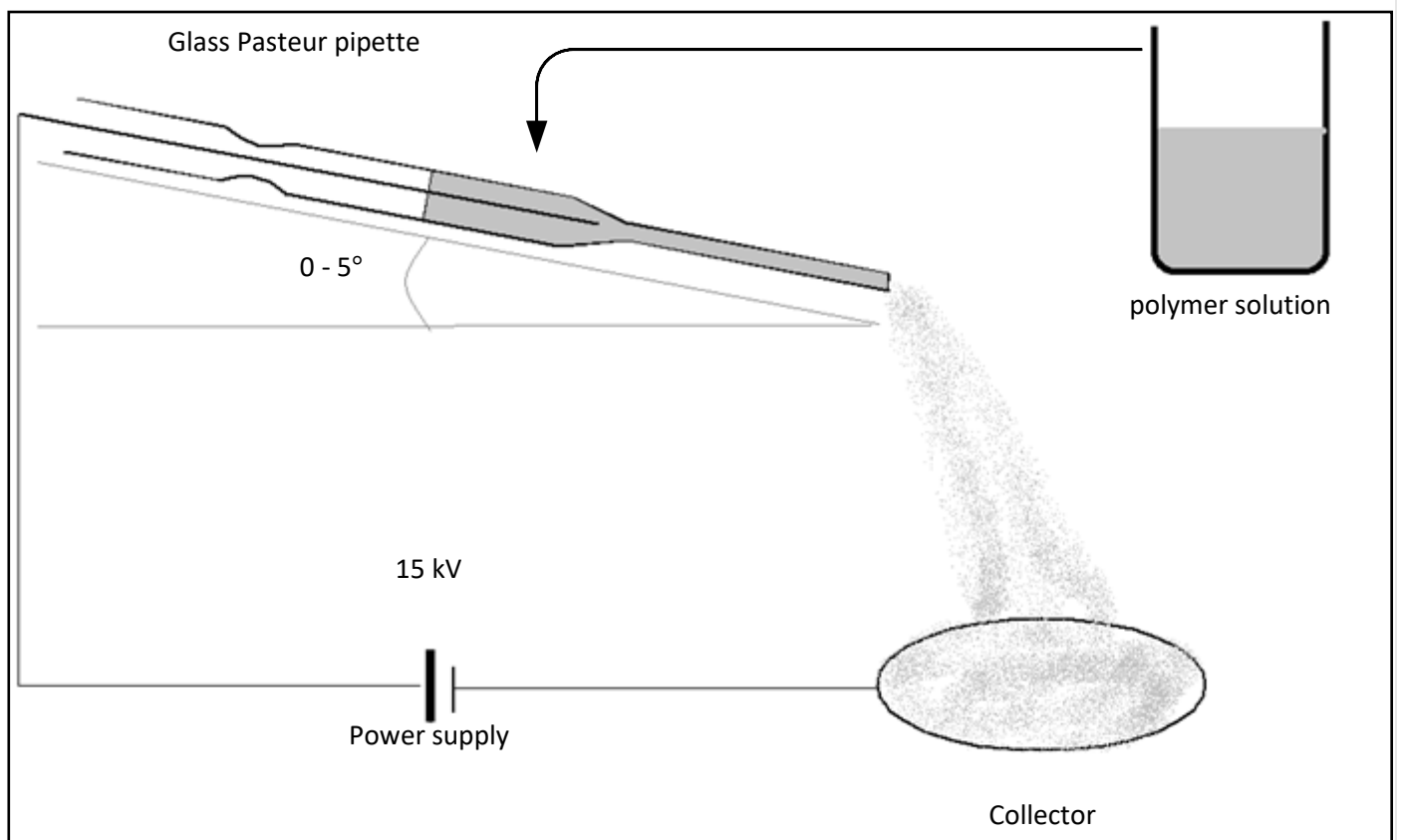


FIG 1: Diagram of the electrospaying setup used to produce PLGA nanoparticles. PLGA was dissolved in DMF (15% w/v) (organic phase), vancomycin was dissolved in DMSO (50 mg/ml) (aqueous phase). The organic and aqueous phase were emulsified and injected into the glass Pasteur pipette. The anode was connected to the glass Pasteur pipette (15kV) and the cathode to a collector (-5Kv). The glass Pasteur pipette was placed at an angle to allow flow of the emulsified solution. The relative humidity was kept below 30% and temperature at 25°C.

Characteristics. The hydrodynamic diameter of the nanoparticles was determined by using dynamic light scattering (DLS) instruments (Malvern zetasizer nano S series). Briefly, 1 mg nanoparticles was dissolved in 1 ml DMSO (1 mg/ml). Samples were mixed continuously during particle size analysis to prevent aggregation. The samples were measured in triplicate and the hydrodynamic diameter of the nanoparticles calculated by the Stokes-Einstein equation, the polydispersity factors (μ_2/Γ^2) were calculated from the cumulative method. (μ_2 : the second cumulant of the decay function; Γ^2 : average characteristic line width).

The morphology of the nanoparticles was analysed using a scanning electron microscope (SEM; Zeiss Merlin SEM). Nanoparticles were placed on a SEM carbon adhesive tape and coated with gold and visualized at 5kV.

Minimum inhibitory concentration (MIC). Agar well diffusion was used to determine the MIC of the nanoparticles. The nanoparticles were suspended in agarose gel plugs (Cylindrical shaped disks, diameter = 5mm and height = 5mm) at various concentrations. Overnight cultures of *S. aureus* Xen 31 (MRSA) and *S. aureus* Xen 36 (300 μ l) were inoculated into 30 ml melted Brain Heart Infusion (BHI) Agar (1%, w/v, agar, cooled to 40°C), swirled and plated out. A sterile glass Pasteur pipette (diameter = 5 mm) was used to make wells in the solidified agar. Cylindrical gel plugs with nanoparticles were inserted in the wells and the plates were incubated at 37°C for 24 h. Zone size was measured and analysed using ImageJ image analysis software (version 1.51 J8).

The micro-broth dilution assay (26) was used to determine the MIC of vancomycin against *S. aureus* Xen 31 and Xen 36. Vancomycin was dissolved in double distilled H₂O. The Staphylococcal strains were incubated overnight in BHI broth at 37°C and adjusted to an A₆₀₀ of 0.1 using fresh BHI broth. Various concentrations of vancomycin were added to each strain (final volume of 200 μ l) and treated bacteria were incubated at 37°C. The change in growth was observed by recording absorbance readings at 600 nm. Absorbance readings were recorded immediately after addition, and 6 h and 24 h later.

Drug release kinetics. A diffusion cell was produced using a 3-D printer (**FIG 2**). A 5 kDa MWCO PES ultrafiltration membrane separated the donor and acceptor compartments of the diffusion cell. The walls of the diffusion cell were constructed from acrylonitrile butadiene styrene (Z-ABS, Zortax). The donor compartment contained 10 mg of nanoparticles dispersed in 2.5 ml 0,3% (w/v) vitamin E and the acceptor compartment 15 ml of 0.3% (w/v) vitamin E. The acceptor compartment was stirred magnetically at 600 rpm. At predetermined sampling times 500 μ l of vitamin E solution was removed from the acceptor compartment and replaced with 500 μ l fresh vitamin E solution. Samples were analysed and quantified using a Waters UHPLC (CAF, Stellenbosch University), as described elsewhere. These values were converted to a percentage value with 0.293 mg/ml set as the maximum (7.338% of 4 mg/ml).

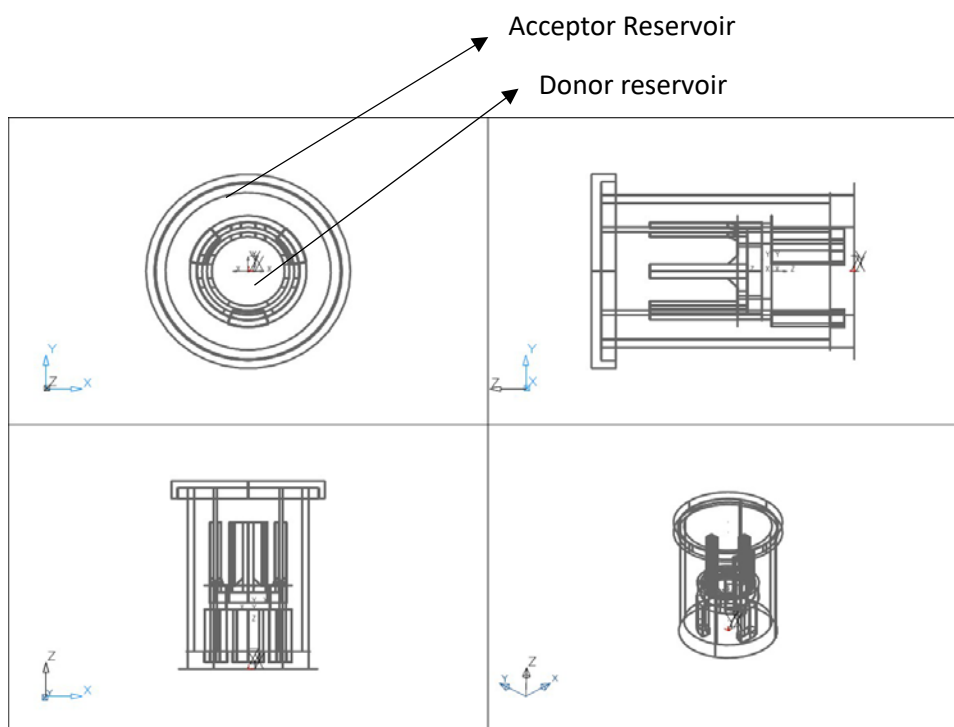


FIG 2: The reservoirs used to determine the release profile of the nanoparticles. A solution consisting of 0,3% (w/v) vitamin E and nanoparticles (10 mg/ml) were placed in the inside donor reservoir. The acceptor reservoir contained 0,3% (w/v) vitamin E solution. At predetermined time intervals, 500 μ l was sampled from the acceptor reservoir and replaced with 500 μ l fresh vitamin E solution.

RESULTS AND DISCUSSION

Drug loading capacity and efficiency. The DLC of VNP produced with electro spraying was 7.33% (w/w) and the EE% was 73.9%. The average DLC reported in similar studies is 30.38% (6, 23). The DSEE method appears to be superior to electro spraying, but in contrast to these results the EE% achieved with electro spraying is higher. This suggests that electro spraying is a more efficient method for encapsulation of water-soluble drugs in PLGA, since less vancomycin was wasted during nanoparticle formation.

Characteristics of CNP and VNP. The mean hydrodynamic size of the CNP as determined by DLS was 384 nm with a polydispersity index of 0.212 (**FIG 3A**). While the mean hydrodynamic size of vancomycin associated nanoparticles (VNP) as determined by DLS was 247 nm with a polydispersity index of 0.385 (**FIG 3B**). The size difference observed for the CNP vs the VNP could be due to an interaction between the vancomycin and the polymer, forming a denser polymer matrix and thus a smaller nanoparticle. When comparing the sizes of the nanoparticles on the micrographs, the same difference in size for CNP and VNP is observed thus supporting the DLS results (**FIG 4**).

The polydispersity index of VNP, produced with electro spraying, is higher compared to those reported by Loftipour and co-authors (6, 23). This suggests that nanoparticles produced by DSEE are larger, with a mean size of 400 nm, and more uniform in size. In contrast to the DSEE method, the polydispersity index of PLGA encapsulated vancomycin produced with the nanoprecipitation method, is similar to that reported in this study (27). In contrast, the polydispersity index and mean hydrodynamic size of un-associated PLGA nanoparticles produced by DSEE as reported in two separate studies by García-Díaz (28) and Menale (29), were considerably smaller compared to results obtained in this study by electro spraying. Since the conventional setup uses a syringe pump to control the flow of the polymer solution (30), the higher polydispersity index in this study could be due to uneven flow of the polymer solution from the Pasteur pipette.

The linked and rough surface structure of the nanoparticles can also be attributed to the electro spray setup, since with small modifications this setup is often used to produce

nanofibers (31). Nanofibers are long fibres with diameters less than 1000 μm and are produced by electrospinning.

Minimum inhibitory concentration. The MIC of vancomycin against *S. aureus* Xen 31 and *S. aureus* Xen 36, as determined by the micro-broth dilution assay, is 5 $\mu\text{g}/\text{ml}$ and 3 $\mu\text{g}/\text{ml}$ respectively, and the MIC of VNP for both indicator strains is 1 $\mu\text{g}/\text{ml}$. This indicates that by encapsulating antibiotics, their antimicrobial activity can be enhanced. This supports the results obtained by Daniel Lim (10). This is likely due to a higher concentration, compared to free-vancomycin, since the hydrophobic nanoparticles bind to hydrophobic chains present on the cell wall of pathogens. The vancomycin is released in closer proximity to the bacteria, thus no “dilution” effect is observed. Further studies are needed to elucidate the exact mechanism of action of PLGA encapsulated nanoparticles.

Drug release kinetics. In an aqueous environment, therapeutic drugs encapsulated in PLGA are released via bulk erosion of the particle (6). The release rate of vancomycin from PLGA depends on the ratio of poly(lactide) (PLA) and poly(glycolide) (PGA), the higher the PLA concentration the more hydrophobic the particle thus the slower the release rate (32). Vancomycin release was monitored for 240 h (10 days) and followed first-order release. Within 24 h, 5 $\mu\text{g}/\text{ml}$ vancomycin was released from the nanoparticles and detected in the acceptor reservoir; thus, nanoparticles are therapeutically active within 24 h. Only 50% (1.47 mg vancomycin) of the total encapsulated vancomycin was released in 10 days, suggesting that these nanoparticles will stay therapeutically active for a minimum of 14 days. This indicated that antibiotic administration can be reduced to once every 2 weeks, thus increasing patient compliance and reducing hospitalization costs. A burst release was observed after 48 h, rendering vancomycin PLGA nanoparticles perfect for use as a prophylaxis treatment to prevent post-surgical infections.

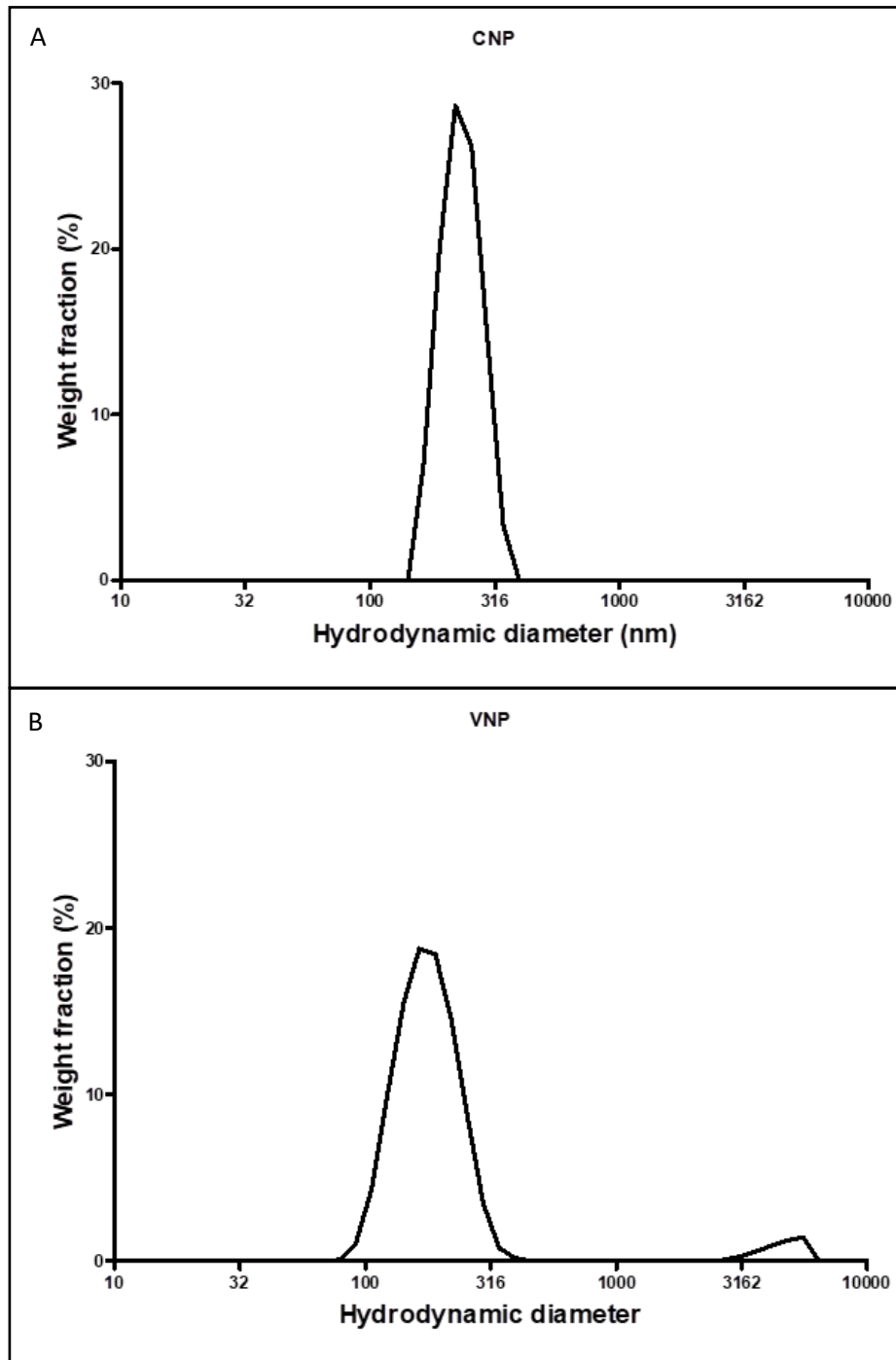


FIG 3: The hydrodynamic diameter distribution of a) un-associated nanoparticles (CNP) and b) vancomycin associated nanoparticles (VNP) as determined by DLS. Particles were dissolved in DMSO (1 mg/ml), mixed continuously and measured in triplicate. The hydrodynamic diameter was determined by the Stokes-Einstein equation. The mean size of CNP was 384 nm, with a polydispersity index of 0.212 and of VNP was 247 nm with a polydispersity index of 0.385.

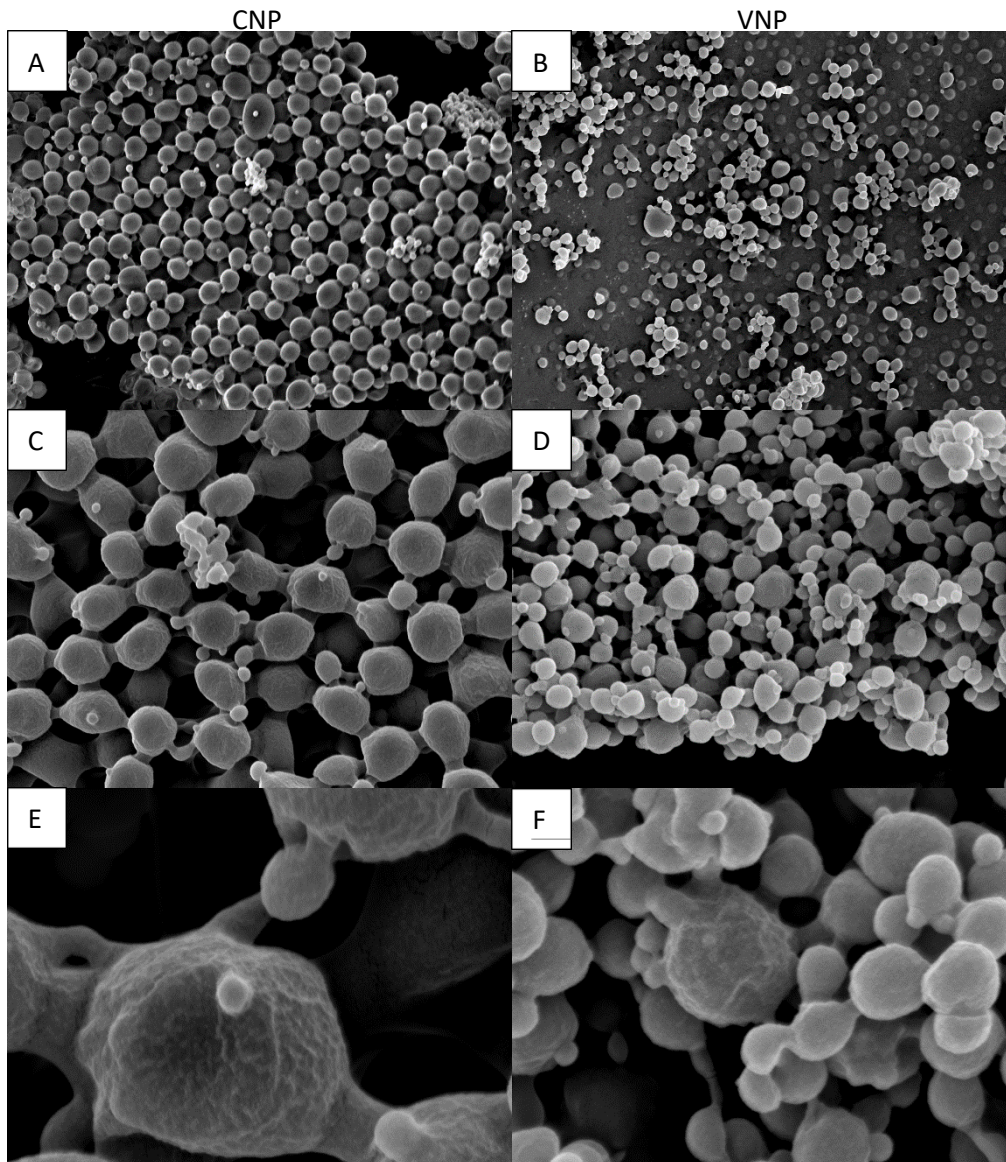


FIG 4: SEM micrographs of un-associated nanoparticles (CNP) and vancomycin encapsulated nanoparticles (VNP). Micrographs A and B are at 5000 x magnification, Micrographs C and D are at 10 000 x magnification and micrographs E and F are at 50 000 x magnification.

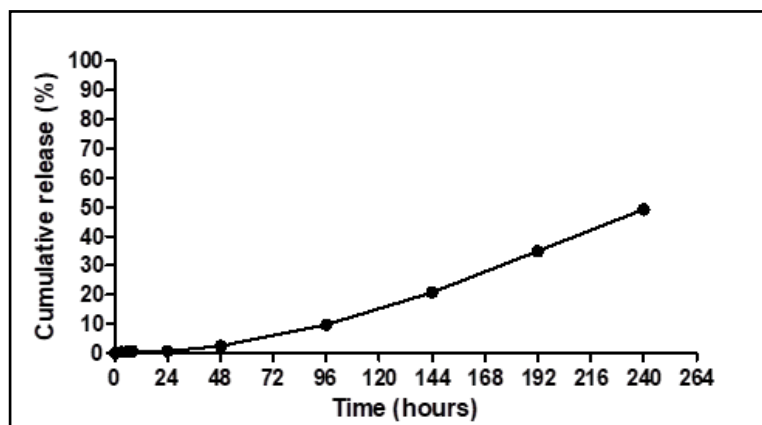


FIG 5: The cumulative release rate of VNP as determined by UHPLV for 240 h (10 days). Release followed a first-order release rate and within 24h enough vancomycin was released to be deemed therapeutically active.

CONCLUSION

PLGA nanoparticles loaded with vancomycin were prepared by the electrospraying method. The antibacterial activity of free vancomycin and encapsulated vancomycin were compared *in vitro*. Results indicated that encapsulating vancomycin in PLGA nanoparticles improved the antibacterial activity of vancomycin against MRSA. VNP had a MIC of 1 $\mu\text{g}/\text{ml}$, even though only 7% of the total particle consisted of vancomycin. Further studies are needed to elucidate the exact mechanism of action, but one possibility is that the nanoparticle binds to the cell wall of the bacterium. This increases the effective concentration of vancomycin in close proximity to the target of inhibition (D-Ala-D-Ala terminal end of peptidoglycan). These results suggest that the pressure of antibiotic resistance can be partially alleviated by encapsulating antibiotics in nanoparticles. Another advantage of encapsulating antibiotics is targeted or location delivery, thus reducing the spread in antibiotic resistance and reducing the death of commensal bacteria seen with conventional administration of antibiotics. The VNPs and CNPs had a rough surface structure and were spherical in shape, showing that vancomycin had no influence on the shape of the particles. The polydispersity index of VNPs and CNPs was above 0.2. We suggest using a syringe pump to improve size distribution. Vancomycin release was evaluated for 10 days; burst release was observed after 48 h and by the end of the assay only 50% of the encapsulated vancomycin had been released. These results indicate that encapsulated vancomycin can be used as a prophylaxis treatment, preventing hospital acquired infections post-surger

References

1. Wagner V, Dullaart A, Bock AK, Zweck A. 2006. The emerging nanomedicine landscape. *Nat Biotechnol* 24:1211–1217.
2. Yao S, Liu H, Yu S, Li Y, Wang X, Wang L. 2016. Drug-nanoencapsulated PLGA microspheres prepared by emulsion electrospray with controlled release behavior. *Regen Biomater* 3:309–317.
3. Salouti M, Ahangari A. 2014. Application of nanotechnology in drug delivery. *InTech*.
4. Danhier F, Ansorena E, Silva JM, Coco R, Le A, Pr at V. 2012. PLGA-based nanoparticles : An overview of biomedical applications. *J Control Release* 161:505–522.
5. Dillen K, Vandervoort J, Mooter G Van Den, Verheyden L, Ludwig A. 2004. Factorial design, physicochemical characterisation and activity of ciprofloxacin-PLGA nanoparticles 275:171–187.
6. Zakeri-milani P, Loveymi BD, Jelvehgari M, Valizadeh H. 2013. The characteristics and improved intestinal permeability of vancomycin PLGA-nanoparticles as colloidal drug delivery system. *Colloids Surfaces B Biointerfaces* 103:174–181.
7. Adair JH, Parette MP, Altinoglu EI, Kester M. 2010. Nanoparticulate alternatives for drug delivery. *ACS Nano* 4:4967–4970.
8. Farokhzad OC, Langer R. 2009. Impact of nanotechnology on drug delivery. *ACS Nano* 3:16–20.
9. Turos E, Reddy GSK, Greenhalgh K, Ramaraju P, Abeylath SC, Jang S, Dickey S, Lim D V. 2007. Penicillin-bound polyacrylate nanoparticles: Restoring the activity of β -lactam antibiotics against MRSA. *Bioorganic Med Chem Lett* 17:3468–3472.
10. Turos E, Shim JY, Wang Y, Greenhalgh K, Reddy GSK, Dickey S, Lim D V. 2007. Antibiotic-conjugated polyacrylate nanoparticles: New opportunities for development of anti-MRSA agents. *Bioorganic Med Chem Lett* 17:53–56.
11. Hartsel S, Bolard J. 1996. Amphotericin B: new life for an old drug. *Trends Pharmacol Sci* 12:445–449.
12. Kim H, Jones MN. 2004. The Delivery of Benzyl Penicillin to *Staphylococcus aureus* Biofilms by Use of Liposomes. *J Liposome Res* 14:123–139.
13. Pandey R, Khuller GK. 2005. Solid lipid particle-based inhalable sustained drug delivery system against experimental tuberculosis. *Tuberculosis* 85:227–234.

14. Cavalli R, Gasco MR, Chetoni P, Burgalassi S, Saettone MF. 2002. Solid lipid nanoparticles (SLN) as ocular delivery system for tobramycin. *Int J Pharm* 238:241–245.
15. Sanna V, Gavini E, Cossu M, Rassu G, Giunchedi P. 2007. Solid lipid nanoparticles (SLN) as carriers for the topical delivery of econazole nitrate: in-vitro characterization, ex-vivo and in-vivo studies. *J Pharm Pharmacol* 59:1057–1064.
16. Pandey R, Sharma A, Zahoor A, Sharma S, Khuller GK, Prasad B. 2003. Poly (DL-lactide-co-glycolide) nanoparticle-based inhalable sustained drug delivery system for experimental tuberculosis. *J Antimicrob Chemother* 52:981–986.
17. Magallanes M, Dijkstra J, Fierer J. 1993. Liposome-incorporated ciprofloxacin in treatment of murine salmonellosis. *Antimicrob Agents Chemother* 37:2293–2297.
18. Omri A, Suntres ZE, Shek PN. 2002. Enhanced activity of liposomal polymyxin B against *Pseudomonas aeruginosa* in a rat model of lung infection. *Biochem Pharmacol* 64:1407–1413.
19. Jain D, Banerjee R. 2008. Comparison of ciprofloxacin hydrochloride-loaded protein, lipid, and chitosan nanoparticles for drug delivery. *J Biomed Mater Res - Part B Appl Biomater* 86:105–112.
20. Fielding RM, Lewis RO, Moon-McDermott L. 1998. Altered tissue distribution and elimination of amikacin encapsulated in unilamellar, low clearance liposomes (MiKasome®). *Pharm Res*.
21. Kirby A, Graham R, Williams NJ, Wootton M, Broughton CM, Alanazi M, Anson J, Neal TJ, Parry CM. 2010. *Staphylococcus aureus* with reduced glycopeptide susceptibility in Liverpool, UK. *J Antimicrob Chemother* 65:721–724.
22. Hachicha W, Kodjikian L, Fessi H. 2006. Preparation of vancomycin microparticles: Importance of preparation parameters. *Int J Pharm* 324:176–184.
23. Lotfipour F, Abdollahi S, Jelvehgari M, Valizadeh H, Hassan M, Milani M. 2013. Study of antimicrobial effects of vancomycin loaded PLGA nanoparticles against *Enterococcus* clinical isolates. *Drug Res (Stuttg)* 64:348–352.
24. van Staden ADP. 2011. Developing bone cement implants impregnated with bacteriocins for prevention of infections.
25. Branowska I, Wilczek A, Baranowski J. 2010. Rapid UHPLC method for simultaneous determination of Vancomycin, Terbinafine, Spironolactone, Furosemide and their metabolites: application to human plasma and urine. *Anal Sci* 26:755–759.

26. Andrews JM. 2001. Determination of minimum inhibitory concentrations. *J Antimicrob Chemother* 48:5–16.
27. Barichello JM, Morishita M, Takayama K, Nagai T. 1999. Encapsulation of hydrophilic and lipophilic drugs in PLGA nanoparticles by the nanoprecipitation method. *Drug Dev Ind Pharm* 25:471–476.
28. García-Díaz M, Foged C, Nielsen HM. 2015. Improved insulin loading in poly(lactic-co-glycolic) acid (PLGA) nanoparticles upon self-assembly with lipids. *Int J Pharm* 482:84–91.
29. Menale C, Piccolo MT, Favicchia I, Aruta MG, Baldi A, Nicolucci C, Barba V, Mita DG, Crispi S, Diano N. 2015. Efficacy of piroxicam plus cisplatin-loaded PLGA nanoparticles in inducing apoptosis in mesothelioma cells. *Pharm Res* 32:362–374.
30. Luo C, Okubo T, Nangrejo M, Edirisinghe M. 2015. Preparation of polymeric nanoparticles by novel electrospray nanoprecipitation. *Polym Int* 64:183–187.
31. Ahire JJ, Neppalli R, Heunis TDJ, van Reenen AJ, Dicks LMT. 2014. 2, 3-Dihydroxybenzoic acid electrospun into poly(D, L-lactide) (PDLLA) / poly(ethylene oxide) (PEO) nanofibers inhibited the growth of Gram-positive and Gram-negative bacteria. *Curr Microbiol* 69:587–593.
32. Makadia HK, Siegel SJ. 2011. Poly Lactic-co-Glycolic Acid (PLGA) as biodegradable controlled drug delivery carrier. *Polymers (Basel)* 3:1377–1397.

STELLENBOSCH UNIVERSITY

Chapter 6

General discussion and conclusion

General discussion and conclusion

Total hip arthroplasty (THA) is considered the most successful orthopaedic operation, with a failure rate of 5% (1). The major cause for early THA revisions is periprosthetic joint infections (PJI) (2), which places an immense burden on the medical industry. Methicillin-resistant *Staphylococcus aureus* (MRSA) is the main causative agent of PJI and is isolated from 19% of cases (3). Traditionally, vancomycin is used to treat MRSA infections, but Kirby and co-workers recently reported on the isolation of MRSA with reduced vancomycin susceptibility (4). This rise in antibiotic resistance has made it nearly impossible to treat these infections. Thus, the discovery of novel antibiotics with a broad activity spectrum is of utmost importance. Radical PJI treatment entails removal of the infected prosthesis, direct application of antibiotics to the infected tissue, followed by a 12-week antibiotic course and insertion of a new prosthesis once the infection has cleared (5). However, direct application (as opposed to systemic administration) of antibiotics on bone formation and remodelling has not been studied in depth.

Prophylaxis treatment is suggested to reduce the occurrence of PJI (6). Traditionally drug impregnated cement was used in prophylactic treatment (7, 8), but the advances in nanotechnology has made it possible to encapsulate antibiotics in nanoparticles. Studies have also shown that by encapsulating antibiotics, their bio-absorption, antimicrobial activity and half-life can be improved (9).

Characterization of *Xenorhabdus khoisanae* antibiotics

Three antimicrobial agents were isolated from a *X. khoisanae* strain. Two were xenocoumacin-2 like and one a novel antibiotic with a mass-to-charge (m/z) ratio of 671, designated rhabdin. Xenocoumacin-2 has previously been isolated from *Xenorhabdus miraniensis* and *Xenorhabdus nematophilia* (10, 11). This is the first report on the isolation of xenocoumacin-2 like antimicrobials from *X. khoisanae*. Rhabdin was analysed with ultra-high-pressure liquid chromatography coupled to electrospray ionization mass spectrometry (UHPLC-MS/MS). A MS/MS fragmentation profile was obtained, indicating the presence of four fragments with m/z ratios of 473, 350, 268 and 144. Antimicrobial studies revealed that rhabdin is active

against *Staphylococcus aureus* Xen 31 (methicillin-resistant) and *S. aureus* Xen 36 (methicillin-sensitive) at levels as low as 3.5 µg/ml (minimum inhibitory concentration = MIC).

The cytotoxic and osteogenic effects of rhabdin were evaluated on two populations of rat derived femora mesenchymal stem cells (MSCs), bone marrow-derived mesenchymal stem cells (bmMSCs) and proximal femur-derived mesenchymal stem cells (pfMSCs). The second population, pfMSCs, was recently described by Jacobs and co-authors (12) as a phenotypically similar, but functionally distinct population of femora derived MSCs. This study revealed that rhabdin was cytotoxic to bmMSCs at levels exceeding 3.5 µg/ml, but pfMSCs were more sensitive as levels below 1 x MIC (3.5 µg/ml) was completely cytotoxic. Rhabdin had no anti-osteogenic effects on bmMSC at 3.5 µg/ml.

Although the toxicity and instability of rhabdin might impede the FDA approval of this antibiotic for use in PJIs, further cytotoxicity studies are needed to evaluate the potential of rhabdin in a clinical setting, especially since rhabdin is equally active against MRSA and methicillin-sensitive *S. aureus*. The cytotoxicity of rhabdin also indicates that it might have anti-cancer properties, but further studies are required to verify this claim.

Cytotoxic and osteogenic effect of vancomycin

Vancomycin, a glycopeptide, is commonly used to treat MRSA infections (13), yet no studies have been done on the cytotoxic and osteogenic effects of vancomycin on femora derived MSCs. In this study, we report that vancomycin had no cytotoxic effects on bmMSCs or pfMSCs at high doses (20 µg/ml), but had anti-osteogenic effects on pfMSC.

Although vancomycin had anti-osteogenic effects, our study indicates that applying vancomycin directly to the infected bone tissue will not have any long-term negative effects, since the pfMSCs should recover once vancomycin treatment is stopped.

Nanoparticle encapsulation of vancomycin

Vancomycin was encapsulated in PLGA nanoparticles by electrospraying and its efficiency compared to vancomycin-free PLGA nanoparticles. The drug-loading content of the vancomycin nanoparticles (VNP) was 7.33%, while the encapsulation efficiency was 73.9%. This indicates that 100 mg of nanoparticles contains 7 mg of vancomycin and that 73.9% of the initial vancomycin was incorporated into the particle. The hydrodynamic diameter of the VNP was 247 nm, while the diameter of un-associated nanoparticles (CNP) was 384 nm. This size reduction is most likely due to an interaction between the vancomycin and polymer used. Antimicrobial studies indicated that encapsulated vancomycin (MIC = 1 µg/ml) was more antimicrobially active compared to free vancomycin (MIC= 5 µg/ml). Vancomycin release was monitored for 10 days and within the first 24 h, 5 µg/ml vancomycin was released from the nanoparticles. After 10 days, only 50% of the encapsulated vancomycin was released, indicating that VNP will stay therapeutically active for a minimum of 14 days.

This study indicates that encapsulated antibiotics can be used in prophylactic treatments. One possibility is incorporating the nanoparticles in a specially designed prosthesis with micro-channels, fitted with a one-directional membrane. This would ensure the release of the encapsulated drug at the desired location and prevent removal of nanoparticles by circulation and macrophage engulfment, ultimately reducing the chance of THA failure due to infection. Although this study focused on hip replacements and MRSA infections, the data can be applied to other joint replacement surgeries and infections.

Conclusion

In conclusion, the *in vitro* cytotoxicity assays showed that rhabdin is cytotoxic to bmMSCs at levels exceeding 3.5 µg/ml, but further *in vitro* studies on other cell lines is needed before rhabdin can be deemed toxic to humans. Further research is needed to determine the structure of rhabdin.

Vancomycin had no toxic effects on bmMSCs or pfMSCs, but had an anti- osteogenic effect on pfMSCs at low levels. The antimicrobial activity of vancomycin was enhanced by encapsulation in nanoparticles, indicating that vancomycin nanoparticles have potential to be used for prophylaxis treatment during THA. Further research and *in vivo* studies are needed to support the vancomycin findings obtained in this study.

References

1. Ulrich SD, Seyler TM, Bennett D, Delanois RE, Saleh KJ, Thongtrangan I, Kuskowski M, Cheng EY, Sharkey PF, Parvizi J, Stiehl JB, Mont MA. 2008. Total hip arthroplasties: What are the reasons for revision? *Int Orthop* 32:597–604.
2. Song Z, Borgwardt L, Høiby N, Wu H, Sørensen TS, Borgwardt A. 2013. Prosthesis infections after orthopedic joint replacement : the possible role of bacterial biofilms. *Orthop Rev (Pavia)* 5:65–71.
3. Pulido L, Ghanem E, Joshi A, Purtill JJ, Parvizi J. 2008. Periprosthetic joint infection. *Clin Orthop Relat Res* 466:1710–1715.
4. Kirby A, Graham R, Williams NJ, Wootton M, Broughton CM, Alanazi M, Anson J, Neal TJ, Parry CM. 2010. *Staphylococcus aureus* with reduced glycopeptide susceptibility in Liverpool, UK. *J Antimicrob Chemother* 65:721–724.
5. Parvizi J, Aggarwal V, Rasouli M. 2013. Periprosthetic joint infection: Current concept. *Indian J Orthop* 47:10–17.
6. Shahi A, Parvizi J. 2015. Prevention of periprosthetic joint infection. *Arch bone Jt Surg* 3:72–81.
7. Jones Z, Brooks AE, Ferrell Z, Grainger DW, Sinclair KD. 2016. A resorbable antibiotic eluting bone void filler for periprosthetic joint infection prevention. *J Biomed Mater Res - Part B Appl Biomater* 104:1632–1642.
8. Hsu Y, Hu C, Hsieh P, Shih H, Ueng SWN, Chang Y. 2017. Vancomycin and Ceftazidime in bone cement as a potential effective treatment for knee periprosthetic joint infection. *J Bone Jt Surg* 99:223–231.
9. Yao S, Liu H, Yu S, Li Y, Wang X, Wang L. 2016. Drug-nanoencapsulated PLGA microspheres prepared by emulsion electrospray with controlled release behavior.

Regen Biomater 3:309–317.

10. Reimer D, Luxenberger E, Brachmann AO, Bode HB. 2009. A new type of pyrrolidine biosynthesis is involved in the late steps of xenocoumacin production in *Xenorhabdus nematophila*. ChemBioChem 10:1997–2001.
11. McInerney B V, Taylor WC, Lacey MJ, Akhurst RJ, Gregson RP. 1991. Biologically active metabolites from *Xenorhabdus* spp., Part 2. Benzopyran-1-one Derivatives with Gastroprotective activity. J Nat Prod 54:785–795.
12. Jacobs FA, Sadie-Van Gijzen H, van de Vyver M, Ferris WF. 2016. Vanadate impedes adipogenesis in mesenchymal stem cells derived from different depots within bone. Front Endocrinol (Lausanne) 7:1–12.
13. Fair RJ, Tor Y. 2014. Antibiotics and Bacterial Resistance in the 21st Century. Perspect Medicin Chem 6:25–64.

